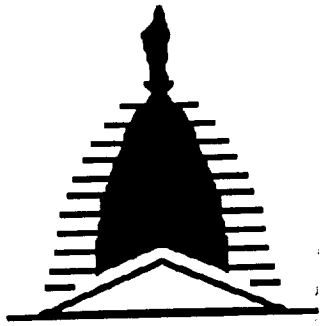

NASA/USRA UNIVERSITY ADVANCED DESIGN PROGRAM 1991-1992

UNIVERSITY SPONSOR
BOEING COMMERCIAL AIRPLANE COMPANY

FINAL DESIGN PROPOSAL

EXODUS - PRIME MOVER

Air Transport System Design Simulation

May 1992

Department of Aerospace and Mechanical Engineering
University of Notre Dame
Notre Dame, IN 46556

DESIGN PROPOSAL

MAY 4, 1992

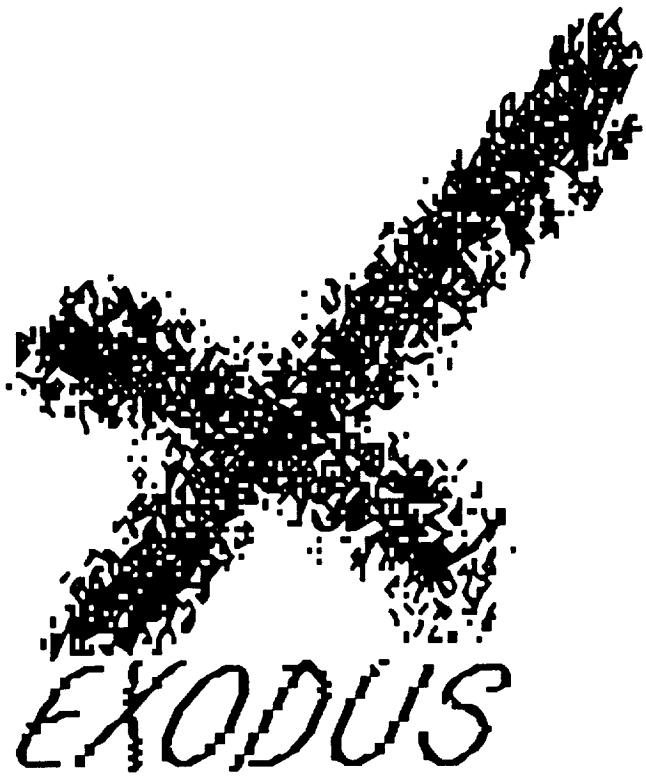

PRIME MOVER

NIKKOL BAUER
PETE CONWELL
MATT JOHNSON
RICH MCMANUS
WENDY SHIELDS
TIM THORNTON
ROB TOKARZ

Table of Contents

Nomenclature

ac	aerodynamic center
AR	aspect ratio
b	wing span
c	chord
Cl	section lift coefficient
$C_{l\alpha}$	section lift slope
C_L	aircraft lift coefficient
C_d	section drag coefficient
C_{do}	section zero lift drag coefficient
C_D	airrcraft drag coefficient
C_{D0}	aircraft zero lift drag coefficient
C.G.	center of gravity
$C_{L\alpha v}$	lift curve slope of vertical stabilizer
$C_{L\alpha w}$	lift coefficient of wing
$C_{Lcruise}$	lift coefficient at cruise of aircraft
$C_{L\delta e}$	change in lift due to elevator deflection
$C_{m\alpha}$	moment coefficient about C.G.
C_{m0}	moment coefficient about C.G. at zero lift
$C_{n\beta}$	yaw stability coefficient
c_{root}	root chord
e	span efficiency factor
E	endurance
E_m	max lift to drag ratio
i	current
I_x	moment of inertia about x axis
J	propellor advance ratio
$L_{\delta a}$	roll moment due to aileron deflection
l_v	distance from C.G. to ac of vertical stabilizer
mAh	milliamp hours
n	load factor
N.P.	neutral point
Q	dynamic pressure
R	range
RPM	revolutions per minute
S	planform area
S.M.	static margin
Sv	planform area of vertical stabilizer
t	time

TO	take-off
V	volts
V_{cruise}	cruise velocity
V_{stall}	stall velocity
V_{TO}	take-off velocity
V_v	vertical tail volume ratio
V_∞	freestream velocity
α	angle of attack
α_{cruise}	angle of attack at cruise
α_{stall}	stall angle of attack
Γ	dihedral angle
$\delta_{ecruise}$	elevator deflection at cruise
η	propellor efficiency
η_v	dynamic pressure ratios
Φ	rolling angular acceleration
φ	bank angle
θ	bank angle
σ_{max}	maximum allowable stress
τ	control surface area ratio
ω	roll rate

1.0 Executive Summary

The Exodus *Prime Mover* is an overnight package delivery aircraft designed to serve the Northern Hemisphere of Aeroworld. The preliminary design goals originated from the desire to produce a large profit. The two main driving forces throughout the design process were first to reduce the construction man-hours by simplifying the aircraft design, thereby decreasing the total production cost of the aircraft. The second influential factor affecting the design was minimizing the fuel cost during cruise. The lowest fuel consumption occurs at a cruise velocity of 30 ft/s. Overall, it was necessary to balance the economic benefits with the performance characteristics in order create a profitable product that meets all specified requirements and objectives.

The SPICA airfoil section and a rectangular planform were selected to reduce construction hours neccessary to produce the wing. Its flat bottom and lift characteristics provide a balance between aircraft performance and construction simplicity. The wing area of 9.62 square feet ensured the necessary lift both during cruise and take-off. In addition, cruise conditions occur at maximum lift to drag ratio.

The Astro 15 electric motor and the ZingerJ 11-5 propeller comprise the propulsion system of the *Prime Mover*. The propeller selection was based upon the take-off distance requirement of 60 feet; the ZingerJ 11-5 provided the highest efficiency while still meeting this requirement. Twelve batteries of 1.2 volts and 1000 mah each were selected to power the system. The battery pack provides the voltage needed for take-off and the capacity required for the flight time of the aircraft.

Directional and longitudinal control has been achieved through the use of a rudder and an elevator. A polyhedral concept has also been adopted for roll control. The polyhedral was chosen over the dihedral to decrease the amount of structure needed to withstand the bending moment at the root of the wing.

The *Prime Mover* is capable of guaranteeing overnight delivery for the entire Northern Hemisphere due to the proposed fleet size of 42 airplanes and the high range and endurance capabilities. The design objectives required the aircraft to meet a 8600 foot range minimum.

The final design has displayed a cruise range of 24,000 feet, enabling the aircraft to complete its nightly schedule without the need to refuel. This reduces the operating costs of the aircraft. The maximum range and endurance of the fully loaded aircraft is 31,000 feet and 13.5 minutes, respectively. The take-off distance at maximum take-off weight is 59 feet.

The *Prime Mover* has a rectangular frontal area of 4.625 inches by 4.375 inches and a fuselage length just under 5.0 feet to provide 800 cubic inches of cargo space. The fuselage, wing, and empennage were designed to withstand a landing load factor of 4.0, a cruise load factor of 2.5, and a catapult launch load factor of 2.0.

The wing and the empennage will be removable in order to fit the disassembled aircraft within a 2ft x 2ft x 5ft box. Although this design increases the complexity of the structure, it enables the use of a modular construction technique. Each component of the aircraft may be built separately and assembled at a later time. This construction method will decrease the construction man-hours.

As a result of the previously mentioned design characteristics, Exodus confidently presents the *Prime Mover*, an aircraft created to harmonize technical and economic considerations. The total production cost is estimated at $376,000. Based upon the production, operating, maintenance, and fuel costs Exodus recommends the price per cubic inch for intracontinental and overseas shipping be $8.74 and $11.01, respectively, in order to break even on the original investment.

EXODUS
PRIME MOVER

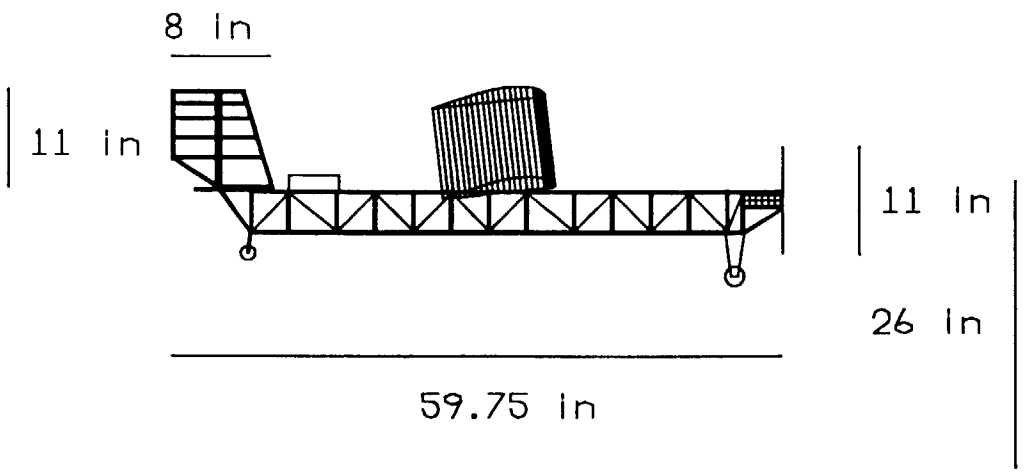

Prime Mover Specifications

Aerodynamics

Wing Area	9.62 ft^2
Aspect Ratio	9.62
Chord	12.0 in
Span	9.62 ft
Taper Ratio	1.
Sweep	0°
Polyhedral	17°
C_{Do} (aircraft)	0.018
Airfoil Section	SPICA
Wing Mount Angle	7°
Stall Angle	14°
CL_{max} (aircraft)	1.18
L/D_{max} (aircraft)	17.8

Structure

Empennage	
Hor. and Ver. Tail Airfoil Sections	flat plate
Horiz. Tail Area	208 in^2
Vert. Tail Area	77 in^2
Fuselage	
Length	5.0 ft
Height	9.36 in
Volume	1130 in^3
Payload Volume	800 in^3
Frontal Area	20.2 in^2
Landing Gear	
Type	Tail Dragger

Economics

Fleet Life Cost /Volume Moved	$6.47
Overseas Price/in^3	$11.01
Intercont. Price /in^3	$8.74
Production Cost	$376,000

Performance

Minimum Velocity	10 ft/s
Maximum Velocity	51 ft/s
Stall Velocity	22.3 ft/s
Take-Off Velocity	26.8 ft/s
Cruise Velocity	30 ft/s
R/C_{max}	5.4 ft/s
Min Glide Angle	3.33°
Take-Off Distance	59 ft
Landing Distance	44 ft
Max Range	31,000 ft
Max Endurance	13.5 min
Turning Radius	60 ft

Propulsion

Engine	Astro 15
Propeller	ZingerJ11-5
# of Batteries	12
Total Voltage	14.4 volts
Battery Capacity	1000 mahs

Weights

Gross T.O. Weight	6.7 lb
Empty Weight	4.7 lb
Zero Fuel Weight	3.45 lb
C.G. position	
x (from nose)	30.5 in
y (from bottom of fuselage)	3.12 in

Parameter	Design Completion	Prototype Completion
DESIGN GOALS:		
V cruise	30 ft/s	30 ft/s
Altitude cruise	25 ft	25 ft
Turn radius	60 ft	60 ft
Endurance	13.2 min	13.2 min
Max Payload Volume	800 in^3	800 in^3
Range-max payload	24,000 ft	24,000 ft
Payload at Max R (wgt)	0. oz	0. oz
Range-min payload	26,200 ft	26,200 ft
Weight (MTO)	6.7 lb	6.8 lb
Design life cycles	600	600
Aircraft sales price	$376,000(actual cost)	$376,000(actual cost)
Target cost/in^3 payload	$6.47(actual cost)	$6.47(actual cost)
Target cost/oz payload	N/A	N/A
BASIC CONFIGURATION:		
Wing Area	9.62 ft^2	9.62 ft^2
Weight (no payload)	4.7 lb	4.8 lb
Weight (maximum)	6.7 lb	6.8 lb
Wing loading (max Wgt)	0.7 lb/ft^2	0.7 lb/ft^2
length	5.0 ft	5.0 ft
span	9.62 ft	9.62 ft
height (fuselage)	4.375 in	4.375 in
width (fuselage)	4.625 in	4.625 in
location of ref. axis origin	nose/bottom of fuselage	nose/bottom of fuselage
WING:		
Aspect Ratio	9.62	9.62
Span	9.62 ft	9.62 ft
Area	9.62 ft^2	9.62 ft^2
Root Chord	12.0 in	12.0 in
Tip Chocrd	12.0 in	12.0 in
Taper ratio	1.	1.
C_{mac} -MAC	-.05	-.05
Leading edge sweep	0.	0.
1/4 chord sweep	0.	0.
Dihedral	17°	17°
Twist (washout)	0.	0.
Airfoil section	SPICA	SPICA
Design Reynolds number	190,806	190,806
t/c	11.7%	11.7%
Incidence angle (root)	7°	7°
Hor. pos. of 1/4 MAC	2.08% of chord	2.08% of chord
Ver. pos. of 1/4 MAC	16.7% of chord	16.7% of chord

e - Oswald efficiency	0.76	0.76
C_{Do} - wing	0.0087	0.0087
C_{Lo} - wing	0.1474	0.1474
$C_{L\alpha}$ - wing	0.0737/deg	0.0737/deg
FUSELAGE:		
Length	5.0 ft	5.0 ft
Diameter - max	N/A	N/A
Diameter - min	N/A	N/A
Diameter - avg	N/A	N/A
Finess ratio	13.0	13.0
Payload volume	800.0 in^3	800.0 in^3
Total volume	1130.0 in^3	1130.0 in^3
Planform area	240.0 in^2	240.0 in^2
Frontal area	20.2 in^2	20.2 in^2
CD_0 - fuselage	0.004	0.004
$C_{L\alpha}$ - fuselage	0.344	0.344
EMPENNAGE:		
HORIZONTAL TAIL		
Area	208.0 in^2	208.0 in^2
Span	26.0 in	26.0 in
Aspect ratio	3.25	3.25
Root Chord	8.0 in	8.0 in
Tip Chord	8.0 in	8.0 in
Taper ratio	1.	1.
L.E. sweep	0.	0.
1/4 chord sweep	0.	0.
Incidence angle	+5°	+5°
Hor. pos. of 1/4 MAC	-2 ft from cg	-2 ft from cg
Ver. pos. of 1/4 MAC	+1.09 in from cg	+1.09 in from cg
Airfoil section	flat plate	flat plate
e - Oswald efficiency	0.82	0.82
C_{Do} - horizontal	0.0016	0.0016
C_{Lo} - horizontal	0.	0.
$C_{L\alpha}$ - horizontal	3.89/rad	3.89/rad
C_{Lde} - horizontal	0.226/rad	0.226/rad
C_{Mmac} - horizontal	0.	0.
VERTICAL TAIL		
Area	77.0 in^2	77.0 in^2
Aspect ratio	1.57	1.57
Root chord	8.0 in	8.0 in
Tip chord	6.0 in	6.0 in
Taper ratio	0.75	0.75
L.E. sweep	0.	0.
1/4 chord sweep	0.	0.

Hor. pos. of 1/4 MAC	-2.3 ft from cg	-2.3 ft from cg
Ver. pos. of 1/4 MAC	+5.76 in from cg	+5.76 in from cg
Airfoil section	flat plate	flat plate
SUMMARY AERODYNAMICS:		
C_{lmax} (airfoil)	1.4	1.4
C_{Lmax} (aircraft)	1.18	1.18
Lift curve slope (aircraft)	0.0737/deg	0.0737/deg
C_{Do} (aircraft)	0.0179	0.0179
Efficiency - e (aircraft)	0.746	0.746
Alpha stall (aircraft)	14°	14°
Alpha zero lift (aircraft)	-2°	-2°
L/D max (aircraft)	17.80	17.80
Alpha L/D_{max} (aircraft)	8.64°	8.64°
WEIGHTS:		
Weight total (empty)	75.74 oz	76.7 oz
C.G. most forward - x&y	(30.4,3.3)in	(30.4,3.3)in
C.G. most aft - x&y	(30.5,3.3)in	(30.5,3.3)in
Avionics	5.95 oz	6.63 oz
Payload (max)	32 oz	32 oz
Motor	10.25 oz	9.7 oz
Propeller	1.0 oz	1.0 oz
Fuel (battery)	20.04 oz	17.99 oz
Structure	38.5 oz	40.57 oz
Wing	15.0 oz	15.34 oz
Fuselage/emp.	19.0 oz	20.48 oz
Landing gear	4.5 oz	5.58 oz
lcg - max weight		
lcg - empty		
PROPULSION:		
Type	Astro 15	Astro 15
Number	one	one
Placement	nose	nose
Pavail max @engine	200 Watts	200 Watts
Preq cruise	15.4 Watts	15.4 Watts
Max. current draw	25 amps	25 amps
Cruise current draw	4.45 amps	4.45 amps
Propeller diameter	11.0 in	11.0 in
Propeller pitch	5 in	5 in
Number of blades	2	2
Max. Prop. RPM	18690	18690
Cruise Prop. RPM	4700	4700
Max. Thrust	1.5 lbs	1.5 lbs
Cruise Trust	.38 lbs	.38 lbs
Battery type	Panasonic	Panasonic
Number	12	12

Individual capacity	1000 mahs	1000 mahs
Individual voltage	1.2 volts	1.2 volts
Pack capacity	1000 mahs	1000 mahs
Pack voltage	14.4 volts	14.4 volts
STABILITY AND CONTROL:		
Neutral point	42.4% chord from LE	42.4% chord from LE
Static margin %MAC	15.6%	15.6%
Hor. tail volume ratio	0.3	0.3
Ver. tail volume ratio	0.01	0.01
Elevator area	39 in^2	39 in^2
Elevator max deflection	+/- 20°	+/- 20°
Rudder Area	49.5 in2	49.5 in2
Rudder max deflection	+/- 20°	+/- 20°
Aileron Area	N/A	N/A
Aileron max deflection	N/A	N/A
$C_{m\alpha}$	-0.672/rad	-0.672/rad
$C_{n\beta}$	0.054/rad	0.054/rad
$C_{l\alpha}$ tail	3.89/rad	3.89/rad
C_{lde} tail	0.226/rad	0.226/rad
PERFORMANCE:		
V_{min}	10.0 ft/s	10.0 ft/s
V_{max}	51.0 ft/s	51.0 ft/s
V_{stall}	22.3 ft/s	22.3 ft/s
Range max - R_{max}	31,000 ft	31,000 ft
Endurance @ R_{max}	11.5 min	11.5 min
Endurance max - E_{max}	13.5 min	13.5 min
Range @ E_{max}	27,000 ft	27,000 ft
ROC_{max}	5.4 ft/s	5.4 ft/s
Min Glide angle	3.33°	3.33°
T/O distance	59.0 ft	59.0 ft
T/O rotation angle	11.5°	11.5°
Landing distance	44.0 ft.	44.0 ft.
Catapult Range	not available	not available
SYSTEMS:		
Landing gear type	tail dragger	tail dragger
Main gear position	6.0 in	16.25 in
Main gear length	5.0 in	5.0 in
Main gear tire size	1.25 in	1.25 in
tail gear postion	57 in	57 in
tail gear length	4.7 in	4.7 in
tail gear tire size	1.1 in	1.1 in
Engine speed control	Tekin Speed Controller	Tekin Speed Controller
Control surfaces	elevator/rudder	elevator/rudder

TECH. DEMONSTRATOR:		
Payload volume	800.0 in^3	800.0 in^3
Payload weight	32.0 oz	32.0 oz
Gross Take-Off Weight	6.7 lb	6.8 lb
Empty Operating Weight	4.7 lb	4.8 lb
Zero Fuel Weight	3.45 lb	3.67 lb
Wing Area	9.62 ft^2	9.62 ft^2
Hor. Tail Area	208.0 in^2	208.0 in^2
Ver. Tail Area	77.0 in^2	77.0 in^2
C.G. position	30.5 in	30.5 in
1/4 MAC position	30.25 in	20.25 in
Static margin %MAC	17%	15.6%
V_{TO}	26.8 ft/s	26.8 ft/s
Range max	31,000 ft	31,000 ft
Endurance max	13.5 min	13.5 min
V cruise	30.0 ft/s	30.0 ft/s
Turn radius	60.0 ft	60.0 ft
Airfram Struct. Weight	38.5 oz	40.57 oz
Propulsion Syst. Weight	11.25 oz	10.7 oz
Avionics Weight	5.95 oz	6.63 oz
Landing Gear Weight	4.5 oz	5.58 oz
Est. Catapult Range	not available	not available
ECONOMICS:		
Unit materials cost	$127	$164
Unit propulsion system cost	$213	$213
Unit control system cost	$300	$300
Unit total cost	$640	$677
Scaled unit total cost	$256,000	$270,800
Unit production manhours	120	112
Scaled production costs	$120,000	$112,000
Total unit cost	$376,000	$392,800
Cargo cost ($/$in^3$)	$6.47	$6.51
Single Flight gross income	$2891	$2891
Single flight op. costs	$1638	$1638
Single flight profit	$1253	$1253
#flights for break even	12,600	12,600

2.0 Mission

2.1 Design Requirements and Objectives

After carefully reading the request for proposal, Group Exodus strove towards developing a mission that would result in the maximum return on investment. In order to do this, the design requirements had to be assessed. Some of the primary requirements were as follows. The aircraft had to be able to take off and land under its own power within 75 ft. . It had to be able to sustain a level 60 ft. radius turn. The aircraft had to travel at a velocity less than 30 ft./sec. The disassembled aircraft had to fit within a 2'x2'x5' box. The aircraft had to be able to reroute to the nearest airport and loiter for 1 minute in case of an emergency. Lastly, the aircraft could utilize no more than 4 servos. These were thought to be the most important design requirements.

Group Exodus was now prepared to analyze the Aeroworld market and develop the most profitable mission. In doing so, a set of design objectives was formulated. The complete list of these objectives is as follows:

Structural:

1. The aircraft design should be as simple as possible in order to minimize construction costs.
2. The aircraft should maintain structural integrity throughout a life cycle of 600 flights.
3. The aircraft must be able to survive a forced landing.
4. The total payload volume will be between 576 and 768 cubic inches. This will allow for a minimum frontal area while maintaining a fuselage length of under five feet.
5. Battery exchange should take less than 1 minute to reduce maintenance costs.
6. The cargo must be easily accessible to decrease handling time.

Performance:

1. The average speed must be greater than 16 ft./sec so that the furthest destination can be reached in the allotted time.
2. Aircraft must complete the furthest run twice within 12 minutes to allow time for package handling.
3. The maximum aircraft weight will be less than 7 pounds, the perceived maximum weight for previous aircraft of this class.
4. The minimum range must be greater than 8600 ft. in order to accommodate the furthest projected flight.

Economic:

1. The total cost of the aircraft structure should not exceed $200.00.
2. Based on initial estimated production cost of $340,000 per aircraft, which is believed to comprise of 90% of the total life cost, the average price per cubic inch will be approximately $2.25.

There were a few alterations to our original design objectives and these will be discussed in the following chapters. These objectives would now guide Group Exodus in formulating the complete mission statement.

2.2 Mission Analysis

Group Exodus, in arriving at the mission, realized the importance of the fact that we were designing for an inexperienced company in a new and uncharted market. Consequently, the fleet was designed for a restricted area which would result in excellent efficiency and dependability; as opposed to spreading the fleet thin throughout all of Aeroworld and decreasing the efficiency and dependability of the service. This dependable service would consequently attract more customers. Therefore, the *Prime Mover* fleet was designed to operate in the Northern Hemisphere only.

There was another good reason to stay within the Northern Hemisphere. After further analyzing the economics of the mission,

fuel costs were estimated to be approximately 73% of the total fleet life cost. Therefore, restraining the total mileage flown by the fleet would result in a less expensive service for the customer. As a result, a hub system was decided on. By centrally locating the hub city, the fuel cost for each plane could be kept to a minimum consequently reducing the total fleet life cost. City J was chosen as the hub city due to its central location and the large daily cargo load of this city.

Another reason for chosing the Northern Hemisphere was the results calculated from the market analysis. After reviewing the daily cargo load departing from all of the Southern hemisphere cities (C, D, E, and O), there was no city that was delivering more than 1000 cubic inches. City C ships 980 cubic inches, city D ships 690 cubic inches, city E ships 960 cubic inches and cty O ships only 280 cubic inches. After refering to Appendix I, it can be seen that the Northern Hemisphere city with the least amount of cargo, city H, ships almost 590 cubic inches more than the Southern Hemisphere city that ships the most, city C. The Southern Hemisphere accounts for only 9% of the total departing cargo load of the world. Consequently, besides expending a lot of money in fuel costs, the prospect for profit in the Southern Hemisphere is quite weak and therefore Group Exodus recommends that only the Northern Hemisphere should be served at this point. Though our analysis does not include the Southern Hemisphere, the aircraft does have the capability to accommadate this area. Future servicing of this hemisphere may be considered using a different pricing system.

There will be 42 planes in the *Prime Mover* fleet. The cargo area of each plane will be 800 cubic inches. This exceeded the 768 cubic inch objective which was set to allow for single-stacked cargo. Single-stacked cargo reduces the frontal area and allows for better control over the cargo CG. We were able to increase our allowable cargo capacity by making the empennage removable, thus enabling the fuselage to be longer without exceeding the five foot storage restriction. This increase in volume will reduce the number of planes in the fleet and consequently greatly reduce the total fleet life cost. Each plane will make only two flights per day resulting in low fuel

cost per plane as mentioned before. The plane will simply fly to city J, unload its cargo, reload, and return to its original destination. The planes that arrive at the hub city first can be unloaded and then the other planes can be unloaded as they arrive. Therefore, the loading and unloading process runs smoothly and is accomplished in less time. There is also the possibility of rotating the planes that fly a longer distance with those that fly a relatively short distance. This will even out the effects of fatigue on each of the aircraft. The simplicity of this mission will also result in basically no problems with the designing of routes and the scheduling of flights. This service will be able to accommodate 100% of the daily cargo load in the Northern Hemisphere or Aeroworld. The *Prime Mover* was also designed to be able to handle a full load of parcels at the maximum density. As a result, no customer will be turned away. Creating this peaceful state of mind in our customers will result in more customers which translates into more of a profit.

The longest flight time for any route will be no more than 9 minutes. This includes a flight to the hub city and back with a one minute loiter during each flight. This will leave 6 minutes for loading, unloading, and daily servicing. This is more than enough time in Aeroworld. As a result of this efficient time schedule, the service becomes as dependable as possible. The price of one aircraft will be $376,000, in order for the company to break even in half of the fleet life. The price breakdown is available in Section 12.1.

3.0 Concept Selection Studies

The design process was begun by developing a number of design concepts to meet the request for proposal. Acknowledging the strengths and weaknesses of each proposal allowed Exodus to determine the best possible final aircraft design.

3.1 Concept #1

Concept one is a conventional aircraft with a high mounted rectangular planform wing with dihedral. It has a conventional tail and a single forward mounted engine. This concept emphasizes simplicity, reducing construction hours and thus construction costs.

Control would be achieved by use of the elevator and the rudder-dihedral combination. Therefore, only two servos would be required for the control surfaces, which decreases operational costs. The dihedral joint would be subject to a large moment due to it's location at the root of the wing. This would require a costly increase in structural support.

Tail dragging landing gear is used to maintain landing stability. It allows for the option of attaching the rear landing gear to the rudder for increased ground control.

3.2 Concept #2

Concept two is a canard configuration. The main wing is high mounted with dihedral and the canard is mounted low and forward on the fuselage. This configuration of the lifting surfaces would minimize the inerference of the control surfaces on the main wing. Again the aircraft would be driven by one forward mounted engine. For this design, tricycle landing gear would implemented.

A canard configuration would require the construction of two wings; hence, increasing the production hours and cost. The extra lift produced by the canard could be used to lift a larger payload. It

becomes necessary to consider the power required to take off with such a large weight.

3.3 Concept #3

Concept three uses a low mounted wing with a tapered planform. The empennage is a T-tail, and the landing gear is a tail dragger.

The tapered wing decreases the induced drag by increasing the wing efficiency and aspect ratio. However, the spanwise change in airfoil sections would increase the construction time and cost. Though the use of a T-tail would be beneficial in avoiding downwash, construction simplicity would suggest placing the horizontal stabilizer on the top of the fuselage Structurally, the empennage of a T-tail would be subjected to larger bending moments than a conventional tail. Control difficulties would arise in running the control wire from the fuselage to the top of the vertical stabilizer.

Concept #1

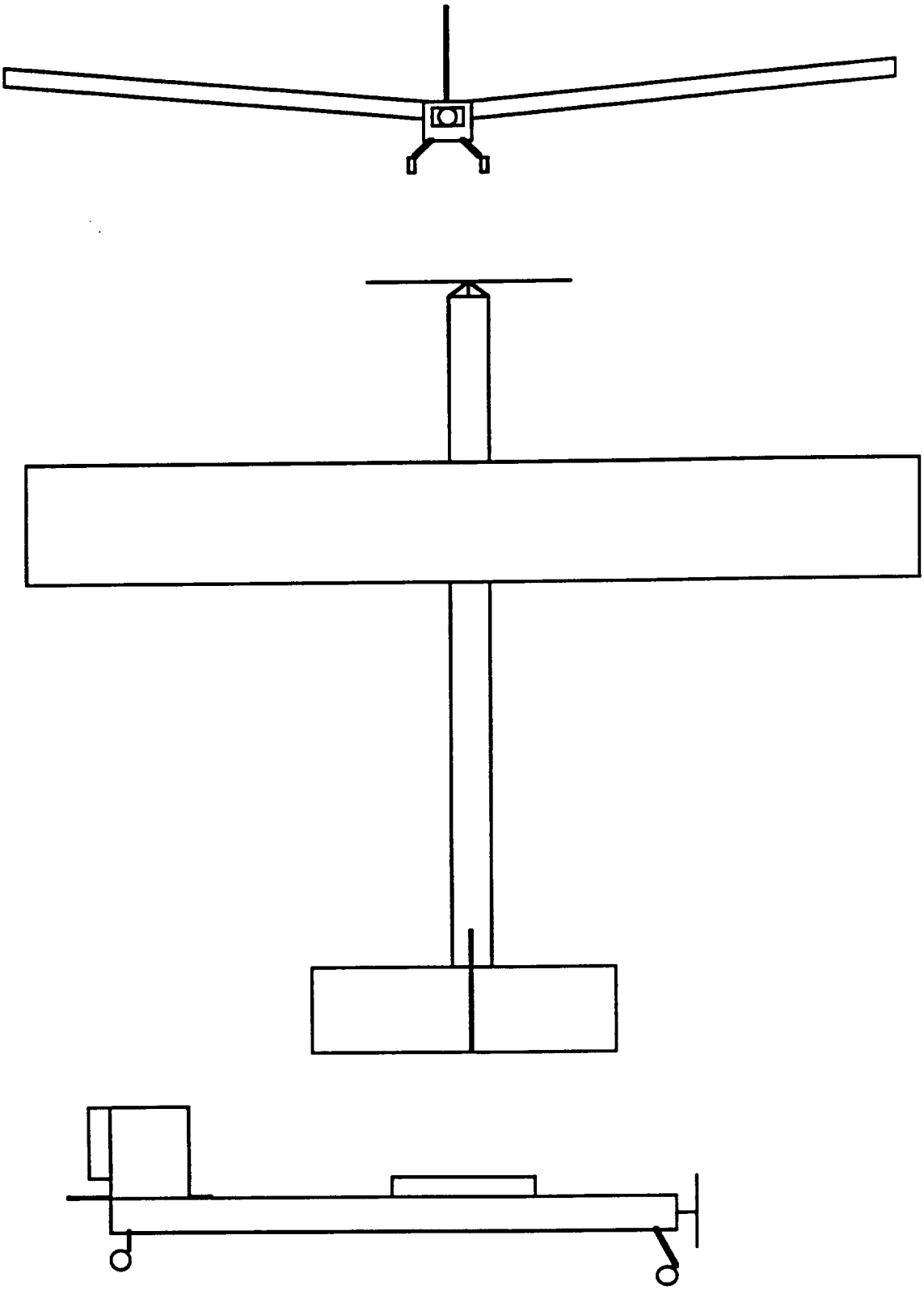

Concept #2

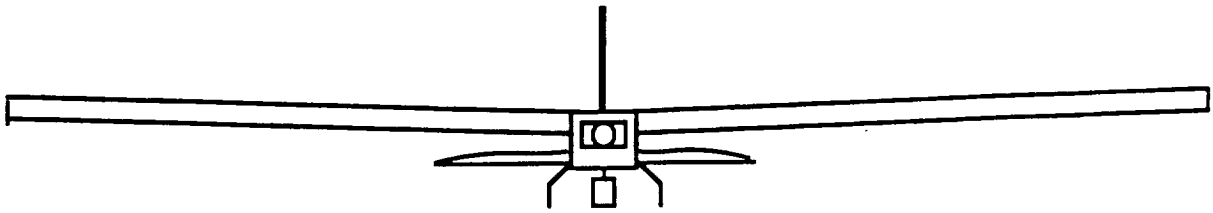

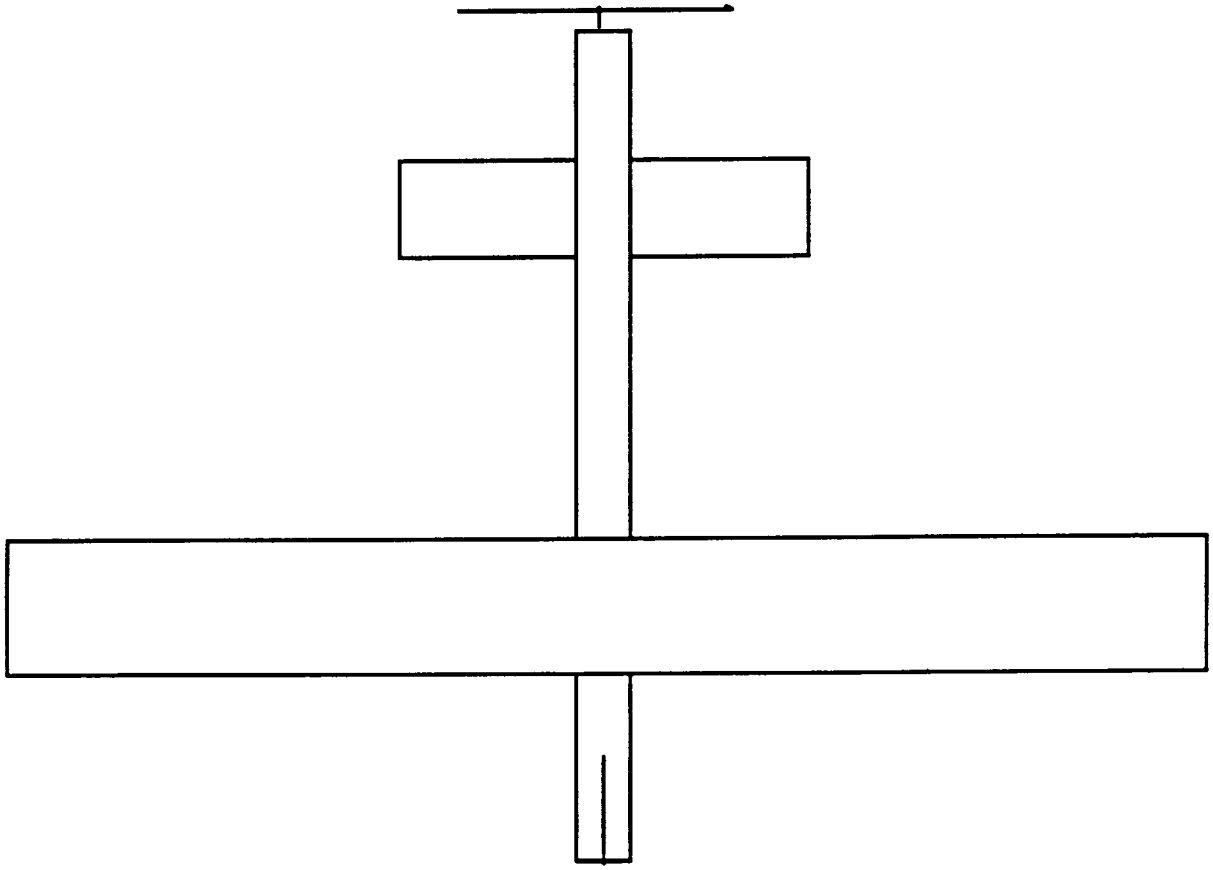

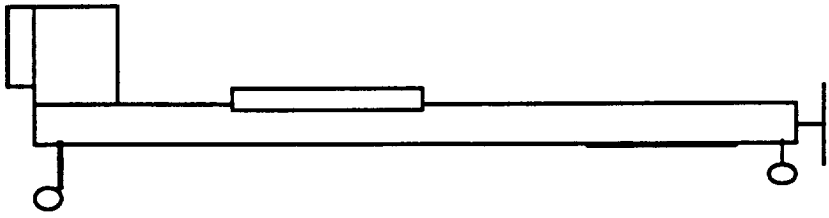

Concept #3

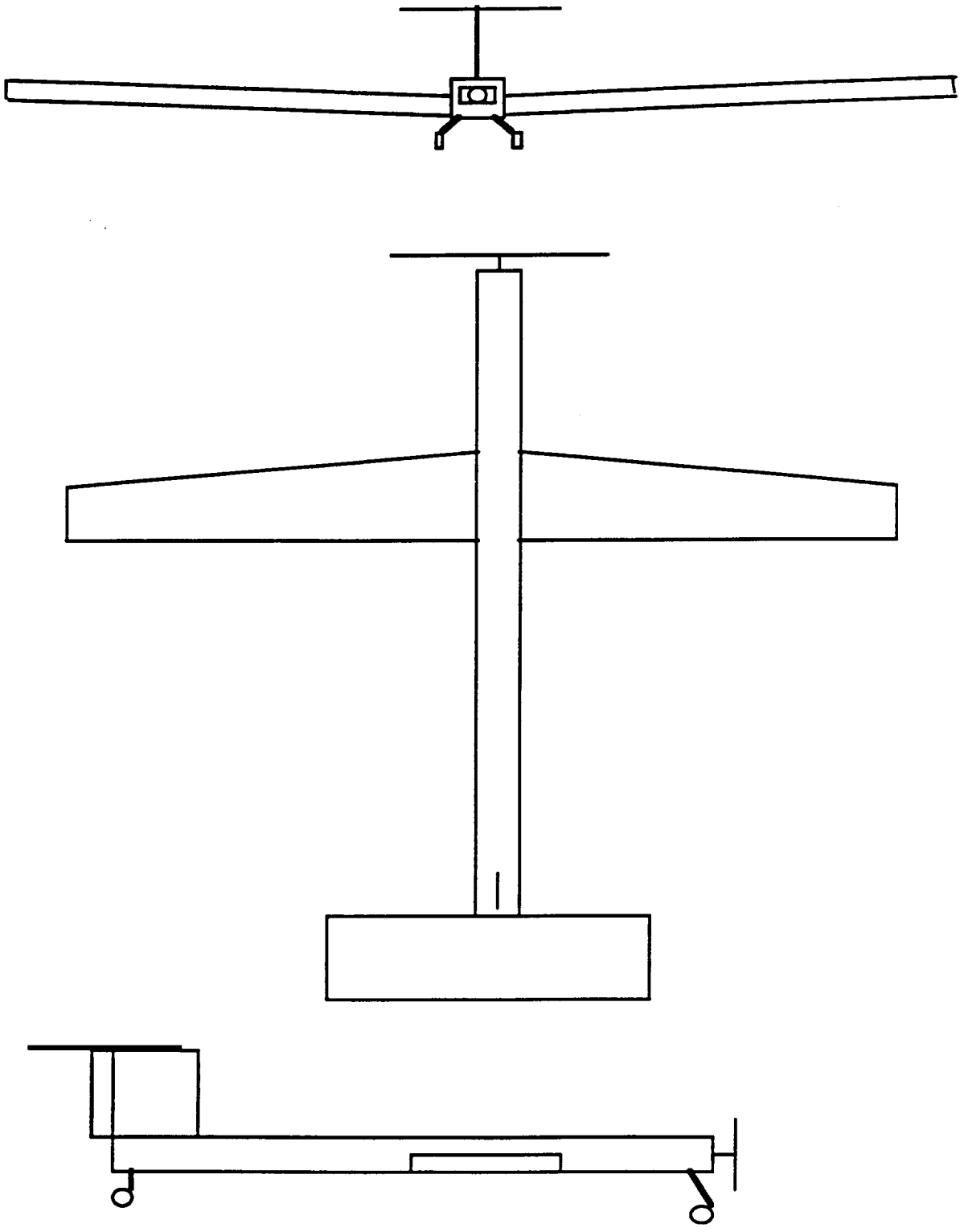

Table 3.1
Concept Evaluation

Concepts	Advantages	Disadvantages
Concept #1	-Reduced Construction Costs -Landing Stability -Less Operational Cost	-Increased Drag -Increased Wing Weight
Concept #2	-Extra Lifing Surfaces -Decreased Downwash Effects	-Increased Weight -Increased Construction Costs
Concept #3	-Decreased Downwash -Decreased Drag	-Increased Construction Costs -Empennage Structural&Control Difficulties

3.4 Final Concept

The *Prime Mover* took on a concept similar to that of the first concept. The wing is mounted above the fuselage in order to maintain a continuous cargo area. The high mounted wing is inherently stable and reduces the size of dihedral angle necessary to control the aircraft. A larger dihedral angle must be complemented with a larger wing area to produce the equivalent lift. This would result in a heavier wing. However, the actual area increase is fairly small.

Exodus decided to use a polyhedral wing in place of a dihedral wing. The advantages of the dihedral are used without subjecting

the wing juncture to the high bending moments located at the root of the wing. Lift of the Exodus *Prime Mover* is made comparable to that of a tandem design by using a large wing area.

The wing planform is rectangular in order to decrease the construction hours and cost. For the same reason, the empennage will consist of flat plate stabilizers located on top of the aircraft.

The *Prime Mover* will implement a single forward mounted engine and tail dragger landing gear. Exodus feels this design will fully meet the requirement and objectives of a profitable overnight delivery service.

4.0 Aerodynamic Design Detail

4.1 Airfoil Selection

The process of selecting an airfoil began with the determination that the airfoil must demonstrate good characteristics at low Reynolds numbers in the estimated range of 150,000 to 200,000. Airfoils in this category were then judged on three design criteria: lift, drag, and geometry of the airfoil. An optimal airfoil design for our aircraft has a high C_{lmax} at a large stall angle and gradual stall characteristics, minimum drag, flat bottom and thick trailing edge. The geometric characteristics were identified as important because they result in less construction time, and therefore reduce production costs. Four airfoils that best fulfilled the design criteria were selected from reference 7 for closer examination. These airfoils included the Wortmann FX63-137, Clark-Y, S3010, and the SPICA. The merits of each airfoil are listed in Table 2.1.

Merits of Selected Airfoils

Airfoils	Merits
Wortmann FX63-137	High C_{lmax}, High lift curve
Clark-Y	Thick trailing edge
S3010	Low Cdo
SPICA	Large a_{stall}, Flat bottom

The Wortmann FX63-137 has the highest Clmax of 1.6 at a stall angle of 12 degrees but the cambered airfoil with the thin trailing edge would be difficult to duplicate and especially difficult to monokote, thus greatly increasing production costs. The Clark-Y has a relatively flat bottom and the thickest trailing edge of the four airfoils examined. However, the airfoil's lift characteristics are poor for it has a C_{lmax} of only 1.2 and stalls at an angle of 10 degrees. The S3010 airfoil has lower drag at zero lift than the other airfoils with

lift characteristics similar to the Clark-Y. Also, the bottom is not as flat as the Clark-Y and the trailing edge is thin.

The SPICA airfoil was selected primarily for economic reasons. Its flat bottom and relatively thick trailing edge as shown in Figure 4.1 make machining and handling easier, and therefore reduce production costs. In addition, the airfoil produces high lift coefficients with a C_{lmax} of 1.45 at a Reynolds number of 151,000 and stalls at an angle of 14 degrees as illustrated in Figure 4.2. The large stall angle is important so that the wing may be mounted at an incidence angle for increased lift at cruise with an adequate margin of safety. The airfoil exhibits gentle stall characteristics. However, the airfoil has high drag at low lift coefficients with a C_{do}=.03. The SPICA airfoil was selected despite this fact due to the early determination that production costs were 90% of the total cost of an aircraft. It is important to note that greater consideration would have been given to the high section drag coefficients had the actual 73% fuel costs been realized earlier.

Figure 4.1
SPICA Airfoil

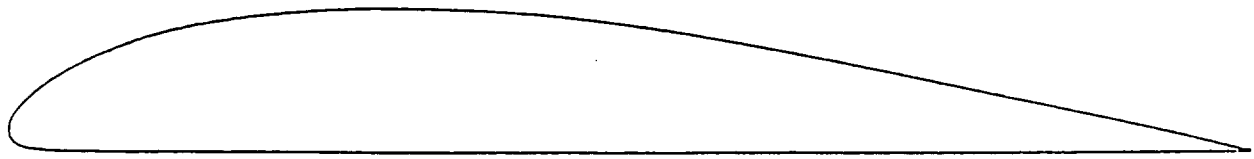

Thickness 11.70% Camber 4.75%

4.2 Wing Design

Once the airfoil was selected, the aerodynamic analysis focused on the design of the wing. The goal was to design a cost effective wing that provided sufficient lift during take-off, cruise, and landing with minimum drag. The design parameters for the wing included the planform area, aspect ratio, taper, twist, and sweep.

Difficulties in constructing a tapered wing and a wing with twist would greatly increase construction time and costs as well as the possibility of wing warp, and therefore were not considered in the design process. Also, sweep was not considered since the aircraft was designed to fly at a low cruise speed of 30 ft/s and decreasing the effective velocity along the wing was undesirable. Therefore, a rectangular planform was selected for the wing and an analysis was conducted to determine the wing dimensions that provide optimum performance.

The SPICA airfoil exhibits desirable characteristics for Reynolds numbers between 150,000 and 250,000. Thus, chord values ranging from 10 inches to 14 inches were selected. Given an estimated planform area of 9.5 square feet, based on minimum take-off requirements for a weight of 6.5 pounds and C_{Lmax} of 1.18, the range of corresponding spans was 6.97 feet to 13.68 feet. These dimensions resulted in a range of aspect ratios from 7 to 13 to be examined. The effects of varying aspect ratio on the drag polar, lift-to-drag ratio, and lift curve slope are illustrated and explained in Appendix A. The aerodynamic analysis revealed that a larger aspect ratio is desired to decrease induced drag, increase the maximum lift-to-drag ratio, and increase the lift coefficient for a given angle of attack. Minimizing drag decreases the amount of fuel required for flight, and therefore minimizes the operating expense. The maximum lift-to-drag ratio signifies that the aircraft is flying most efficiently and expending the least amount of fuel. A large lift coefficient at a small angle of attack is desired so that an adequate margin of safety exists between the angle of incidence and the stall

angle. However, increasing the aspect ratio also increases the weight of the wing.

Another important measure of merit is a minimum ratio of wing weight to lift. Minimizing the wing weight ensures that fuel is spent lifting the greatest percentage of cargo weight, thus maximizing the revenue earned each flight. Since the required lift of the wing is defined as the overall weight of the aircraft, our goal is to reduce the bulk of the wing while minimizing the induced drag that the wing develops at cruise conditions. However, these two objectives are contrary.

As can be seen in the drag equation, $C_D=C_{Do} + C_L^2/\pi eAR$ (Ref 1), the wing's effect on drag can only be diminished by increasing the aspect ratio and/or increasing the wing efficiency, since the parasite drag and lift coefficient are effectively defined by the aircraft's total weight for a given a planform area and cruise speed. In order to achieve a maximum efficiency, the wing must be tapered, which would necessitate the construction of many different rib sizes and would significantly increase construction costs as stated previously. A more effective means of reducing drag is to increase the aspect ratio. However, since the effective lift force on higher aspect ratio wings is further from the fuselage, the bending moment at the root, and therefore the stress on the wing structure, is greater for higher aspect ratio wings. In order to accommodate this increased stress, the structure of the wing must be reinforced, making it heavier. As a simple model of this trade-off, the wing was modeled as the minimum rectangular spruce spar necessary to maintain a load factor of 2.5. Figure A.4 in Appendix A relates the approximation of the relation between wing weight and drag as the aspect ratio varies. This study determined that an aspect ratio of approximately 9.5 provides the desired aerodynamic characteristics at an acceptable spar weight.

A polyhedral wing configuration was designed to minimize the weight of the wing by utilizing continuous members across the fuselage and lighter joints near the tips. The polyhedral configuration functions like a dihedral wing by allowing the *Prime Mover* control authority without the additional weight and cost of

ailerons. For ease of construction, the wing is divided into three sections with a 3.89 foot middle section and two 3 foot additions mounted at a 17 degree angle. This results in a 9.62 effective span and, with a one foot chord, a 9.62 effective planform area. Therefore, the effective aspect ratio is also 9.62.

The two-dimensional lift curve slope for the airfoil was corrected for three-dimensional effects using the relation $dC_L/d\alpha = a_0/(1+57.3a_0/\pi eAR)$ where a_0=.0906/degree was determined from the lift curve slope for the two-dimensional airfoil (Ref 1). The efficiency factor was estimated to be .746 for an aspect ratio of 9.62. This value was determined by averaging the efficiency factors obtained from the two methods outlined in Appendix B. The lift curve slope for the wing is illustrated in Figure 4.3. Based on the given stall angle of the airfoil, the maximum lift coefficient was conservatively estimated to be 1.18. The lift coefficient required for cruise conditions was calculated to be .65 using the relation $C_L=2W/\rho V_\infty^2 S$ where the lift equals the weight of the airplane during steady, level flight (Ref 1). Therefore, the wing will be mounted at a 7 degree angle of incidence to provide sufficient lift. An additional concern was tip stall. The change in angle of attack for the outboard wing sections may be approximated as $\Delta\alpha=B\Gamma$ (Ref 6). At maximum yaw angle of 10° and effective dihedral angle of 13.6°, one wing tip will at +2.3° while the other will be at -2.3° in reference to the center wing section. In a steady, level turn the maximum total angle of attack is 9.3°, an angle well below the stall angle.

The variation of the lift-to-drag ratio is illustrated in Figure 4.4. The maximum lift-to-drag ratio is 17.80 at an angle of attack of 8.6 degrees. During cruise, the airplane flies at a lift-to-drag ratio only 2% less than the maximum value. Thus, the *Prime Mover* will fly efficiently at cruise conditions.

Figure 4.2

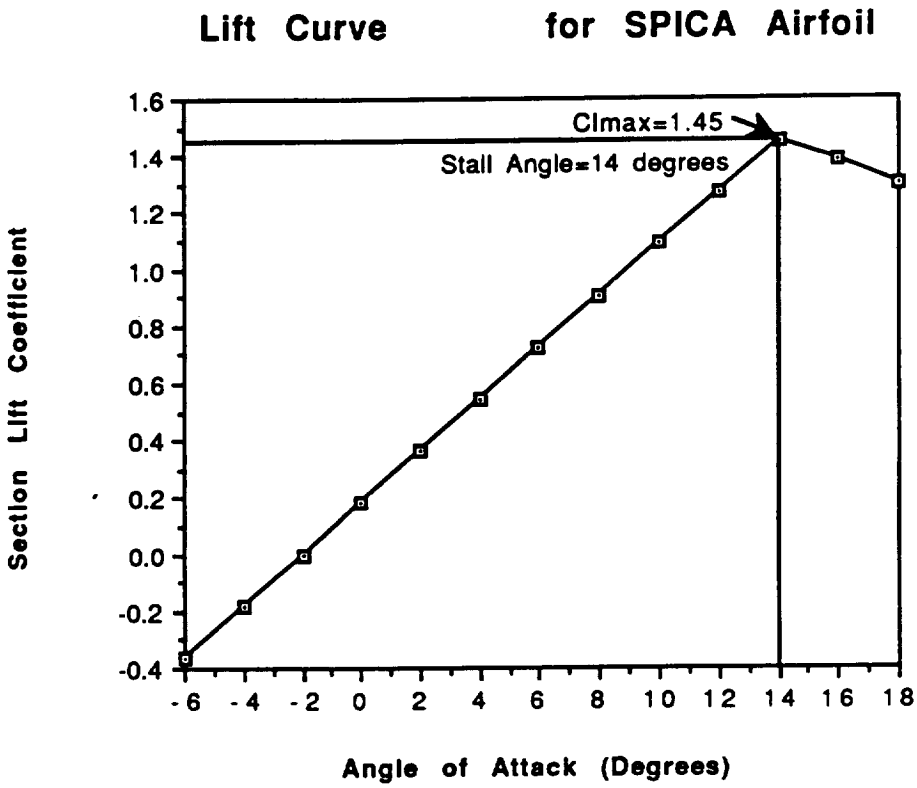
Lift Curve for SPICA Airfoil
Clmax=1.45
Stall Angle=14 degrees
Section Lift Coefficient
1.6
1.4
1.2
1.0
0.8
0.6
0.4
0.2
0.0
-0.2
-0.4
-6 -4 -2 0 2 4 6 8 10 12 14 16 18
Angle of Attack (Degrees)

Figure 4.3

Lift Curve

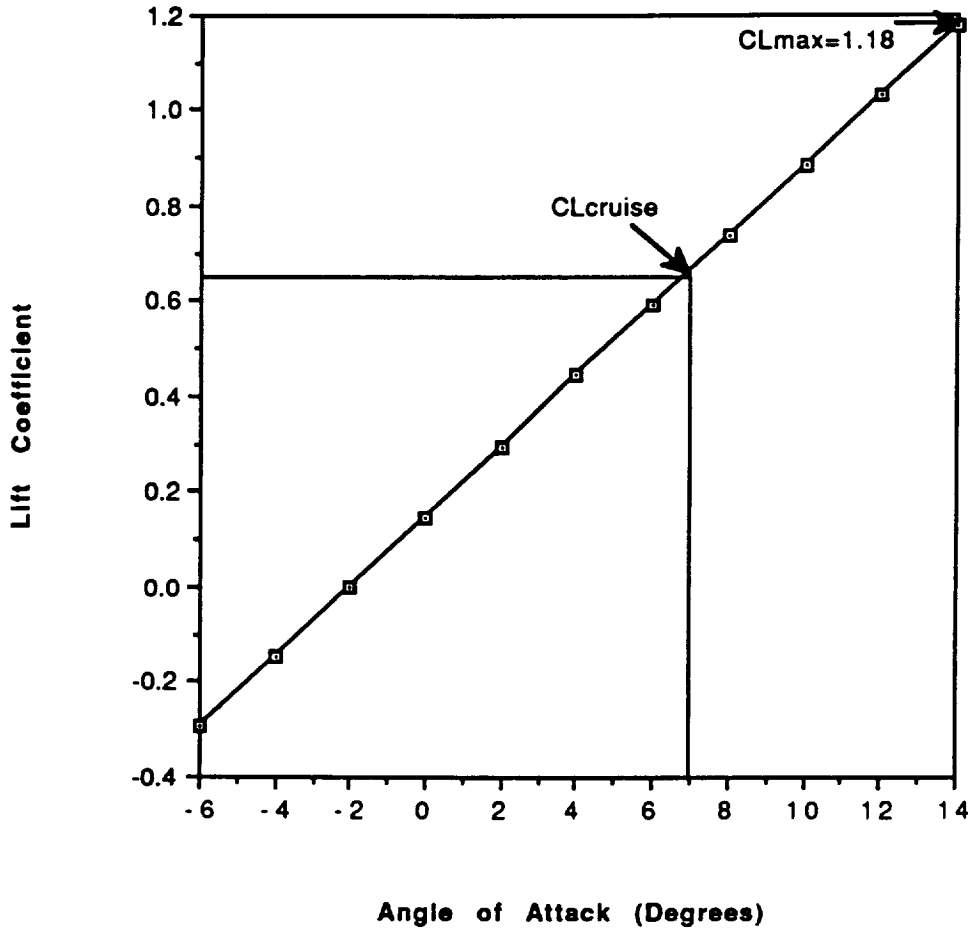

Figure 4.4

Variation of Lift-to-Drag Ratio with Angle of Attack

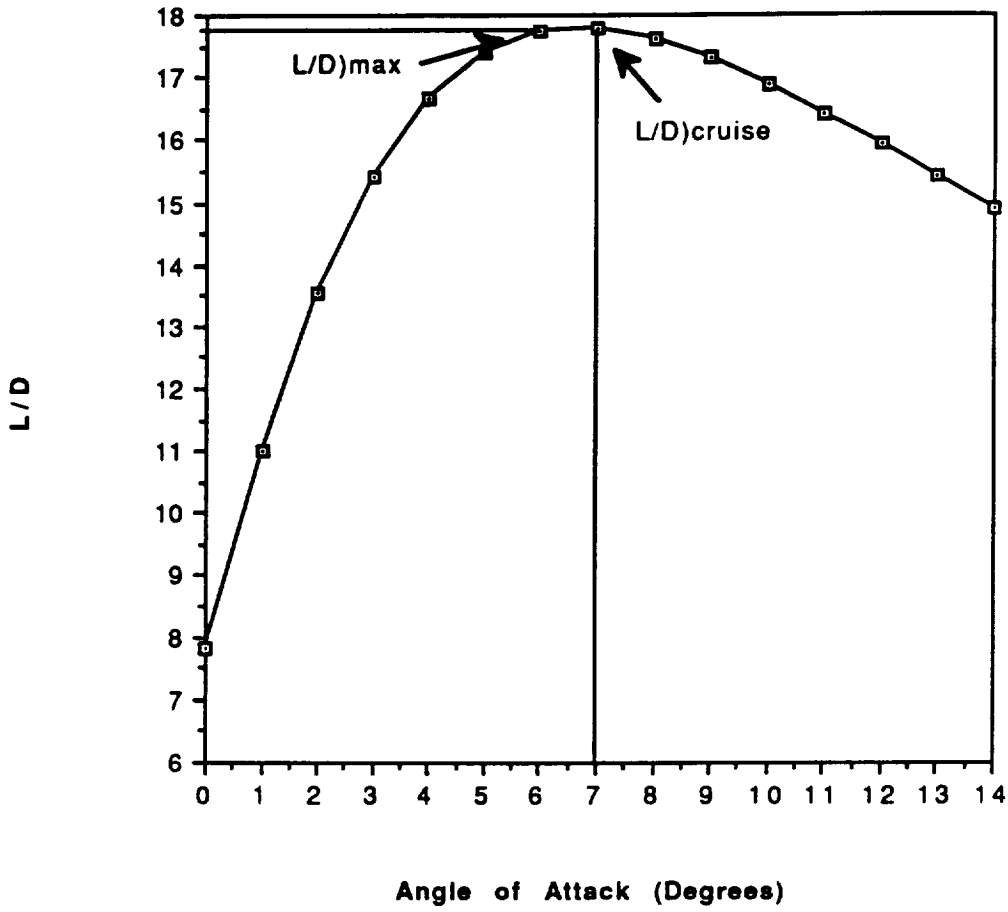

4.3 Drag Prediction

The drag for the entire aircraft was estimated using the relation for the drag coefficient $C_D = C_{Do} + C_L^2/\pi eAR$ where the first term is the parasite drag coefficient at zero lift and the second term includes both induced drag and the contribution of parasite drag due to lift (Ref 1). The method used for the estimation of C_{Do} was the drag breakdown method based on wetted surface area outlined in Jensen's thesis. The total drag was found by adding the contributions from each component according to the formula $C_{Do} = SC_fS_{wet}/S_{ref}$ where a value of C_f=.0055 was obtained from empirical data and the wing planform area was used as S_{ref} (Ref 3). See Appendix A for detailed discussion of the drag breakdown.

Given the values for aspect ratio, efficiency factor, and parasite drag coefficient the equation for the drag polar is $C_D = .0179 + .0441C_L^2$. Figure 4.5 shows the quadratic relation between the drag coefficient and the lift coefficient.

Table 4.2
Drag Component Breakdown

Component	$C_f S_{wet}/S_{ref}$
Wing	.008685
Fuselage	.004156
Horizontal Stabilizer	.001616
Vertical Stabilizer	.000769
Landing Gear	.000310
Interference	Add 5% to C_{Do}
Roughness and Proturberances	Add 10% to C_{Do}
Total C_{Do}	.0179

Figure 4.5

Drag Polar

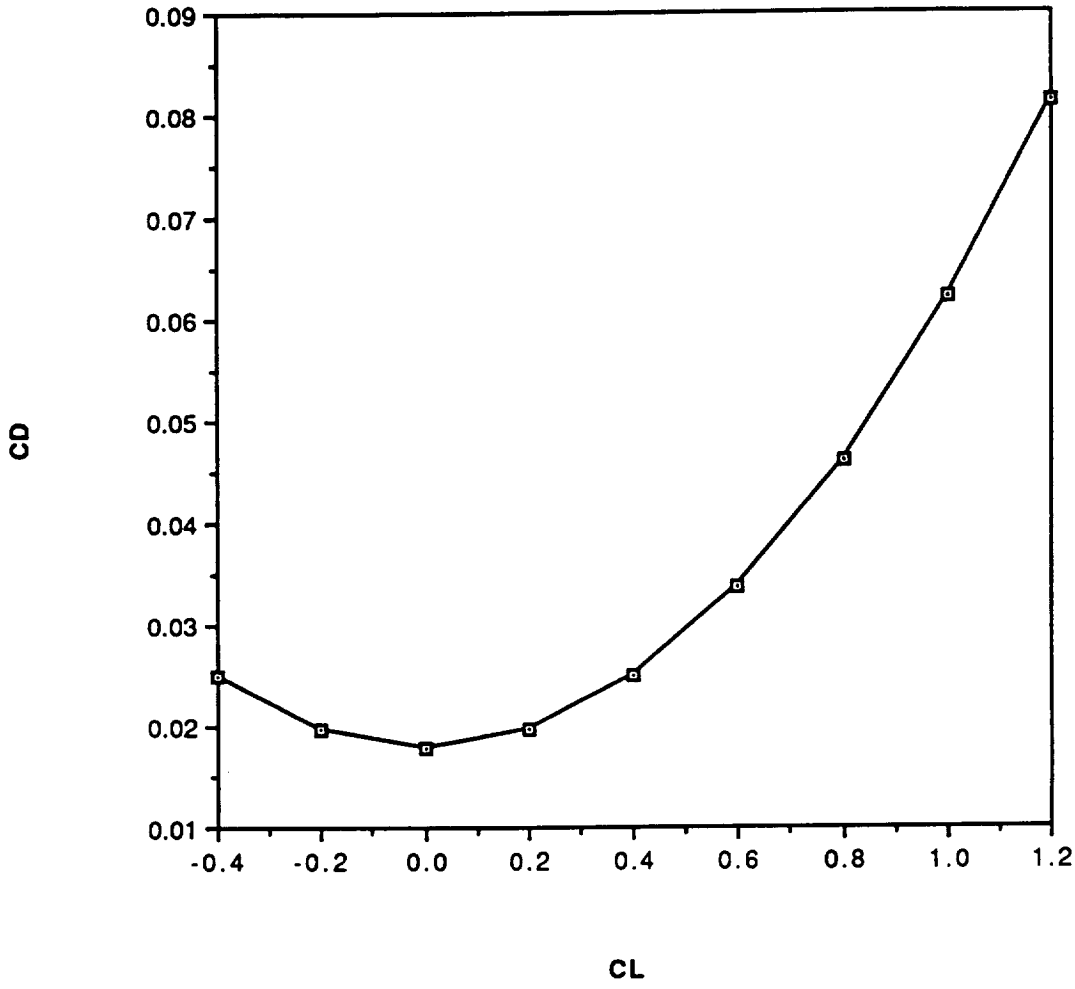

5.0 Propulsion System

5.1 System Selection and Performance Predictions

The Exodus *Prime Mover* requires a propulsion system that conforms to the following requirements:

1. Range > 8600 feet.
2. Velocity ≤ 30 feet per second.
3. Take-off distance ≤ 60 feet.
4. Cost as low as possible.

To achieve these goals, the *Prime Mover* requires a system that works well together through all portions of the flight. The first step in assembling this system was to find a motor capable of providing enough power to enable the *Prime Mover* to meet the takeoff distance requirement. At the same time, the motor needed to be as small as possible to keep the weight of the system down.

It was determined that fuel costs for the *Prime Mover* was 73% the total life cost of the aircraft. A study of current draw versus fleet life cost per volume moved showed that for every one amp increase in the current draw the fleet life cost per volume moved increased 15%. For these reasons, minimizing the fuel consumption became a prime concern for Group Exodus. The *Prime Mover*'s propulsion system consumes 86% of the total fuel per flight during cruise based upon estimates of required power (Figure 5.1). Therefore, it was decided that the studies involved in decreasing the fuel consumption would require an in-depth study of the cruise portion of the flight.

Three motors were studied, the Astro Cobalt 05, 15, and 25. By looking at designs from previous years, it was noted that most aircraft were lighter than our aircraft and used either the 05 or the 15. It was therefore assumed that the 05 would be too small for our aircraft and was ruled out immediately. The 15 was analyzed to see if it would provide enough power for take-off.

Figure 5.1
Fuel Consumption Breakdown

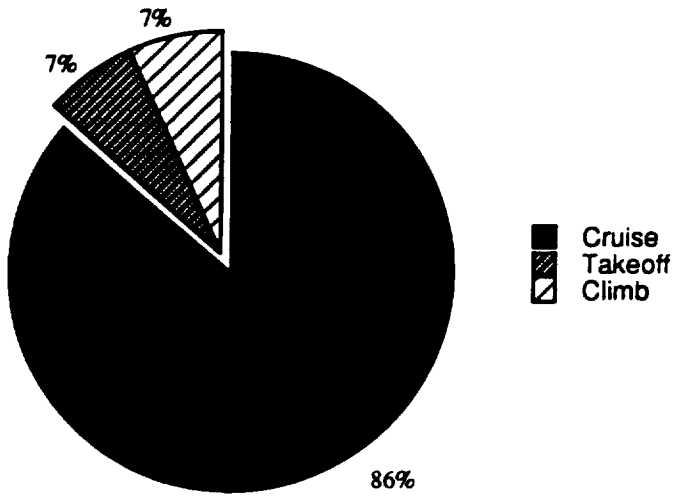

The take-off program and the TK Solver program, electric motor performance, were used for the initial study. Because the motor needed to be ordered early in the design process, the study was done with many initial guesses for the required design parameters. This study showed that the 15 would provide enough power for take-off, even if the design parameters were to change. Cruise conditions were not a concern since there was more than enough power available from the 15. Therefore, the Astro Cobalt 15 was chosen because it provided the required power, weighed 30% less, and cost approximately 20% less than the Astro Cobalt 25.

During the take-off portion of the flight, the motor will be running at 15,192 revolutions per minute at an efficiency of .73. During climb the motor is running at 16,195 revolutions per minute at an efficiency of .75. Finally, the motor will work for the rest of the flight at the cruise condition of 11,186 revolutions per minute at an efficiency of .55. These figures were based on manufacturers specifications and computer analayses found in Appendix G. A graph of the motor efficiencies versus the rpms can be seen in figure 5.2 below.

Figure 5.2
Motor Efficiency versus RPM
Astro 15

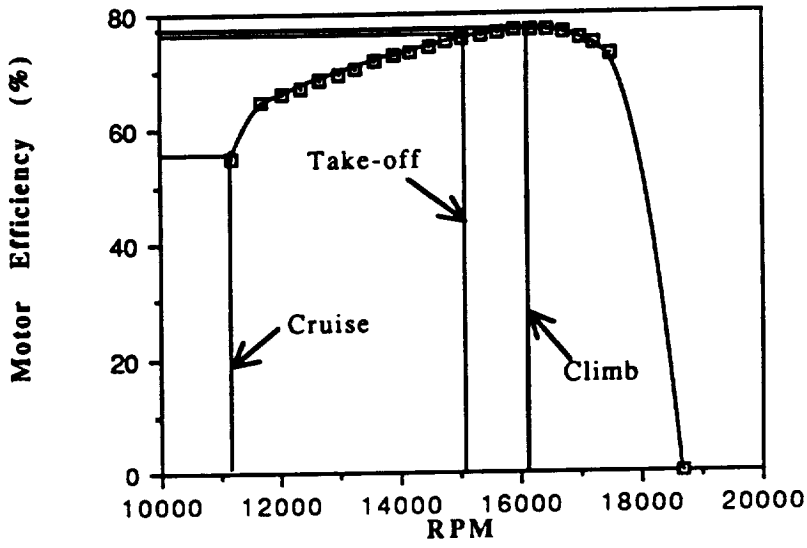

The next piece of hardware that needed to be ordered was the batteries. It was determined from the initial studies on the Astro 15 that during take-off the engine would require 14.4 volts to provide the power required. This voltage requires 12 batteries connected in series, since each battery had an individual voltage of 1.2 volts.

The next step was to determine the capacity of the batteries needed for the *Prime Mover*. The objective of Group Exodus was to have a range larger than 8600 feet, which includes diversion and loiter. For take-off and climb the motor uses a total of only 20 milliamp hours. At 30 feet per second the current draw for the motor was 4.45 amps. To cover the range of 8600 feet the motor would use a total of 354 milliamp hours, for a total of 376 milliamp hours used for the entire flight.

Since each aircraft would be making two flights a day, it was decided to use batteries with the capacity to make this round trip flight without needing to change the batteries. This would provide for a decrease in operational costs as well as a decrease in the length of time on the ground. Therefore, a battery capacity of 752 milliamp hours was needed. The nearest capacity battery to this required amount was a 1000 milliamp hour battery, which provides more than enough fuel for the *Prime Mover*.

5.2 Propeller Design

Determination of a propeller for the system proved to be a difficult task. Picking a propeller to keep the current draw during cruise as low as possible was the main task, for the reasons stated previously. The fuel consumption and total efficiency of the system was studied during this portion of the flight for different propellers. Unfortunately, it was determined that an efficient propeller for the cruise portion of the flight didn't necessarily allow the aircraft to take-off in the required distance. Therefore, a study was made of several different propellers to determine the best for the entire flight regime.

A major tool used in this selection was the propeller program written by Barry N. Young. This program predicts various performance characteristics, such as coefficient of thrust, power, and the efficiency, for a particular propeller design. This is done by use of the blade element theory which included considerations for induced velocity and tip losses, as well as lift and drag coefficient adjustments for the working Mach and Reynold's numbers. The use of this program requires the user to input specific data on the propeller, namely airfoil sections, chord, thickness, and angle of the blade at different radial positions. An example of the propeller input data and the output from the program can be seen in Appendix D. It is important to note that the airfoil section selected for this program should be the NACA44XXLOWRE because it is a low Reynold's number airfoil. The reason for this is that the propeller is working at very low Reynold's numbers, approximately 60,000 at 75% of the diameter, which can be seen on the ZingerJ 11-5 performance estimate sheet in Appendix D. It is believed that by doing this the performance predictions for the propeller will be more accurate.

This program was run for several propellers ranging in diameter from 8 inches to 12 inches and in pitch from 4 inches to 6 inches. The data was compiled onto Cricket Graph in order to obtain more information to be used in the TK Solver program, electric motor performance. An example of the input data and the rules used for the TK Solver program can be seen in Appendix E. This program requires a value for the coefficient of thrust and power for an advance ratio of

zero. This value is not available from the propeller program therefore the values had to be extrapolated for an advance ratio of zero. Once these values were found the electric motor performance was utilized to find the efficiencies and the current draw during cruise for the studied propellers. The results can be seen in Figures 5.3 and 5.4.

From this it can be seen that the best choices would have been either the 8-6 or the 10-4. Unfortunately, neither of these propellers would enable the aircraft to takeoff in the required 60 feet. Therefore, the ZingerJ 11-5 was chosen for our aircraft.

During take-off the propeller will work at an advance ratio of .2 and an efficiency of .61. During climb the propeller will increase it's advance ratio to the cruise condition of .42 and work at it's maximum efficiency of .745. This can be seen in the propeller efficiency versus advance ratio curve, figure 5.5.

Figure 5.3
Current Required at Cruise

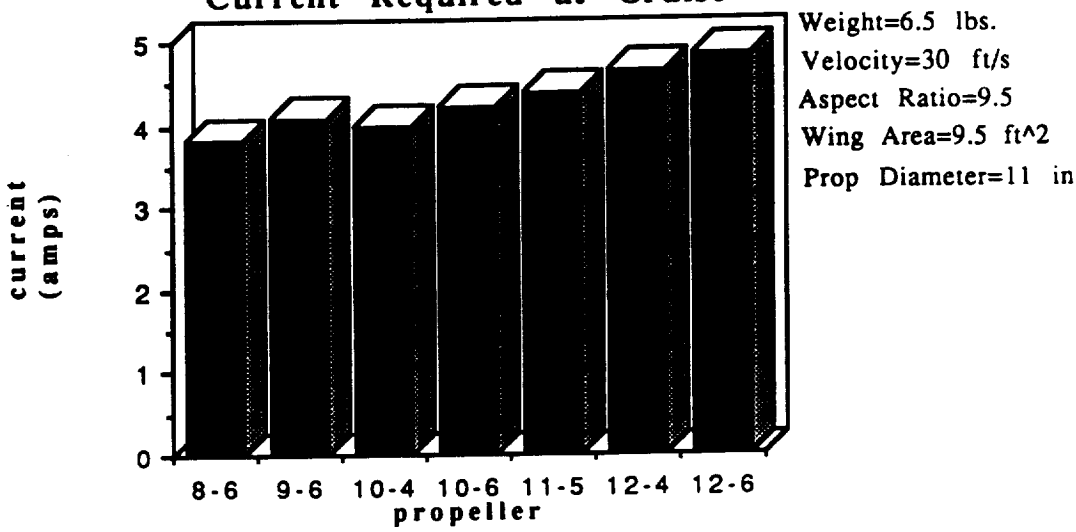

Figure 5.4
Efficiency at Cruise

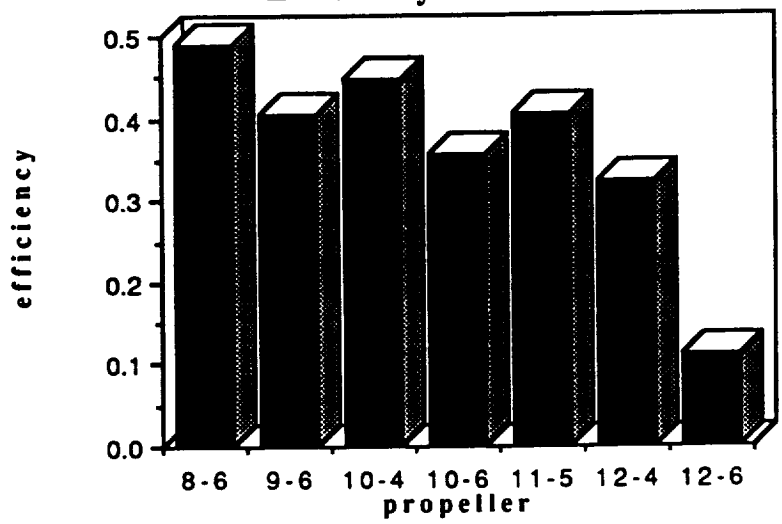

Figure 5.5
Propeller Efficiency versus Advance Ratio
ZingerJ 11-5

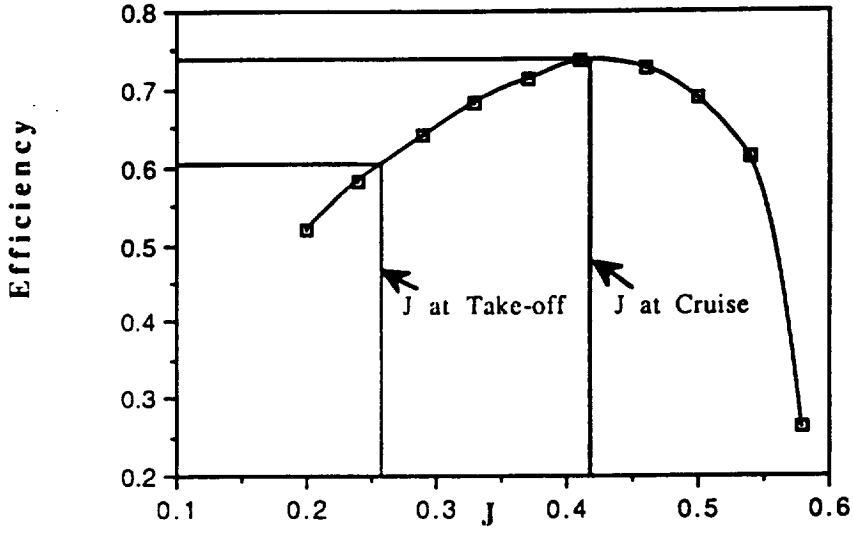

5.3 Engine Control

The motor will be controlled by the Tekin speed controller. Throughout the flight the *Prime Mover* will be operating at two different throttle settings. At take-off the *Prime Mover* will be at full throttle(14.4 volts). This results in a maximum rate of climb of 5.4 feet per second for the aircraft at a forward velocity of 30 feet per second, the *Prime Mover*'s designed cruise velocity. Once the cruise altitude is obtained the *Prime Mover* will be throttled back to 67% full throttle(9.6 volts). This information is shown on the power required and power available versus flight speed curve in Figure 5.6.

Figure 5.6
Power Required, Power Available Curve

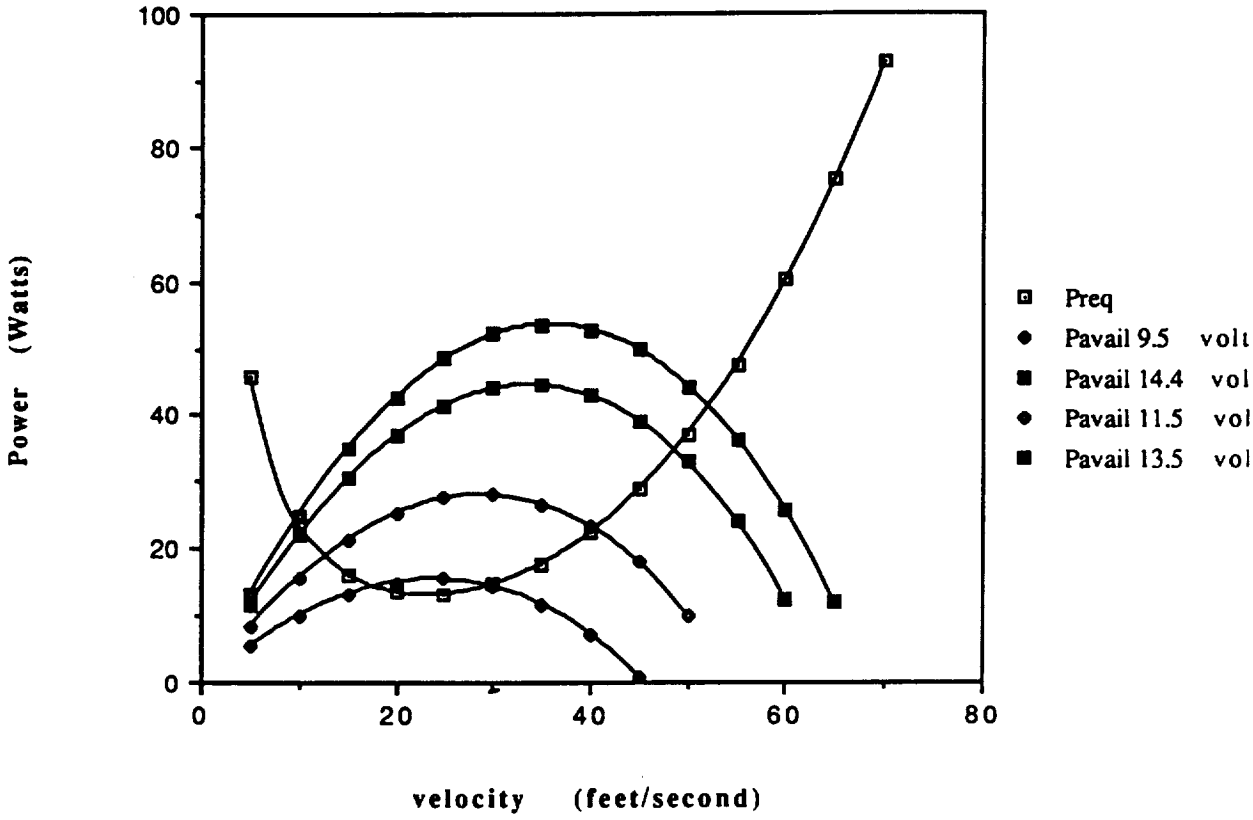

6.0 Preliminary Weight Estimation Detail

6.1 Component Weight Estimates

Based upon an economic analysis of the available Aeroworld overnight delivery market, Group Exodus set out to design a cargo aircraft capable of transporting a 2 pound payload at a velocity of 27 ft/s. A rough estimate of the airplane's total weight, 6 pounds, was obtained by extrapolating from last year's AE441 large-scale, battery-operated aircraft concepts, which were designed for smaller payloads and weighed an average of 4.6 pounds. Using this initial weight estimate, we approximated the weights of the various components to verify the initial guess.

Based upon the total weight, it was determined that a wing planform area of 9 ft^2 would be needed to maintain steady, level flight at cruise conditions with an estimated C_L of .8. From this planform area, an estimate of the wing weight was made based upon a linear extrapolation of the densities of previous wings. As is shown in Table 6.1, the densities of previous wings (wing weight/planform area) vary between .01 and .026 oz/in^2. Since the chord was estimated at 1 foot, we felt that the wing of the Behemoth Apteryx, which was slightly overdesigned, would be most like our wing design. With a few technological advances, we felt that we could design a wing of roughly twice the span at the same density, .011 oz/in^2, for a total wing weight of about 14.5 ounces.

Table 6.1

Wing Density of Existing Aircraft

Aircraft	S (sq in)	Weight (oz)	Density (oz/in2)
Behemoth Apteryx	840	9	.011
Pale Horse	1010	17.6	.017
El Toro	1000	12	.012
Initial Guess	1000	10	.010
Valkyrie	1440	37	.026
Nood Rider	842	11.5	.014

The weight estimate of the fuselage was determined in a similar manner as the wing weight. Since it was desired that the interior of the cargo bay to house a line of 4 inch boxes, the exterior dimensions of the fuselage were estimated at 4.5" x 4.5" x 60". The fuselage of last year's Initial Guess had about the same cross-section, and weighed 11.8 oz. for a 51 inch length. Scaling its weight for our 60 inch fuselage, an approximate fuselage weight of 14 ounces was obtained.

In choosing a propulsion system, it was noticed from the engine specifications that there is a large weight penalty when upgrading from an Astro 15 to an Astro 25; therefore, it was an objective to stay with the lighter Cobalt 15 engine. For the initial weight estimate of the *Prime Mover*, the avionics and propulsion system weight estimates provided in the spec sheet were used.

Finally, since the empennage and landing gear contribute so little to the overall aircraft weight, a very rough estimate on the weights of these components was made based upon comparable components utilized in previous aircraft. These weights, along with the weight estimates and c.g. locations of all of the other components of the *Prime Mover*, are listed is Table 6.2a. From these approximate component weights, the total weight estimate of the *Prime Mover* came to about 6.8 lbs. Since this figure is slightly higher than the initial estimate, the wing area was increased to about 9.5 ft^2 with a weight of 15 oz. These initial weight and location estimates are very close to the actual figures for the technology demonstrator (Table 6.2b), which weighed only 6.7 pounds when fully loaded.

Table 6.2a

Weight Estimates and C.G. Locations of Aircraft Components

Component	Weight (oz)	x position (in)	y position (in)	z position (in)
fuselage	14	-30	0	0.1
engine	10.25	-2	0	0
empennage	5	-57	0	4.5
Landing Gear (front)	5	-3.5	0	-7
Landing Gear (rear)	2	-58	0	-3
Cargo	32	-30.75	0	0
receiver	0.95	-4.95	0	-0.5
servos	1.2	-4.95	0	1.25
system battery	2	-4.95	0	-1.5
speed controller	1.8	-4.95	0	0.5
wing (left)	7.5	-32.25	30	6
wing (right)	7.5	-32.25	-30	6
battery 1	10.02	-49.5	1	2.5
battery 2	10.02	-49.5	-1	2.5
total weight	109.24			

Table 6.2b
Final Weights and C.G. Locations of Aircraft Components

Component	Weight (oz)	x position (in)	y position (in)	z position (in)
fuselage*	16.9	-31.8	0	0.1
engine**	10.25	-3	0	0
empennage	2.8	-58.5	0	4.5
Landing Gear (front)	4.6	-19	0	-5
Landing Gear (rear)	1	-59	0	-4.5
Cargo	32	-32	0	0
control package***	6.6	-9	0	0
wing (left)	4.6	-32	38	7.6
wing (mid)	6.2	-32	0	3.3
wing (right)	4.6	-32	-38	7.6
battery 1	9	-51	1	3
battery 2	9	-51	-1	3
total weight	107.55			

* includes two control rods and 4 ft battery cable (2 oz total)
** includes geared engine and propeller
*** includes receiver, servos, system battery, and speed controller

6.2 Center of Gravity Location and Travel

The center of gravity of the *Prime Mover* is located 1.2 inches above the centerline of the fuselage and 30.5 inches behind the propeller (Figure 6.1). Due to the placement of the batteries atop the rear fuselage, the center of gravity of the *Prime Mover* is practically independent of cargo weight.

Figure 6.1
Position of the Center of Gravity

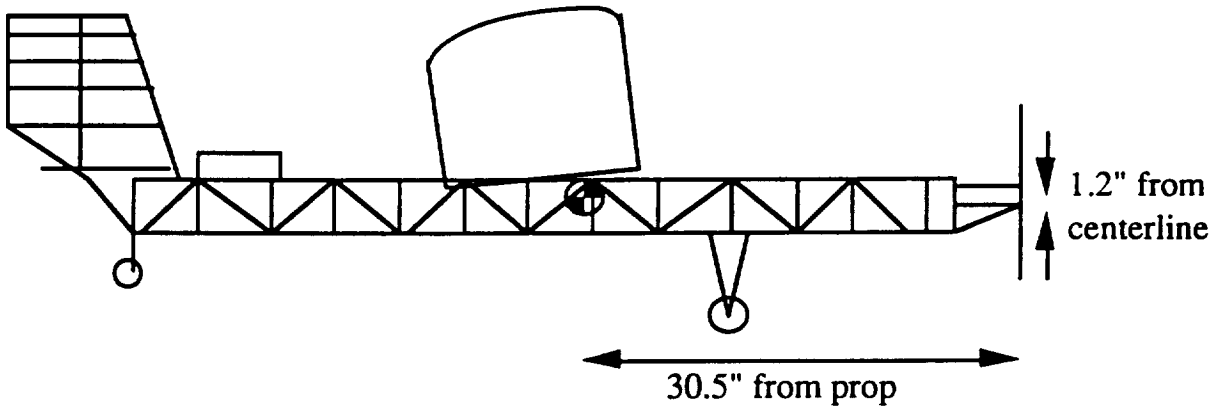

As shown in Figure 6.2, for the range of possible cargo densities, the center of gravity of the entire aircraft deviates only 1% of one chord length. Since the *Prime Mover* possesses a continuous cargo bay, the C.G. of the cargo can be held effectively constant by judicious placement of cargo. The center of gravity may move from design conditions more significantly, however, due to errors in component weight estimates; yet, as can be seen in Figure 6.2, this off-design performance accounts for a C.G. movement of at most 8% of one chord length.

Figure 6.2

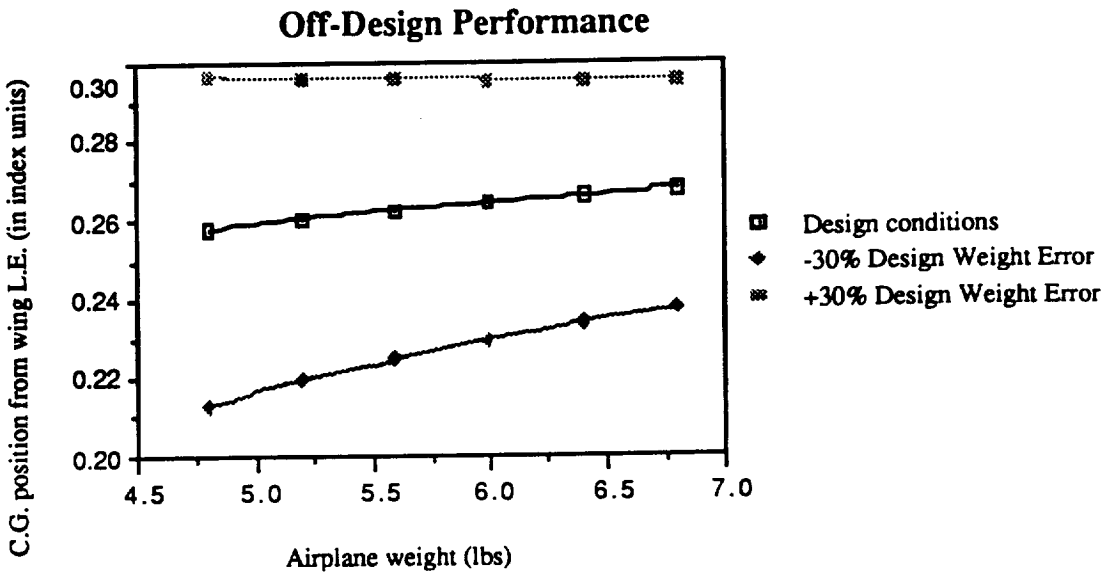
Off-Design Performance
C.G. position from wing L.E. (in index units)
0.30
0.28
0.26
0.24
0.22
0.20
4.5
5.0
5.5
6.0
6.5
7.0
Airplane weight (lbs)
Design conditions
-30% Design Weight Error
+30% Design Weight Error

7.0 Stability and Control

Stability can be divided into three major areas of concern: longitudinal, directional, and roll stability.

7.1 Longitudinal Stability

For an aircraft to have longitudinal static stability, the pitching moment curve must have a negative slope (ie $C_{m\alpha} < 0$). Appendix F.1-F.3 shows the contribution of each component and the assumptions involved. The neutral point of the aircraft is where $C_{m\alpha} = 0$. It is defined by:

$$X_{np}/c = X_{ac}/c - C_{m\alpha f}/C_{l\alpha w} + \eta_h * V_h * C_{l\alpha h}/C_{l\alpha w} * (1 - d\varepsilon/d\alpha)$$

The static margin is a measure of the degree of stability and is defined by:

$$\text{Static Margin} = X_{np}/c - X_{cg}/c$$

The larger the static margin, the more stable an aircraft will be. Through an analysis of similar aircraft from previous years, it was determined that a static margin of approximately 15% should allow safe flight without requiring large control inputs for maneuvering. The static margin values for typical aircraft are between 5° and 10°. The reason for the higher values for this type of aircraft is the larger response time needed by a remote pilot.

There are many factors that effect longitudinal stability, but only a few which are not set by other requirements. These are:

1. Center of Gravity (CG) location
2. Wing Position
3. Horizontal stabilizer incidence angle
4. Horizontal stabilizer moment arm
5. Horizontal stabilizer area/aspect ratio

The CG location plays a major role in longitudinal stability. The more the CG travels, the more the handling characteristics of the *Prime Mover* will vary. In order to reduce this variation, the battery CG was used to make the *Prime Mover* CG approximately independent of payload. Therefore, the CG location, though not set by requirements outside of stability and control, was set to limit the variation in handling characteristics of the *Prime Mover.* The amount of CG travel between full and empty payload cases is only one tenth of an inch. A graph of Static margin versus CG for the *Prime Mover*'s forward and aft CG limits is shown in figure 7.1 (please note that inches from the leading edge should read inches aft of the leading edge). It can be seen that static margin is strongly influenced by CG location. The arrows on this and all figures in this section represent the present design values.

FIGURE 7.1
Effect of CG Travel on Static Margin

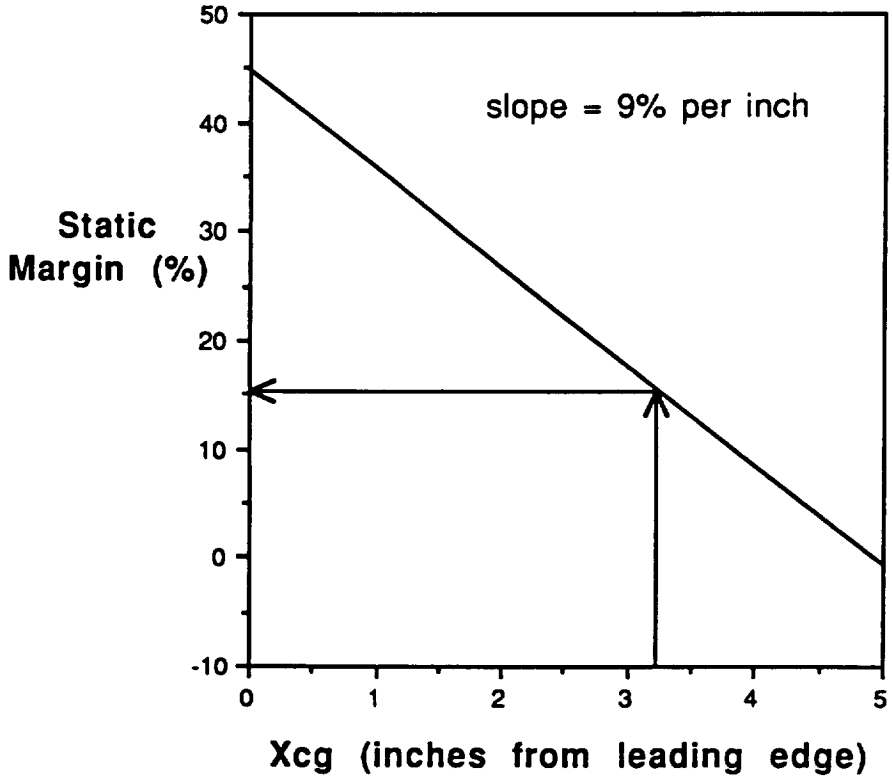

As mentioned earlier, the angle of attack of the fuselage reference line and horizontal stabilizer incidence angle are both desired to be zero at cruise in order to reduce drag. Assuming this, for the aircraft to be in equilibrium during cruise, the wing lift force and pitching moment should be balanced to result in zero moment about the CG. Altering the wing position is very useful in controlling this condition. Appendix F.4 shows how the wing position was set. The CG position was determine as described above and the coefficient of lift and chord were set by cruise conditions. However, there was no data for Cm_{ac} for the SPICA airfoil. It was observed that symmetric airfoils have Cm_{ac} values of zero and cambered airfoils have Cm_{ac} values proportionate to the amount of camber. It was also observed that the more camber, the more negative the value of the $\alpha_{cl=0}$ on the lift curve slope. Combining this information, it was assumed that the SPICA would have a similar Cm_{ac} as an airfoil that has the same $\alpha_{cl=0}$. Therefore, Cm_{ac} was assumed to be -.05. The resulting wing position placed the aerodynamic center at 30% chord point. This is in agreement with traditional conventional aircraft.

A higher angle of incidence of the horizontal stabilizer creates more drag at cruise cruise conditions. To avoid this unnecessary drag, it was desired to have the horizontal stabilizer attached at zero angle of incidence. This would also make construction simpler, hence reduce the construction hours and cost. However it was not possible to have the tail at zero angle of incidence. The angle of incidence for the horizontal stabilizer was set at +5°. The reason for the large angle is directly related to the small moment arm which will be discussed next.

As the horizontal stabilizer moment arm increases, the effectiveness of the horizontal stabilizer increases, hence the smaller the horizontal stabilizer area required to have the same effect. The smaller horizontal stabilizer reduces both drag and weight. Therefore, the horizontal stabilizer was placed as far aft as possible on the fuselage. Since the CG is so far aft on the fuselage, the moment arm is small

relative to the size of the fuselage. This will be a major hindrance in the design process.

The stability of an aircraft can be increased by increasing the horizontal stabilizer area; however, if the horizontal stabilizer is too large it will require a large elevator or elevator deflection to achieve CLmax. Flying at Clmax allows the aircraft to fly at the slowest possible speed (V_{stall}) making landing easier. Horizontal stabilizers with higher aspect ratios are more effective. Large bending moments associated with higher aspect ratios arise because the horizontal tail is a simple flat plate and offers only small amounts of stiffness about the roll axis. The sensitivity of Static Margin to horizontal stabilizer area and aspect ratio is shown in figure 7.2. The *Prime Mover* has a horizontal tail area of 1..44 ft^2 and an aspect ratio of 3.25. This results in a static margin of 15.6%.

FIGURE 7.2
Effect of Horizontal Tail Area and Aspect Ratio on Static Margin

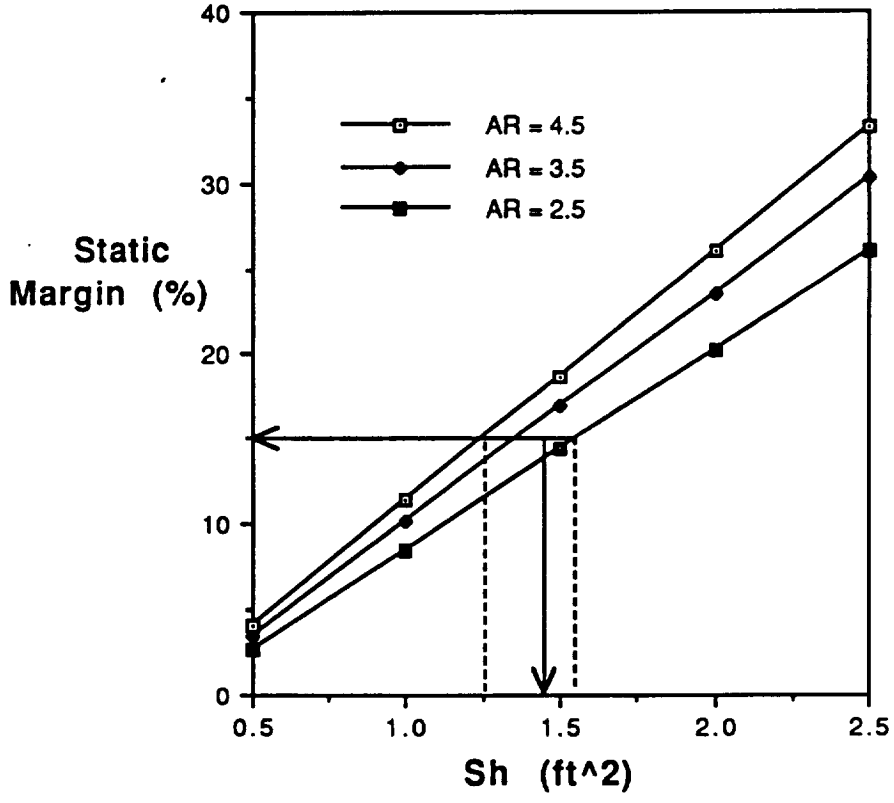

The elevator was sized to allow achievement of CLmax. The deflection angle was limited to +/- 15°. This is because large deflection angles result in high drag. Using an elevator size equal to 18.75% of the horizontal tail area, a graph of Cm versus α for maximum elevator deflection is shown in figure 7.3. Since the CG travel is basically zero, there are no real forward and aft limits for the CG. As long as the Cargo Cg is placed at the center of the cargo bay, the overall CG of the *Prime Mover* will be the same. From this it can be seen that an elevator deflection of 12° will provide the *Prime Mover* with Clmax. Figure 7.1 can be used to determine the allowable limits on CG motion. The limits are set by the neutrally stable condition (SM = 0%) and a static margin 25%. It shows a 2.7 inch CG travel, however, the *Prime Mover* will want to maintain a tolerance of 0.5 inch to maintain adequate handling qualities. This represents the stupidity tolerance of the *Prime Mover*, since it will only be of concern if the cargo is loaded improperly. The elevator will be controlled by a servo in the avionics compartment. The control cables will run along the sides of the cargo bay.

FIGURE 7.3
Pitching Moment versus Angle of Attack
(of the Fuselage Reference Line)

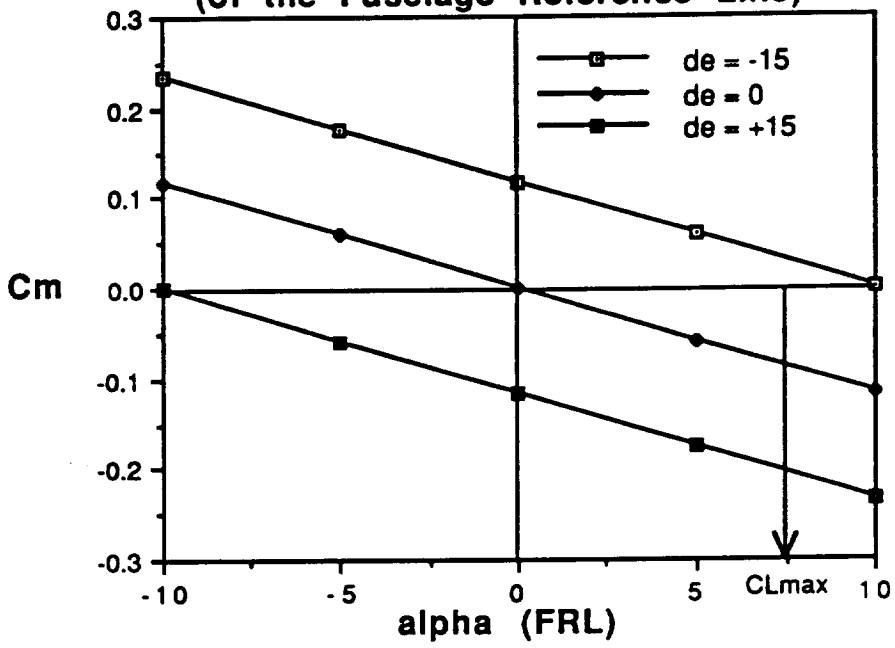

7.2 Directional Stability

For an aircraft to have directional static stability, it must have a positive yawing moment curve slope (ie CnB > 0). The main contributors to CnB are the fuselage and the vertical stabilizer. Appendix F.5-F.6 show how each component's contribution was determined.

The important parameters for directional stability that were not set by other considerations are:

1. vertical stabilizer moment arm
2. vertical stabilizer area/aspect ratio

Vertical stabilizer moment arm was desired to be as large as possible to reduce the size of the required vertical stabilizer, thus reducing drag and weight. Therefore, it was placed as far aft as possible. Again, the relatively short moment arm of the *Prime Mover* adds difficulty to the design.

Large vertical stabilizer area increases weathercock stability. However, if the vertical stabilizer is too large it will have a problem with large control input requirements analogous to the large horizontal stabilizer. The vertical stabilizer aspect ratio increases the effect of the vertical stabilizer, but is limited by structural concerns.

7.3 Roll Stability

For an aircraft to have roll static stability, it must have a negative banking moment curve slope (ie ClB < 0). The main contributor to ClB is effective dihedral angle (EDA). ClB was calculated by the method shown in Appendix F.7.

Since the *Prime Mover* is employing a rudder/dihedral combination, as opposed to ailerons, to meet the turning requirement, it will require a large EDA. Therefore, EDA selection was driven by the turning requirement instead of stability. At the design cruise velocity, and assuming a 25°/second roll rate, the *Prime Mover* requires 13.2° EDA, which results in a 17° panel dihedral since the *Prime Mover*'s break point is at 40% of the span (appendix F.8). Using this information, the *Prime Mover* would require a 10° yaw angle to meet the turning requirement (appendix F.9). The rudder was sized to be able to achieve a 10° yaw angle. The deflection angle was again limited to +/- 15° for

the same reasons. A graph of Cn versus B (figure 7.5) for a rudder area of 56.7% of the vertical tail area shows that a rudder deflection of 15° will satisfy the turning requirement. The rudder will also be controlled by a servo located the the avionics compartment, with a cable running along the sides of the cargo bay.

FIGURE 7.5
Yawing Moment versus Yaw Angle

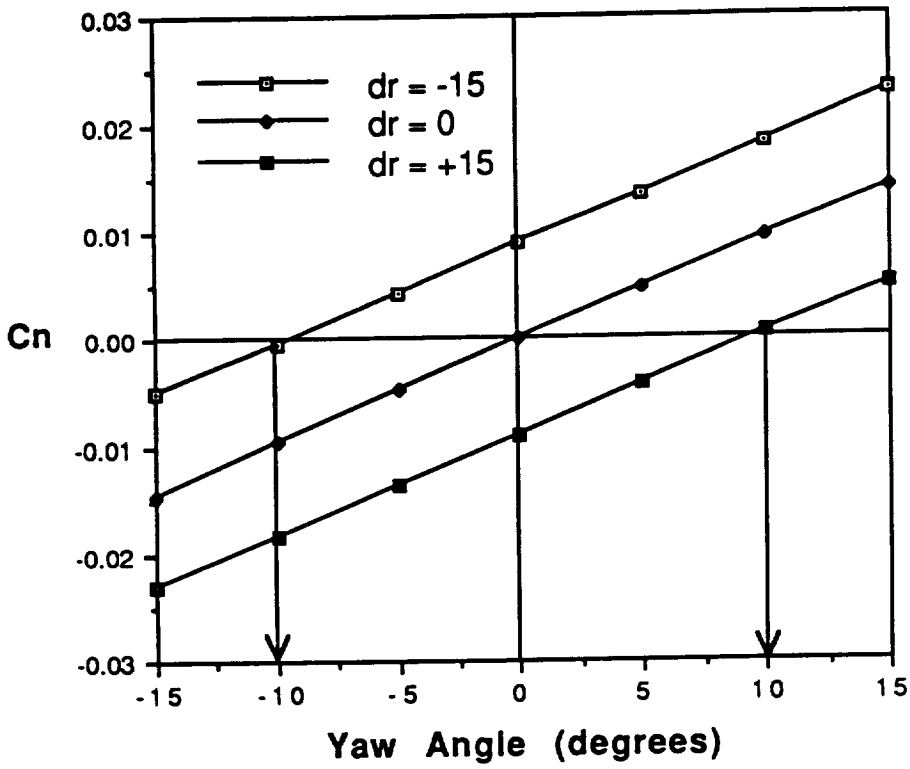

8.0 Performance Estimations

8.1 Take-Off and Landing Estimates

Estimation of take-off performance was a complicated yet crucial task that became the determining factor in the sizing of the aircraft components. The take-off analysis began with the use of a computer code, listed in Appendix G. Following the selection of the motor and batteries, it was determined that the most influential specification on take-off distance was the propeller type. To insure realistic values of the propeller coefficients, corrections were made for velocity and tip losses, Reynold's number, and airfoil section. Because of the mission-set objective, requiring the *Prime Mover* to complete its take-off run under 60 feet, the propeller was limited to a minimum diameter of 11 inches. The final propeller chosen was the ZingerJ 11-5.

Once the sizing of the aircraft was complete, cargo weight and coefficient of friction were varied to test the sensitivity of take-off distance. Figure 8.1 shows the variation of take-off distance with weight and coefficient of friction. The *Prime Mover* was designed to take-off under the required distance, carrying the maximum possible cargo weight, and subject to the estimated coefficient of friction of the targeted run-ways (.15). For larger values of coefficient of friction the cargo weight need be reduced. For a more detailed explanation of the take-off calculations, see Appendix G.

Figure 8.1: Variation in Take-Off Distance with Cargo Weight and Coefficient Friction

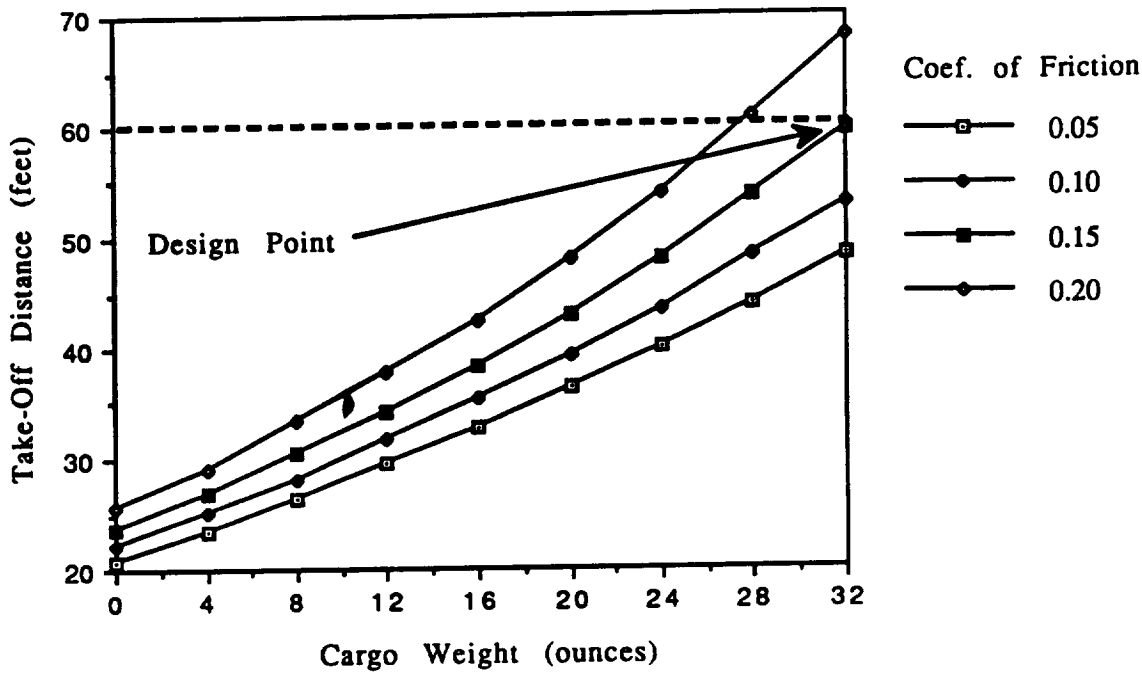

Landing distance was another important estimation. Without the use of brákes these distances can be quite large. Fortunately, the value for coefficient of friction for the run-ways was also large, helping to reduce the landing distance. Estimation of ground roll distance during landing was made with the use of the equations found in Reference 5. Exact calculations are shown in Appendix G. The landing distance for the *Prime Mover* was found to be 44 feet at maximum cargo weight, enabling landing in all targeted cities. Although no braking system will be employed during the flight test, plans for construction of brakes should be completed for manufacturing of the fleet to allow for changes in coefficient of friction.

8.2 Range and Endurance

Range and endurance estimates were found using the computer code listed in Appendix G. Figure 8.2 shows the values for range and endurance of the fully loaded *Prime Mover* varying with velocity. The final results far exceeded the mission objective of a minimum range of

8900 feet. The reason for this occurrence was due to the 1000 milliamp-hour capacity of the selected batteries. A much lower battery capacitance should have been used in order to reduce the amount of over-shoot.

Figure 8.2: Range and Endurance

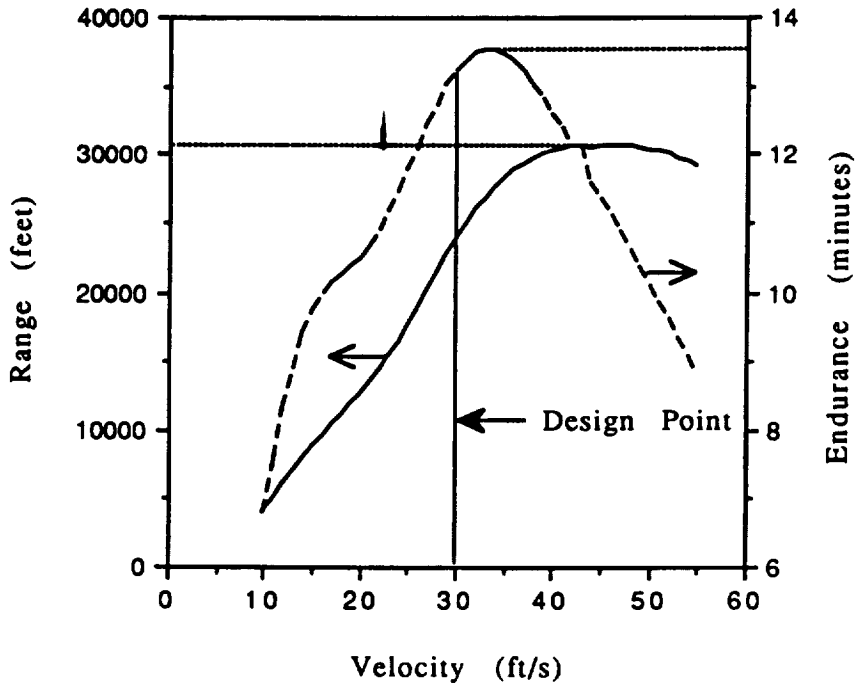

Under the selected cruise velocity of 30 ft/s, the range and endurance were calculated as about 24,000 feet and 13.2 minutes, respectively. The maximum range occurred around 31,000 feet at 45 ft/s with a corresponding endurance of 11.5 minutes. At 33 ft/s, the maximum endurance of 13.5 minutes was discovered with a range of 27,000 feet. Another important consideration was the variation in range with payload weight. Figure 8.3 shows this trend with values of cargo weight from empty to maximum. Again, with the 1000 milliamp-hour batteries, there was no concern with the inability to meet the design objectives.

Figure 8.3: Range-Payload Diagram

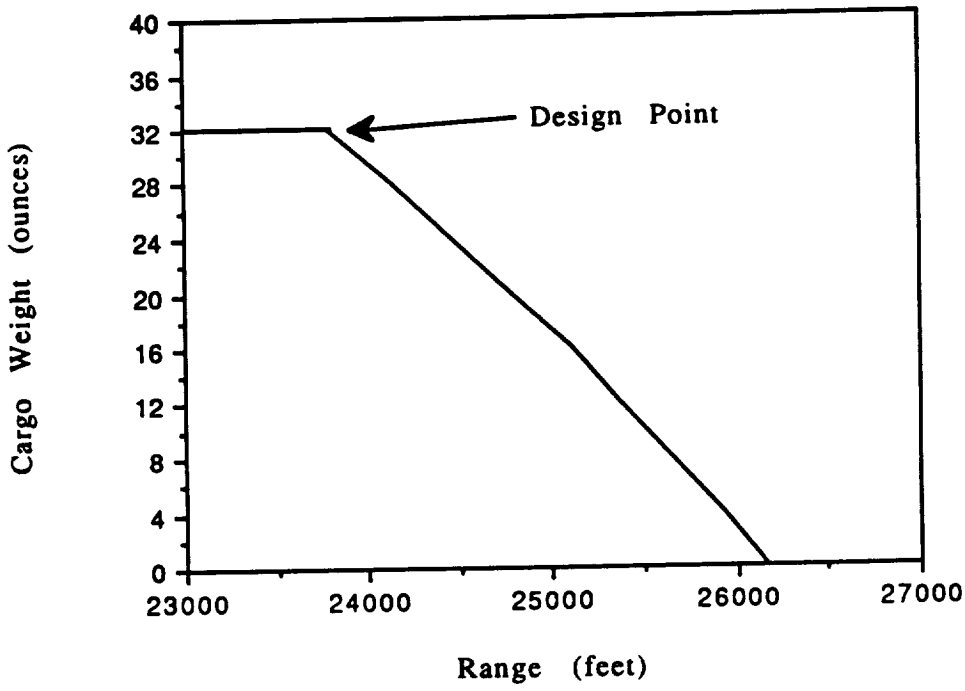

8.3 Power Available and Required Summaries

The power available calculations were completed for various voltage settings, using the computer code in Appendix G. Results of this study are shown in Figure 8.4 for the fully loaded *Prime Mover*. The significant features to note of these results are the values of minimum and maximum velocity and the voltage setting for the desired cruise velocity. Maximum and minimum velocities occur where the power available for maximum voltage setting intersects the power required curve. These values were found to be about 10 ft/s and 51 ft/s, respectively.

Figure 8.4: Power Available and Required for varying voltage settings

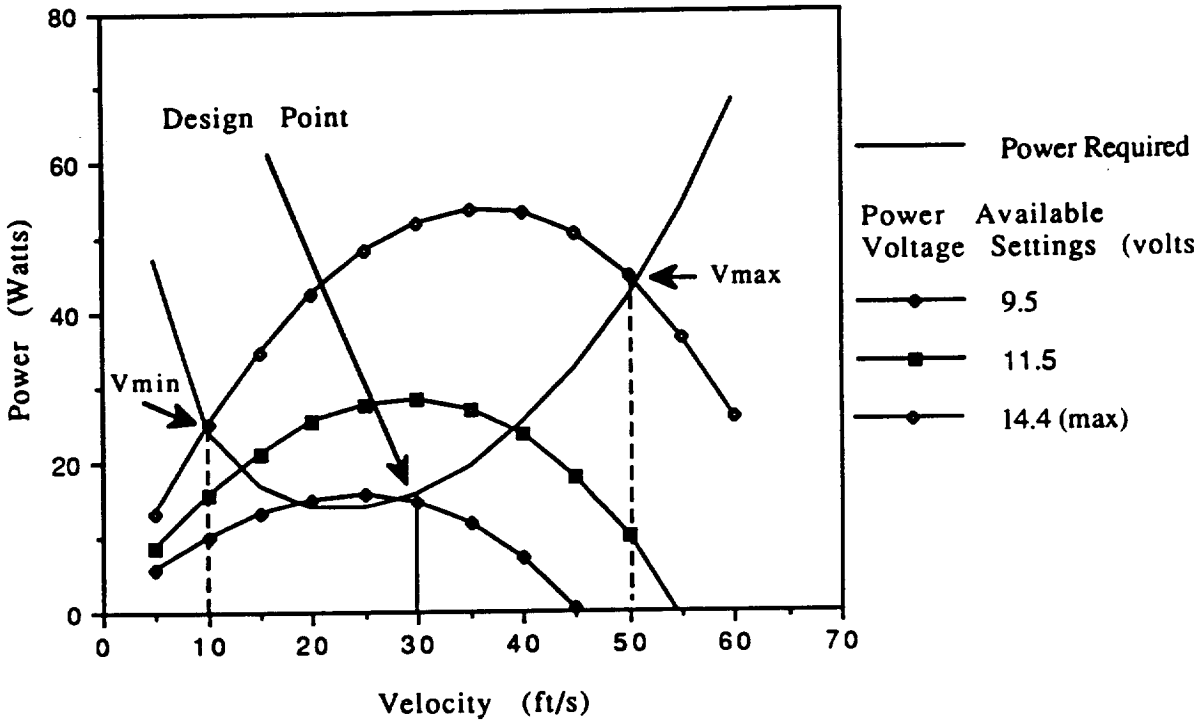

At the cruise velocity of 30 ft/s, the voltage setting was about 9.5 volts. Also shown in the figure is a power available curve for one other voltage setting. This example shows how to determine the voltage setting for various desired cruise velocities and rates of climb.

8.4 Climbing and Gliding Performance

As a result of the power available and required study the rate of climb for various velocities and voltage settings was determined. Of particular importance was the maximum rate of climb, occurring at the maximum voltage setting, found to be 5.4 ft/s. This rate of climb occurs at the desired cruise velocity of 30 ft/s. The ratio of horizontal to vertical distance traveled during maximum rate of climb is 5.56, meaning a significant amount of ground distance must be covered to increase in altitude. To illustrate this fact, assuming the maximum rate of climb can be achieved directly after take-off, about 140 feet will be needed to climb to a 25 foot height, over twice the distance needed for take-off ground roll.

In case of such emergencies as engine failure, it was important to investigate the *Prime Mover*'s gliding performance. The minimum glide angle, giving the maximum horizontal distance covered in gliding flight, occurs when the lift-to-drag ratio is greatest. The minimum glide angle was found to be 3.33°, giving a horizontal distance travelled of 430 feet from a starting altitude of 25 feet.

8.5 Catapult Performance Estimate

The series of flight tests includes a catapult test to test such characteristics as aerodynamics and stability. To estimate the predicted performance during this test, a catapult program, written by Kevin Costello, has been utilized.

One particular problem encountered during the calculations was the difficultly in obtaining a relatively large range while touching down approximately parallel to the ground. Many of the initial flight conditions tested either resulted in the inability to take-off or the occurrence of a nose dive. Employing an elevator deflection helped to alleviate this problem. Figure 8.5 presents the results of one particular catapult estimation in which the variable parameters were as follows:

Distance between hard points : 20 feet
Catapult deformation : 30 feet
Elevator deflection : -0.15 rad

Figure 8.5: Catapult Estimation

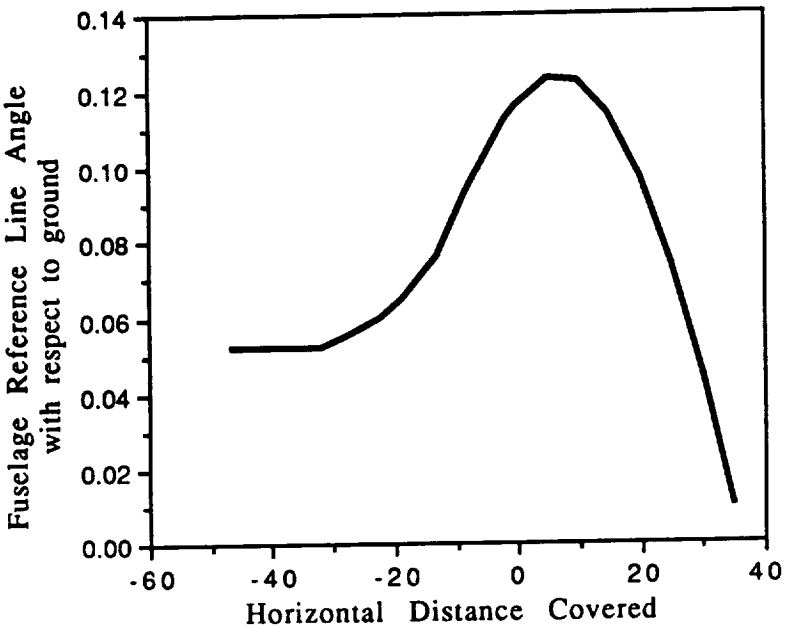

The catapult range measured from the pins was 35 feet with the angle of the fuselage reference line at touch down at 0.009 rad. The maximum altitude achieved was about 2 feet.

9.0 Structural Design Detail

9.1 V-n Diagram

The *Prime Mover* is not only designed to withstand the expected flight conditions, but also, to handle the unexpected loading environments of Aero World. Figure 9.1 shows the load limitations of the aircraft versus the aircraft velocity for an estimated weight of 6.5 lb. The maximum load capacity during flight maneuvers is 2.5 g, and during landing is 4.0 g. The maximum velocity of the Primer Mover is 51.0 ft/sec. However, due to the Aero World constraints on noise, the *Prime Mover* will not fly faster than the speed of sound, 30 ft/sec.

9.2 Basic structural components, substructures, and assembly

The elimination of the need for ailerons makes a dihedral wing configuration very attractive due to savings in both construction and maintenance costs. However, the bulky reinforcement at the root of the dihedral wing means a possible weight penalty. Use of a polyhedral wing eliminates the middle joint, allowing a continuous main spar to carry bending stress. Since the wing joints are further out on the wing and since the bending moment decreases as the square of the distance from the root, the polyhedral wing utilized on the *Prime Mover* provides a lighter solution for aileron elimination than does a dihedral configuration.

Figure 9.1
V-n Diagram

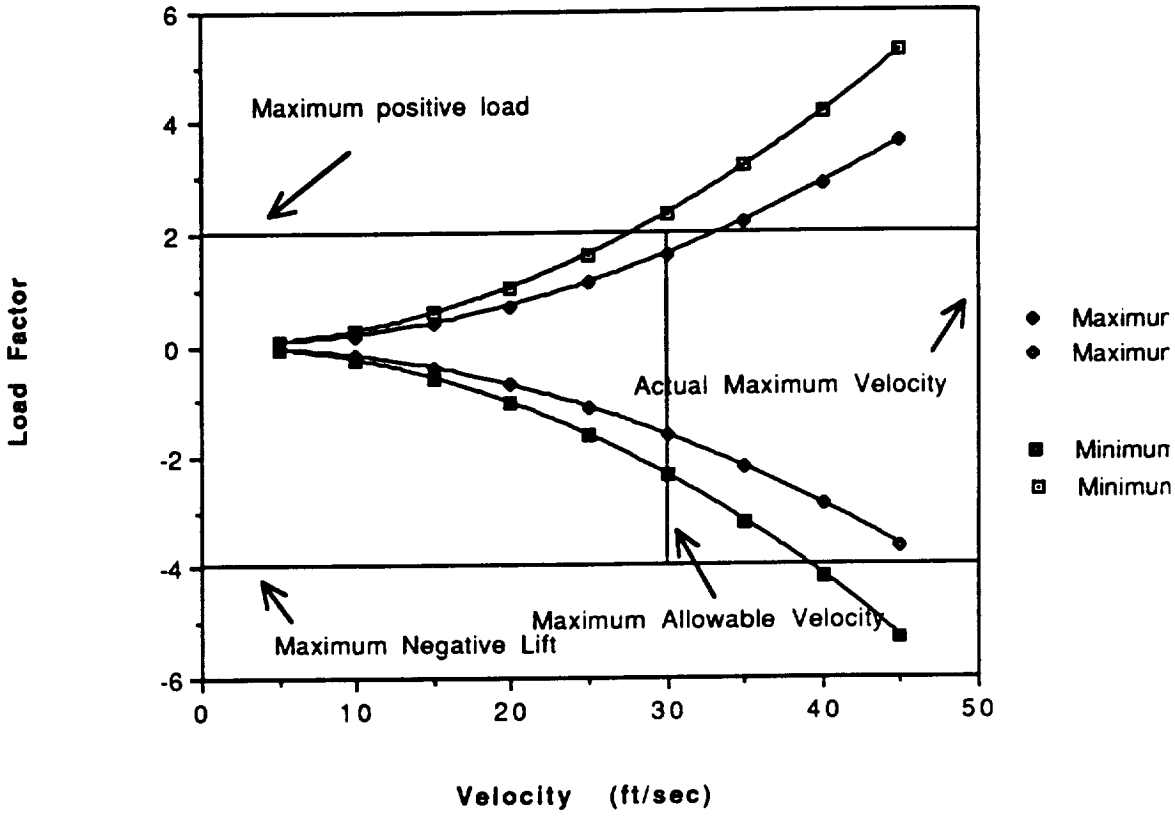

The major stresses in the wing are carried through the C-beam main spar. The spruce spar caps, in particular, are responsible for the integrity of the wing under the stress caused by lift forces. For these caps, spruce, due to a significantly higher yield stress than balsa, was found to weigh less than the amount of balsa necessary to prevent failure at the root of the wing. Balsa spar webs will also be included in the middle-section of the wing, where bending moments are the highest, to prevent excessive shear stresses on the ribs. The leading edge and trailing edge spars are of balsa construction and carry very little structural load. The ribs are also made of balsa and primarily maintain the integrity of the airfoil shape. Since the monokote is most likely to droop at the leading edge, where there is a high pressure gradient, half ribs are employed every six inches to increase the aerodynamic effectiveness of the wing. Toward the trailing edge, less structural mass is wasted supporting level sections of skin, which accounts for a rib weight savings of about 10% over a more closely spaced arrangement of full ribs. Wherever possible, the ribs are cored out to further reduce their mass.

Figure 9.2

Middle section of wing structure

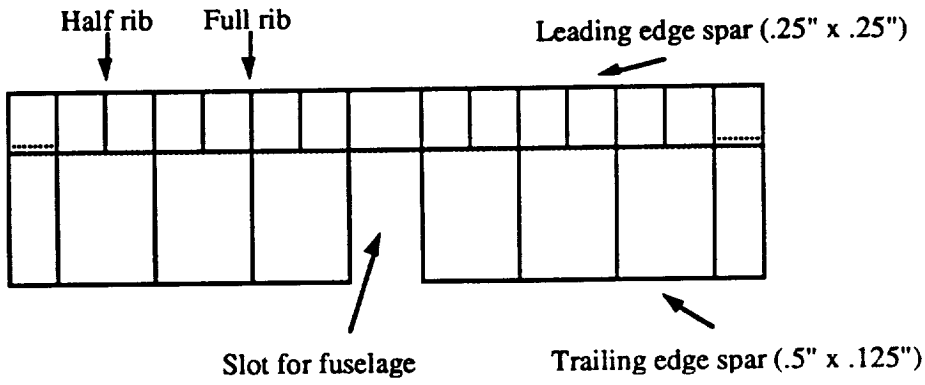

The most complicated piece of the wing is the joint between the main wing section and each canted, exterior wing section. These exterior sections must be detachable so that the *Prime Mover* will meet

storage requirements; yet, the joints must also be strong enough to weather a hard landing. Since an angled joint must be employed to connect the main spar of each section, a light plywood must be used, at a small weight penalty, to avoid failure due to shear along the grain. These plywood joints are affixed to the exterior sections and fit into sleeves between the spar caps of the middle wing section. Pins at the leading and trailing edges and an additional rib along the joint ensure that the wing sections are flush with each other, eliminating lift degradation due discontinuities in the skin.

At the center of the middle wing section, a reinforced spar web drops down and anchors the wing to the top of the fuselage. Screws at the trailing edge of the ribs which flank the fuselage anchor the wing to the aircraft at the proper incidence angle.

The size of the empennage is determined to optimize the control and stability of the aircraft. (See chapter 7). The empennage is designed to be easily removable and light weight in order to meet storage requirements and weight objectives.

Figure 9.3
Empennage Design

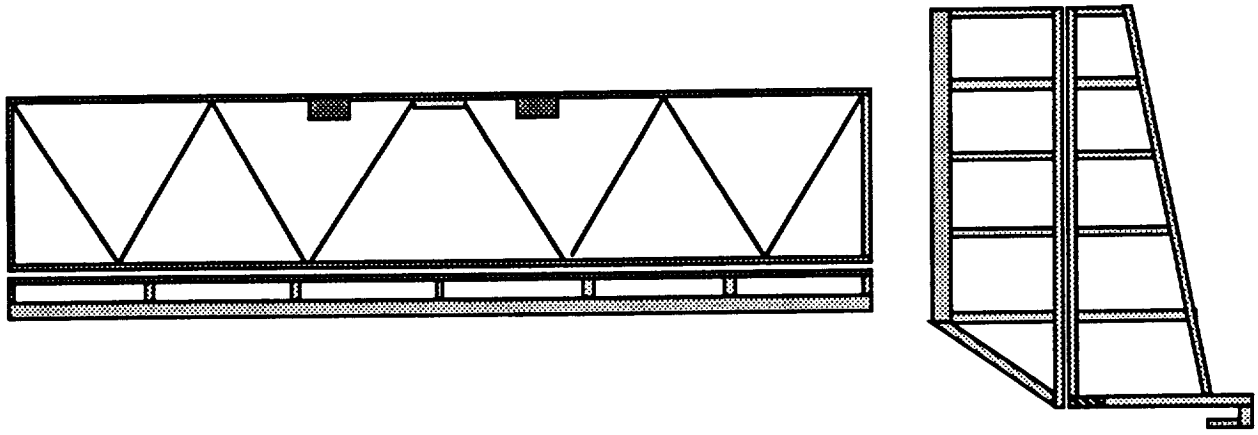

With the exception of the mounting hooks, the entire empennage is made of balsa. The size of the balsa wood was chosen to ensure handling strength while minimizing the weight. The configuration of the empennage components are shown in Figure 9.3. The empennage will be connected by screws in the aft section and a metal mounting hook in front.

The fuselage was designed to keep a minimum frontal area while allowing room for either the two or four inch cubes in the cargo space as illustrated by Figure 9.4. The circular holes in the upper corners represent the location of the control cables with respect to the cargo space.

Figure 9.4
Fuselage Cargo Spacing

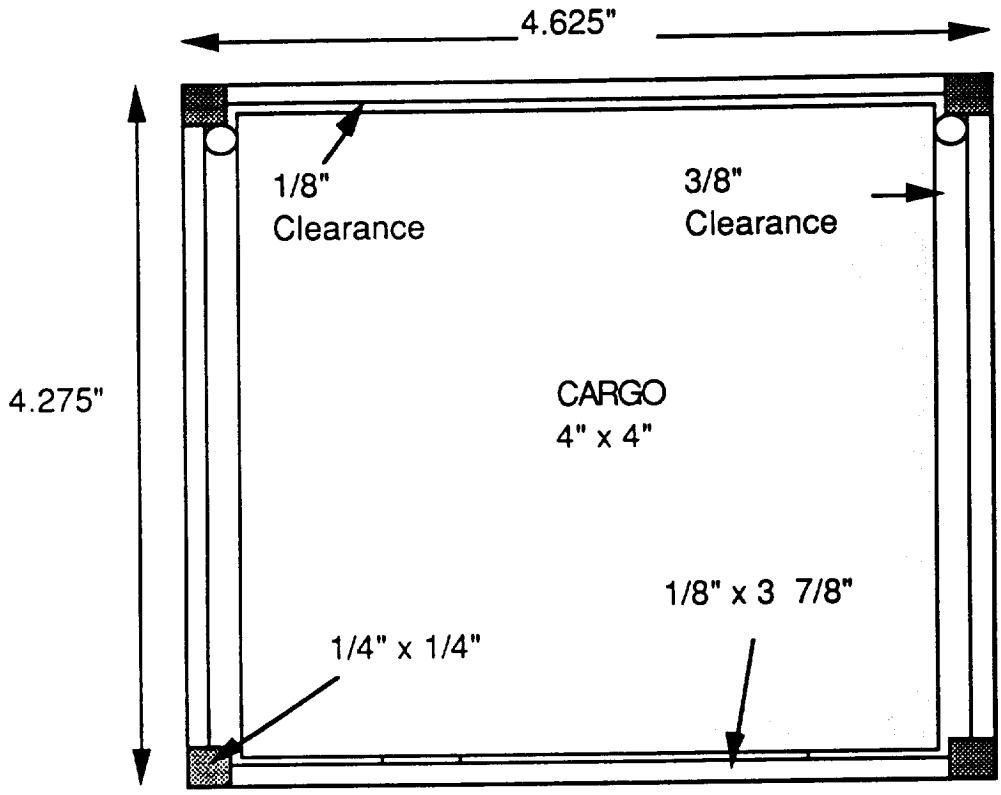

The side of the *Prime Mover* fuselage structure is supported by a sawtooth truss design (Figure 9.5). This was chosen over right angle and left angle truss designs because it is stronger than either in both tension and compression as evaluated by the Exodus internal stress analysis program (See Appendix H). The location of the vertical cross beams were chosen to minimize the fuselage weight while withstanding 4.0 g landing loads, 2.5 g cruise loads, and catapult loads of 2 g's.

In order to simplify construction, the beams where then moved to even intervals and retested. The amount of weight added by this step was only a fraction of an ounce.

Figure 9.5
Fuselage Truss Design

The forward landing gear is located directly under the instrument package where the fuselage is already strengthened. Unfortunately, this is located far forward of the center of gravity, possibly producing an undesirable attitude if landing when the aircraft is subject to large yaw moments. To counter this situation the landing gear is given a wide base.

9.3 Internal Configuration

There are four major internal components. These are:

1. motor
2. batteries
3. avionics
4. cargo

The location of each component plays an important role in the performance of the aircraft. The internal configuration can be seen in figures 9.6 and 9.7.

Figure 9.6
External Configuration of the Exodus *Prime Mover*

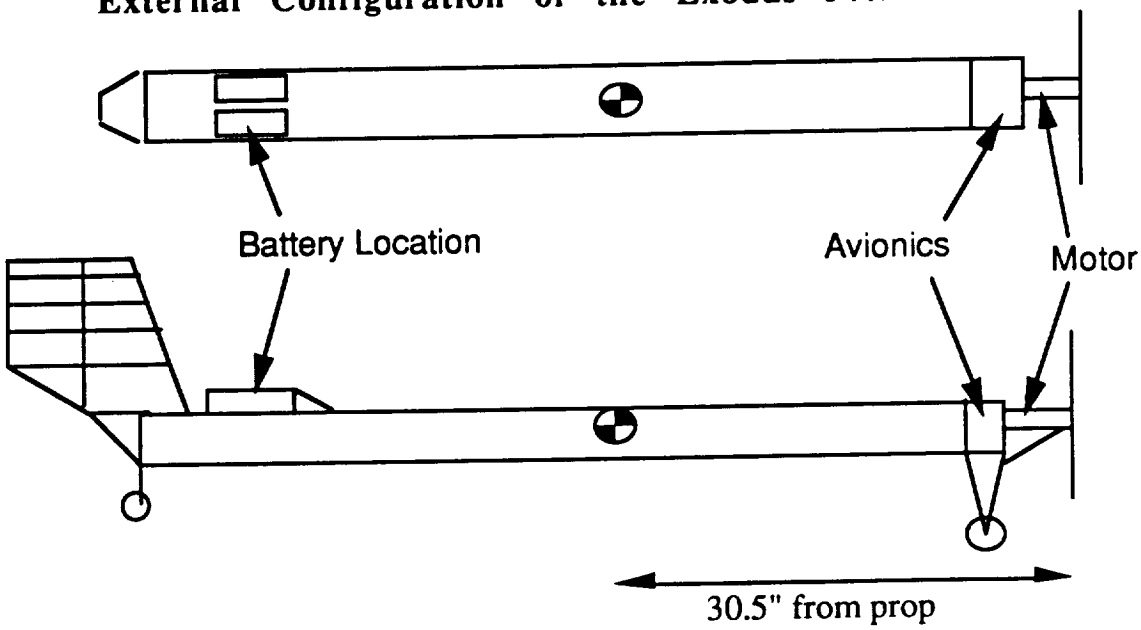

Figure 9.7
Instrument Package Configuration

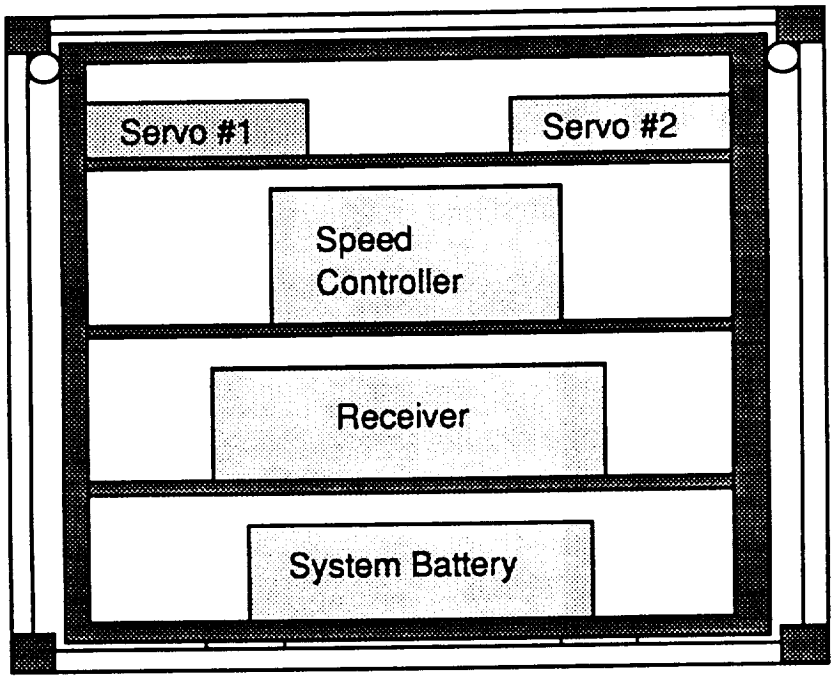

Motor

The motor is located in the front of the Exodus to reduce blockage. This location also reduces the risk of ground contact since the Exodus has tail dragger landing gear. The motor is centered and slightly high

on the fuselage in order to align the motor with the CG of the Exodus and minimize the effects of the propulsion system on the moment about the CG. Another benefit of having the motor slightly high on the fuselage is that it reduces the required landing gear height.

Batteries

Since the fuselage, motor, and cargo (full payload) CGs are fixed, the batteries are the only remaining component with sufficient weight to significantly effect the total CG of the aircraft. It is desirable for the CG of the Exodus to be independent of the payload it is carrying so that the handling qualities are consistent. In order to achieve this it was necessary to make the CG of the complete aircraft with no payload match the CG of the cargo only. This required the batteries to be as far aft on the fuselage as possible.

The batteries are on top of the fuselage in a separate compartment for several reasons. It provides easy access, thus lower maintenance cost. It also maximize internal volume. Another important reason is to provide cooling. The batteries get very hot and ventilation will be much better in a separate compartment where vents can be added. The wires from the batteries will run inside the main fuselage along the sides of the cargo bay.

Avionics

The Avionics is composed of five components:

1. Receiver
2. Speed Controller
3. System Battery
4. Servo #1
5. Servo #2

These components are located close to each other for easy access and to reduce the wire length between them. Easy access is a requirement because the entire system must be able to be installed in less than 30 minutes. Each component will be on a separate platform, and each platform will be connected. This system will have a handle to provide easy removal of the total system. The servos will be connected to control cables for the elevator and rudder. These cables will run along

the sides of the fuselage in a similar manner as the battery wire. This requires the servos to be on top to allow for cable connection after the components are in place. The avionics are located forward on the Exodus to limit the load on the compartment since the aircraft will be at an angle of attack while on the ground.

Cargo

The Exodus has a single uninterrupted cargo bay to provide complete control capability of the cargo CG. The boxes will be supported by strips of wood running the length of the cargo bay. These strips will have holes every inch to allow for a peg to be inserted, thus constraining the boxes during non-full cases. The door to the cargo bay will have 1/8 inch guides to insure the cargo does not interfere with the control cables or battery wires running along the side of the compartment.

10.0 Construction Plans

10.1 Major Assemblies

As with any type of construction, difficulties can be anticipated and overcome by early planning. For this reason, Group Exodus has chosen a number of major assemblies which need extra attention.

The first is the polyhedral joints. These joints will be connected in a sleeve joint assembly. The angle will be constructed into the joint and held by additional slanted rib supports. The joint will be made out of a light plywood which will slide between the spar webs and spar caps of middle wing section (Figure 10.1). The plywood will be designed to maintain a tight fit in the .25" by .9" webb area of the inner and the outer wing sections.

Figure 10.1
Polyhedral Joint

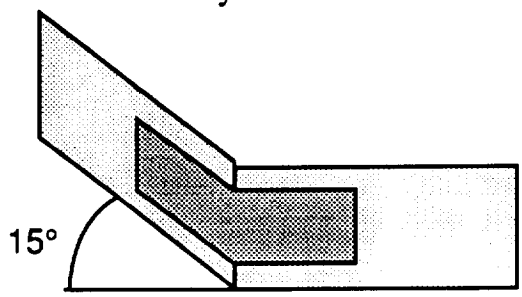

The second obstacle is the wing-fuselage attachment. The wing will be attached to the fuselage by two means. Two hooks originating from the wing spar will attach to a strengthened fuselage cross beam near the outside of the fuselage. The back of the wing will be attached by screwing the interior ribs to the fuselage. The locations of the rear attachment are selected so as to produce the proper wing incidence angle.

The third challenge is the empennage mounting which will be done in a fashion similar to that of the wing. The vertical tail hooks around the horizontal stabilizer which in turn is hooked to the fuselage

near the outer edges of the fuselage. This configuration minimizes the forces exerted on the fuselage support beam. The entire empennage is then fastened to the fuselage at the rear of horizontal and vertical tails just prior to the elevator and rudder by use of a large plastic screw (Figure 9.3).

The instrument package is placed between the engine firewall and the instrument protection wall. Sufficient room is allowed for easy removal and reconnection of the instruments as necessary. The forward landing gear is connected directly under the instrument package.

Figure 10.2
Removable Instrument Package

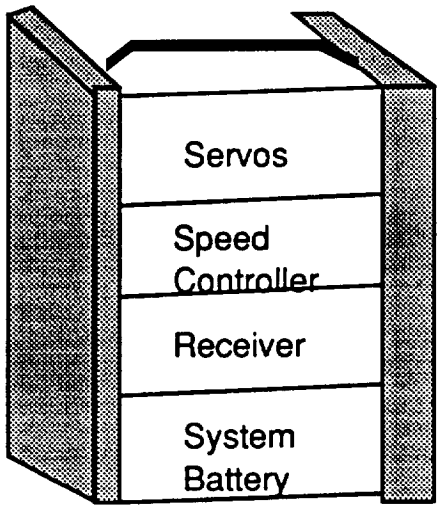

Connecting the rear landing gear offers some difficulty. An attempt must be made to give the rear landing rotational freedom in order to assist in ground handling. This freedom can be assured by attaching the landing gear in a pivot block made of plywood. Washers fastened to the gear will stop landing gear vertical motion while allowing turning capability. See Figure 10.4

Figure 10.3
Rear Landing Gear Attachment

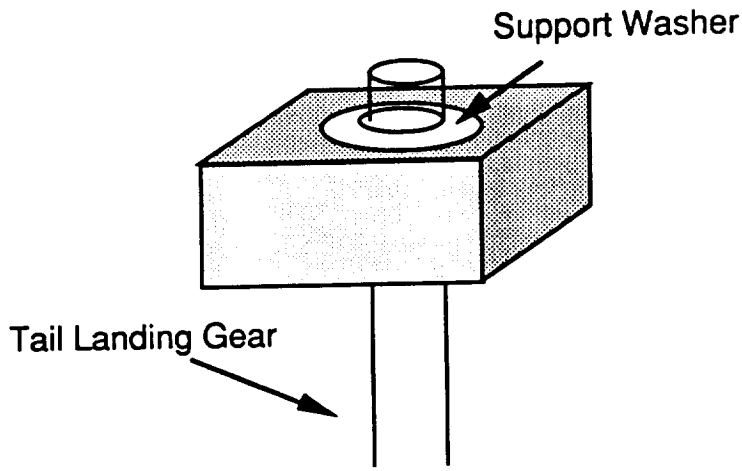

10.2 Complete Parts Count

The parts count is based on the initial blueprint of the *Prime Mover*. Alterations will need to be added as construction begins. For this reason a price inflation of 10% is added to each component to meet unexpected changes in the prototype construction.

Figure 10.4 is a listing of the initial part count.

10.3 Assembly Sequence

Assembly of the vertical tail, horizontal tail, wing sections, and empennage side trusses will all be done independently. At this point the aircraft's center of gravity can be verified. The final stages of construction demand extra attention to assure proper connection with the wing and empennage as well as proper placement of the battery and wing. The complete fuselage will be put together at this point after verifying all connection designs.

The over all production time should be enormously decreased by this modular construction plan. With smart planning, production of the *Prime Mover* should easily be achieved in less then the one hundred and twenty man hour goal.

11.0 Enviromental Impact and Safety Issues

11.1 Disposal of Each Component

The revolutionary success of the Exodus *Prime Mover* will ensure that the first few hundred production units will be sent to miscellaneous museums throughout the world.

Keeping environmental considerations in mind, Exodus plans on reusing or recycling all products to the end of their expected life cycle. For instance, all propulsion units are rechargeable and aircraft control equipment may be reused in other airplanes.

Difficulties arise in recycling wood because all connections between members are joined by toxic glue. All salvageable wood may be recycled for any use (i.e. gardening mulch or firewood). Infected wood and plastic monokote materials must be handled separately as potentially hazardous materials.

11.2 Noise Characteristics

Unfortunately, Aeroworld is free of real world effects associated with the effects of exceeding Mach one. The aircraft itself will be limited to a velocity of mach one; however, the propellor can not meet that limitation. The rotational speed necessary to propel any aircraft results in a tip speed far greater than 30 ft/sec. The noise elements related to the propellor speed can not be avoided.

The actual hub station should be placed outside the residential area of city J in order to reduce the number of complaints related to late night noise. Other suggestions for noise reduction include detoured flight patterns as well as engine muffling or resizing.

11.3 Waste and Toxic Materials

Disposal of waste and toxic materials is generally subcontracted to waste disposal companies. In the event that these companies can not deal with glue or monokote materials City O, the New Jersey of Aeroworld, would be an ideal dump site.

12.0 Economic Analysis

Probably the most important goal of this project was to maximize the return on investment. Consequently, the economic analysis was one of the most crucial studies. In fact, the economic strategy affected the mission and the final design more than originally expected.

Before performing the economic analysis, Group Exodus adopted an economic strategy. We realized that we were designing a fleet of planes for an inexperienced company in a brand new market. Rather than spread the *Prime Mover* fleet thin throughout all of Aeroworld, the fleet was designed to serve a restricted area, the Northern Hemisphere. By doing this, a more reliable and efficient service could be provided. Concentrating on a restricted area and therefore providing an extremely dependable service would install a "piece of mind" among our customers. This eventually would attract more customers. From a marketing and economic point of view, this was deemed to be more important than serving a larger area at first and decreasing the efficiency of our service. The possibility of expanding the service throughout the whole world still exists, but as a new company creating a good reputation is of upmost importance. With this strategy in mind, the economic analysis could begin.

One the most important results obtained from the economic analysis was that fuel costs, using an average price rate of $12.50 per milli-amp hour, accounted for 73% of the total fleet life cost. This differs quite a bit from the original design objectives. This was simply due to the fact the fuel cost equation was not interpreted correctly.

Figure 12.1

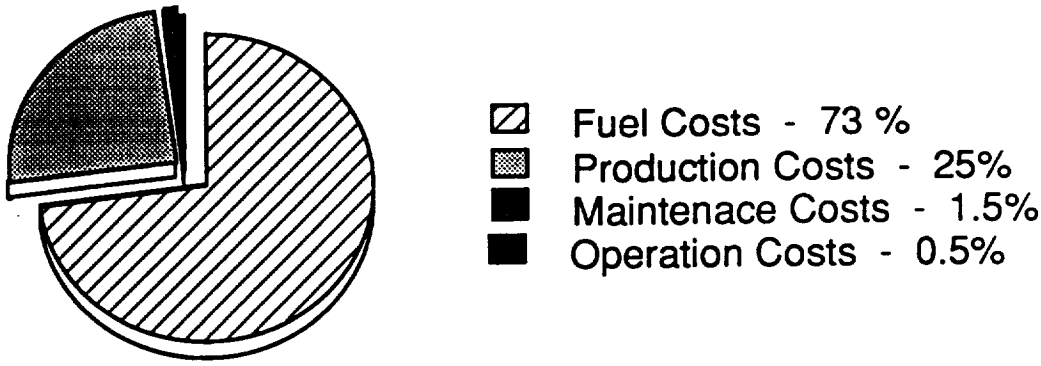

This result had a huge impact on the mission and final design. This large percentage drove Group Exodus to design optimally for a fleet that would serve a restricted area, namely the Northern Hemisphere of Aeroworld. The fuel costs also had repercussions on the final design. As can be seen in Figure 12.2, a one amp increase in the current draw at cruise results in an approximate 15% increase in the fleet life cost per volume moved (FCPVOL).

Figure 12.2

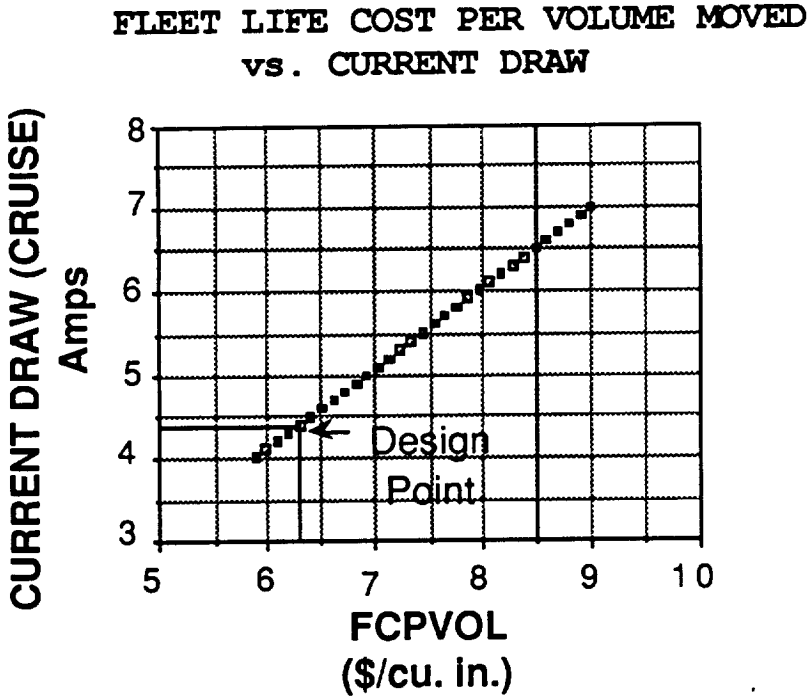

This translates into a more expensive price for our customers. Consequently, it was necessary to keep the current draw as low as possible. It was observed that one of the best ways to accomplish this was to minimize the weight of the aircraft. Therefore, Group Exodus opted for a relatively small cargo volume compared to other groups. The one drawback of this size volume was that the fleet size had to be increased; but, as mentioned before, this larger fleet size would insure the reliability and efficiency that it necessary for good overnight package delivery service.

The pricing scheme adopted for this overnight package delivery service is quite simple. Customers will be charged per volume of the parcel with and added overseas charge for intercontinental shipping. There are two reasons for this overseas charge. The main reason is that after analyzing the daily cargo load for the Northern Hemisphere (Appendix I), it was noticed that 58% of this cargo is shipped overseas. Another reason for this overseas charge, is that customers will expect to pay more for parcels that are shipped overseas. Consequently, overseas shipping proved to be the best avenue for profit. In order to break even on the original investment in half of the fleet's life, 150 days, a price of $8.74 per cubic inch for intracontinental shipping and a price of $11.01 per cubic inch for overseas shipping will be charged. The total fleet life cost is $57,069,600. Other pertinent results of the economic analysis are listed on the spread sheet in Appendix I.

12.1 Production Costs

As can be seen in the cost breakdown, the production cost accounts for 25% of the total fleet life cost, which makes it the second most important cost. Consequently, keeping this cost as low as possible translates into sizable price reductions for our customers. The production cost influenced the overall design of the *Prime Mover*. After reviewing the equation for the production cost, it was realized that the number of man hours was the most controllable aspects of the total production cost. Consequently, Group Exodus chose to keep the overall design as simple as possible in order to keep the cost as low as possible. After reading past reports, it was estimated that 120 man-hours would

be sufficient to build the *Prime Mover* prototype. Construction costs were estimated as follows:

CONSTRUCTION COSTS

PROPULSION COST:	Propeller (Zinger 11-5)	$3.00
	Engine(Astro 15)	$125.00
	Speed Controller	$70.00
	Batteries(12)	$15.00
		$213.00
CONTROLS COST:	Transmitter	
	Receiver	
	Battery Pack	
	2 Servos	
		$300.00
STRUCTURE COST:	Wood (balsa and spruce)	$45.00
	Monokote	$30.00
	Hinges, Clamps, Screws	$10.00
	Landing Gear	$22.00
	Glue, Tape	$20.00
		$127.00
	TOTAL	**$640.00**

Using the given equation for production costs, a value of $376,000 was obtained.

12.2 Maintenance Costs

The cost analysis (Figure 12.1) revealed that the maintenance costs only accounted for 1.5% of the total fleet life cost. As a result, this cost will not have a big impact on the customer. Nevertheless, it was minimized as much as possible. Maintenance costs are based on the time it takes to replace the batteries. Group Exodus therefore designed a removeable portion of the fuselage so that the batteries could be replaced as quickly as possible. It was estimated that a battery change

will take one minute and that the batteries will have to be changed on the average every 2 flights. Therefore, the maintenance costs were calculated to be $25 per flight.

12.3 Operation and Fuel Costs

Operation costs were estimated to be only 0.5 % of the total fleet life cost (Figure 12.1). Along with the maintenance costs, the operation costs have little impact on the customers. The operation costs are based the flight time in minutes at the maximum range and the number of servos in the aircraft. As a result of the simple design of the *Prime Mover*, the number of servos was limited to 2. The maximum flight time in minutes for our designed mission with a one minute loiter included is 4.5 minutes. Consequently, the operation costs total a mere $9.00 per flight.

Fuel costs as stated before, accounted for 73% of the total fleet life cost and therefore had the biggest impact on the customers. As a result these costs were kept to minimum as much as possible. This was described in the introduction of this section. Using an average value of $12.50 per milli-amp hour, the fuel costs were calculated to be $1,604 per flight.

13.0 Results of Technology Demonstrator Development

13.1 Configurational Data, Geometry, Weights and C.G.

The configurational and geometry of the *Prime Mover* remained unchanged from the initial design concept. However, the methods of connecting the wing, tail and landing gear were altered. In addition, weight and C.G. location varied with respect to the predicted values.

The wing was initially designed to be connected by hooks to a piece of spruce glued on top of the fuselage. However, Group Exodus desired to connect the wing in a more secure manner. A 3/16 inch piece of plywood was used to form a bulkhead inside the aircraft with an additional 1.5 inches on top for two holes. The wing had two birch dowel pegs that fit into these holes. The trailing edge was connected in the original manner. In future versions, the fuselage should be made wider so that a 4X4 inch square may be cut out to provide a continuous, uninterrupted cargo space. The tail was originally to be attached by a screw and hook design. The hook was replaced by velcro because it is a simpler technique.

The main landing gear was placed further aft than originally planned. This was done to improve ground handling under the advisement of an expert in the field. Also, the main gear was bolted to the fuselage instead of being glued. This was proven to be an important decision, as several other aircraft with landing gear that did not use bolts were torn off. In future versions, the fuselage should be made slightly higher to account for thickness of the plywood support and the length of the bolt on the inside of the aircraft (approximately 1/4 inch).

The avionics compartment should be changed in future versions. Two inches of available length in the fuselage may be used for the structure of a sturdier compartment. The present compartment is 1/16 inch balsa and is very fragile. It is also a very tight fit and adds difficulty to installation.

The batteries Group Exodus desired were not available, so lighter batteries with less power were used. Our motor was slightly lighter than noted on the specification sheet. The reason for the deviation is unknown. The main landing gear was slightly heavier than expected

because it was purchased instead of built. This was done to increase survivability and was probably one of the most important decisions made since the *Prime Mover* had several hard landings. The fuselage was heavier than expected due to the change in the method used for connecting the wing. Also, battery wire, control cables, and the avionics compartment were not accounted for in the original estimation.

The C.G. was off by 0.5 inches. This was due to a combination of several small weight differences and the relocation of the main landing gear. To correct this, a 3 oz weight was placed in the rear of the aircraft.

13.2 Flight Test Plan and Test Safety Considerations

The flight test plan for the *Prime Mover* prototype consisted of an indoor flight in Loftus Center. The plane was designed to take-off within 20 yards and to safely complete a figure eight flight configuration within an area with a 100 yard length and a 40 yard width. In order to ensure a safe flight, Group Exodus meticulously completed a pre-flight check. Some of the major checks included: shaking the prototype to check for loose parts and the overall integrity of the aircraft, dropping the prototype from a height of three feet to check the soundness of the structure especially the landing gear and polyhedral wing joints, and testing the radio control and the corresponding movement of the control surfaces.

13.3 Flight Test Results-Taxi and Controlled Flight Tests

The taxi test was, for the most part, a success since it was confirmed that the *Prime Mover* prototype does indeed fly and that there were no major mechanical problems. Yet, the design group was alerted to a few minor problems that had to be attended to before the flight test. As the *Prime Mover* began its take-off, a bias in the rear landing gear caused the aircraft to veer to the left. The design group attributed this problem to the asymmetry of the rear wheel axle, which is curved on one side to clear the wheel. For flight tests, the gear was tuned to eliminate the bias and the axles were greased to decrease the force on the axle, but with little success. In retrospect, since the freely rotating rear axle does not provide adequate ground handling, it is

apparent that the rear gear should be attached to the rudder servo. Another factor that contributed to the tendency of the prototype to turn left during the taxi test was the warped rudder. This warp resulted from the monokote clinging too tightly to one side, and therefore creating a bend in the main spar. In an attempting to correct this problem, the heating iron was applied to one side only to try to remove the warp. This attempt was unsuccessful. A better solution would be to make the vertical stabilizer with stiffer material. This would minimize the need for precise monokoting which is difficult for amateur builders. Finally, the taxi test revealed an inadequacy in the wing joints. After a brief, aborted flight, the aircraft made a hard landing, which cracked the spar webs that hold the wing joints in place. These webs were not designed to take such an impactive force, which occurred because a gap between the leading edges of the wing sections allowed a small amount of wing rotation in the yaw axis. To strengthen these joints, the original, 1/16 inch thick webs were replaced with 1/4 inch thick webs with the grain oriented vertically to prevent shear. During flight tests, the gaps between the wing sections were filled with small, pliable rubber shock absorbers to prevent transmission of impactive forces into the joints.

During the controlled flight test, a few additional problems were revealed in the construction of the *Prime Mover*. In flight, the aircraft tended to roll to the left, reducing controllability during right turns. The pilot believed that this was this result of slight wing warp, causing a roll moment during flight. This is the most likely cause of this problem, since the aircraft was balanced along the roll axis. Another possibility is that the rudder was in the wake of the outboard wing sections which are at 17° actual dihedral. This was not accounted for in our calculations. Future analysis may show the need for a larger rudder to compensate for this interference. The inability of the freely rotating rear gear to provide directional stability once again made ground handling difficult. Finally, another hard landing, this time on the nose of the aircraft, cracked the 1/4 inch thick balsa engine mount. Future versions should utilize a more durable material, such as spruce or birch plywood, for this critical structural member.

13.4 Manufacturing and Cost Details

The Exodus DR&O set a limit price of two hundred dollars for construction materials. Exodus believed that the technology demonstrator could be constructed for approximately one hundred and twenty five dollars. This is the figure used in obtaining the initial cargo fee. Though cost overrun kept Exodus from meeting the one hundred and twenty five dollar goal, the DR&O goal was accomplished. Final expenses totaled to $164.22. Figure 13.1 shows the percentage costs breakdown. A more detailed cost per component break down in shown in Figure 13.3.

Major sources of pricing error included the monokote, landing gear, and excess wood. Monokoting the wing required two rolls of monokote instead of one. This increased the monokote price by $10.00. Initial estimates on the price of light weight wheels were off by 30%. Extra expenses in construction materials (balsa and spruce) arose due to manufacturing errors. In continued construction of the Exodus fleet, these additional costs can easily be avoided.

The number of construction manhours spent on the *Prime Mover* prototype was 112. This is within 7% of the initial 120 manhour estimate. Again, this value should be reduced as manufacturing experience is gained. Figure 13.2 shows the component division of manhours

Figure 13.1

Cost Breakdown by Aircraft Component

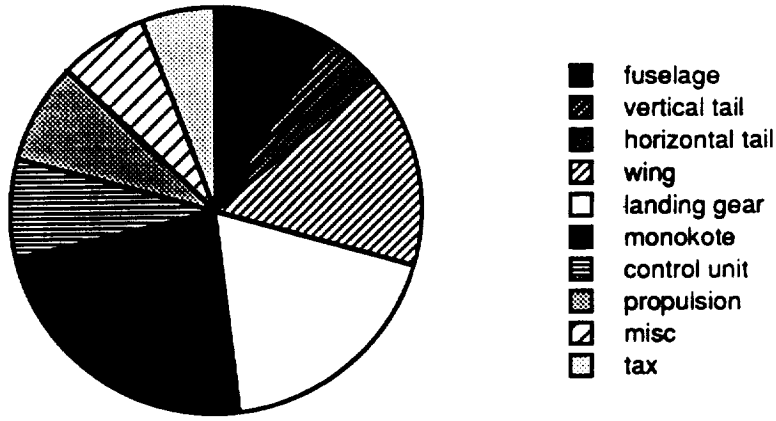

Figure 13.2

Manhours per Component

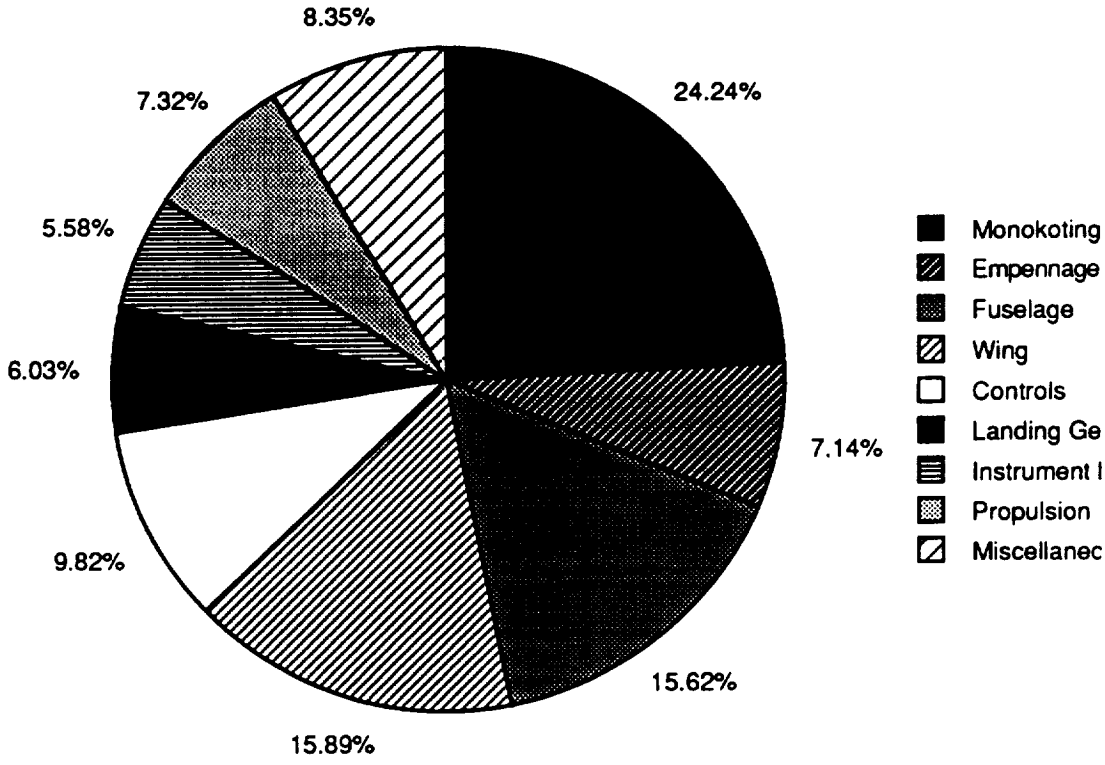

Fuselage (including instrument package)				
9	1/8"x1/8"x36"	spruce	diagonal beams (sides)	3.6
1	1/8"x3"x36"	balsa	instrument prot wall	1.73
1	1/4"x3"x36"	balsa	firewall	2.4
6	1/4"x1/4"x36"	balsa	main frame	3.36
10	1/8"x1/4"x36"	balsa	vertical beams and misc	4
1	1/16"x1"x36"	balsa	cargo support panel	0.42
	Fuselage Total			15.51
Vertical Tail				
1	1/8 x 1/4 x 36"	balsa	Internal	0.4
1	1/8 x 1/2 x 36"	balsa/tria	Trailing Edge	0.69
1	1/4" x 1/4" x36"	balsa	Frame	0.56
1	1/8 x 3 x 36	balsa block	Attaching block	1.73
	Vertical Tail Total			3.38
Horizontal Tail				
1	wing mounting kit			2.29
2	1/4"x1/4"x36"	balsa	Frame	0.56
2	1/8"x1/4"x36"	balsa	Internal	0.8
1	1/8 x 1/2 x 36"	balsa/tria	Trailing Edge	0.69
	Horizontal Tail Total			4.34
Wing				
1	Birch Dow		Wing connection	1.25
1	24"x6"x1/4"	plywood	polyhedral joints	1.99
1	12"x6"x3/16"	plywood	mounting bulkhead	1.99
2	1/4"x1/4"x48"	spruce	main wing spars	1.78
1	1/2"x1/8"x48"	spruce	main wing T.E.	0.89
3	3/16x3/16x48"	spruce	all wing L.E.	2.67
4	1/4"x1/4"x36"	spruce	side wing spars	2.36
2	1/2"x1/8"x36"	balsa	side wing T.E.	0.98
8	3"x36"x1/16"	balsa	ribs	9.54
1	1/8"x3"x36"	balsa	ribs	1.73
	Wing Total			25.18
Landing Gear				
1	Main Gear			9.99
1	Tail Gear			5.39
2	wheels			7.39
1	tail wheel			4.99
2	Collars			2.98
	Landing Gear Total			30.74
Monokote				
3	Clear monokote			28.77
1	trans. blue monokote			9.59
	Monokote Total			38.36
Control Unit				
1	48" Push Rod			4.5
1	36" Push Rod			3.99
1	Control Horn Pack			1.49
1	nylon hinge tabs			2.61
	Control Unit Total			12.59
Propulsion:				
1	12x4 prop			3.49
1	11x5 prop			2.79
2	Velcro mounting			6.9

REFERENCES

1. Anderson, John D. Jr., Introduction to Flight, New York: McGraw-Hill Book Company, 1985.

2. Beron-Rawdon, Blaine, "Dihedral," Model Aviation, Aug.-Nov., 1988.

3. Jensen, Daniel T., A Drag Prediction Methodology for Low Reynolds Number Flight Vehicles, University of Notre Dame, Indiana, 1990.

4. Nelson, Robert C., "Effective Dihedral Derivative."

5. Nelson, Robert C., "Flight Mechanics Notes," Spring 1990.

6. Nelson, Robert C., Flight Stability and Automatic Control, New York: McGraw-Hill Book Company, 1989.

7. Selig, Michael S., John F. Donovan, and David B. Fraser, Airfoils at Low Speeds, Virginia Beach, Virginia: H.A. Stokely, Publisher, 1989.

8. Timoshenko, S. and Gleason H. MacCullough, Elements of Strength of Materials, New York: D. Van Nostrand Company, Inc., 1935.

Appendix A
Selection of Aspect Ratio

The drag polar was determined by calculating the drag coefficient for various lift coefficients. The drag was divided into parasite drag and induced drag in the equation $C_D = C_{Do} + C_L^2/\pi eAR$. The drag polars for the various aspect ratios are illustrated in Figure A.1. For a given lift coefficient, the drag coefficient decreases with increasing aspect ratio. Thus, it is desirable for the wing to have a large aspect ratio so that the drag will be minimal. A larger aspect ratio decreases the induced drag, the greatest contributor to the total drag for large lift coefficients.

Figure A.1

Drag Polars for Various Aspect Ratios

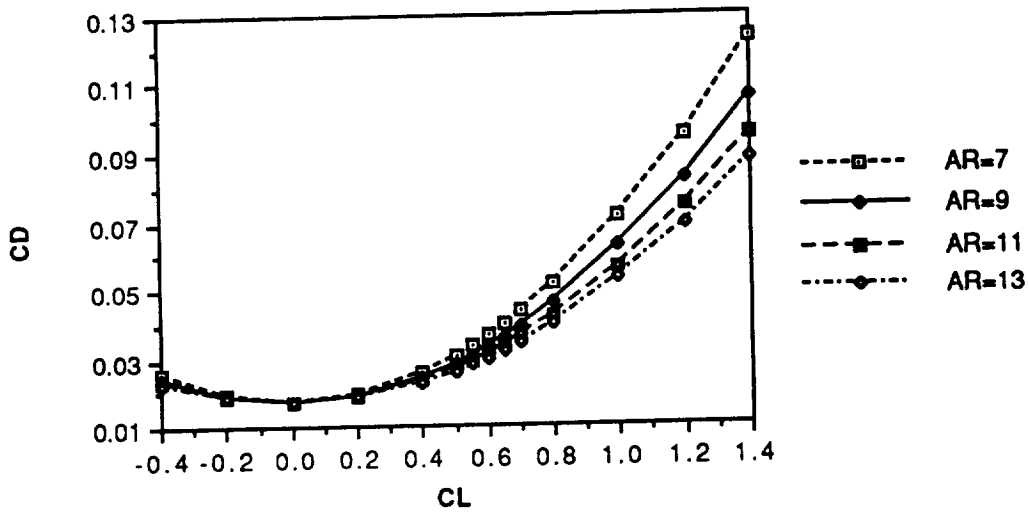

The data from the drag polar was then used to generate the lift-to-drag ratios for the various lift coefficients as shown in Figure A.2. The exact value of the maximum lift-to-drag ratio was determined for various aspect ratios using the relation $L/D)_{max} = (C_{Do}\pi eAR)^{1/2}/2C_{Do}$ and the corresponding lift coefficient was found using $C_{L[atL/D)max]} = SQRT(\pi eARC_{Do})$ (Ref 1). As the aspect ratio varies, the angle of attack for zero lift remains constant at -2 degrees

and the stall angle occurs at an estimated 14 degrees. The efficiency factor was assumed to vary with aspect ratio according to the equation $e=1.78(1.00-0.045AR^{0.68})-0.64$ (Ref 3). Maximum lift-to-drag ratio increases with increasing aspect ratio. The value varies by approximately 20% between an aspect ratio of 7 and 13. The corresponding lift coefficients vary by approximately the same percent and range from .55 to .7. At cruise conditions, C_L must be greater than or equal to .64. It is desired that the airplane cruise at $L/D)_{max}$ for greatest efficiency, however, L/D varies only by a few percent near the maximum value. For example, L/D only varies by approximately 1% for C_L values between .5 and .7 for an aspect ratio of 9. Thus, a large aspect ratio will produce the greatest aerodynamic results.

Figure A.2
Variation of Lift-to-Drag Ratio with Lift Coefficient For Various Aspect Ratios

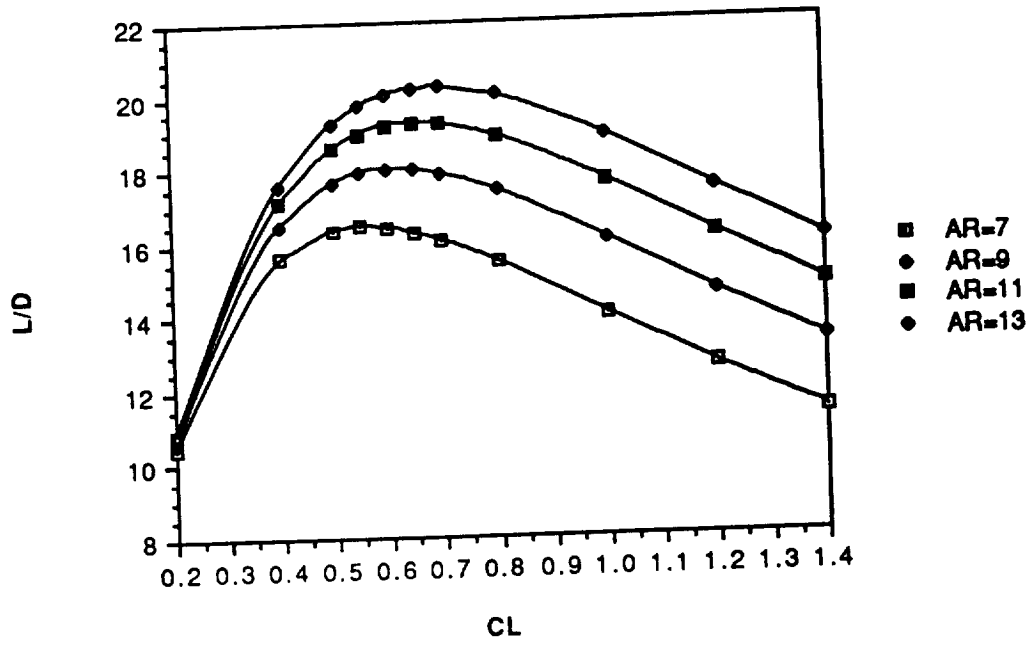

The effect of varying the aspect ratio on the lift curve slope is illustrated in Figure A.3. As the aspect ratio increases, the corrected lift curve slope increases. Thus for a given C_L, the angle of attack decreases with increasing aspect ratio which is desirable. However, the decrease is only minimal. For $C_{Lcruise}$ equal to .65, the angle of attack will fall between 6 and 7 degrees for the range of aspect ratios. Therefore, aspect ratio does not have a great effect on reducing the required incidence angle.

Figure A.3

Lift Curve Slopes for Various Aspect Ratios

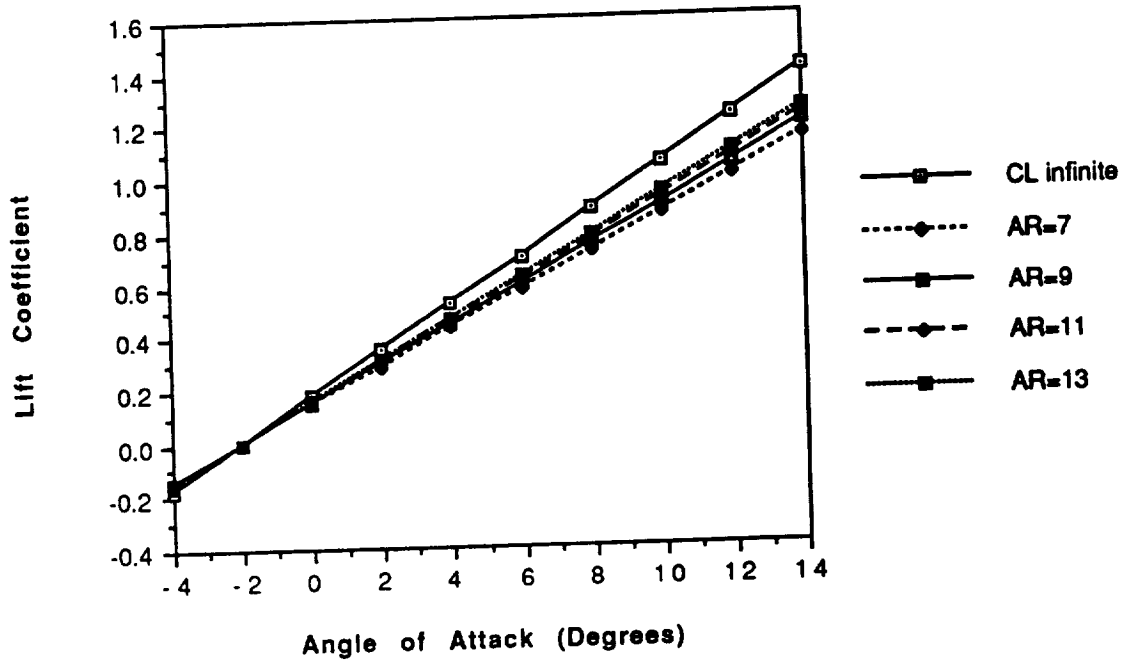

In order to assess the relation between the weight of the wing structure and the aspect ratio, the wing was simplified to a cantilever beam representing the main spar. This is a fairly accurate method for estimating the reaction of the wing to lift forces since the main spar is the primary carrier of stress due to bending about the roll axis. However, the spar weight for each aspect ratio is only a characteristic weight for the wing. Assuming that the excess weight in the relatively ineffective middle of the spar is approximately

equal to the weight of the balsa ribs and leading and trailing edge spars, the total wing weight is approximately equal to the spar weight plus about 5 ounces of monokote.

For each aspect ratio, $AR=b^2/S$, since $S=bc$ is fixed, the span, b, and the chord length, c, are defined. In addition, since the spar height, h, is .117c, this is also determined by the AR. The spar is located at the thickest part of the airfoil since the maximum stress in a symmetric beam, σ_{max}, equals $Mh/2I$, where M is the bending moment and I is the moment of inertia (Ref. 8, p.116). Since the wing from root to tip is effectively a cantilever beam under an even force distribution, the moment equals $Lb/8$, where L is the total lift force (Ref. 8, p.162). For ease of calculation, the beam cross-section was modelled as a rectangle of height, h, and thickness, t, making $I=th^3/12$ (Ref. 8, p.350). For a given aspect ratio and material with known yield stress, a spar thickness is defined. Given a material density, ρ, the weight of the spar is ρtbh.

Using an integral beam-bending analysis, the deflection of the wingtip is found to be $Lb^3/16EI$, where E is the Young's Modulus (Ref. 8, p.163). For spruce, E=1.3e6 psi, $\rho=.016 lb/in^3$, and $\sigma_{max}=2500$ psi.

Figure A.4

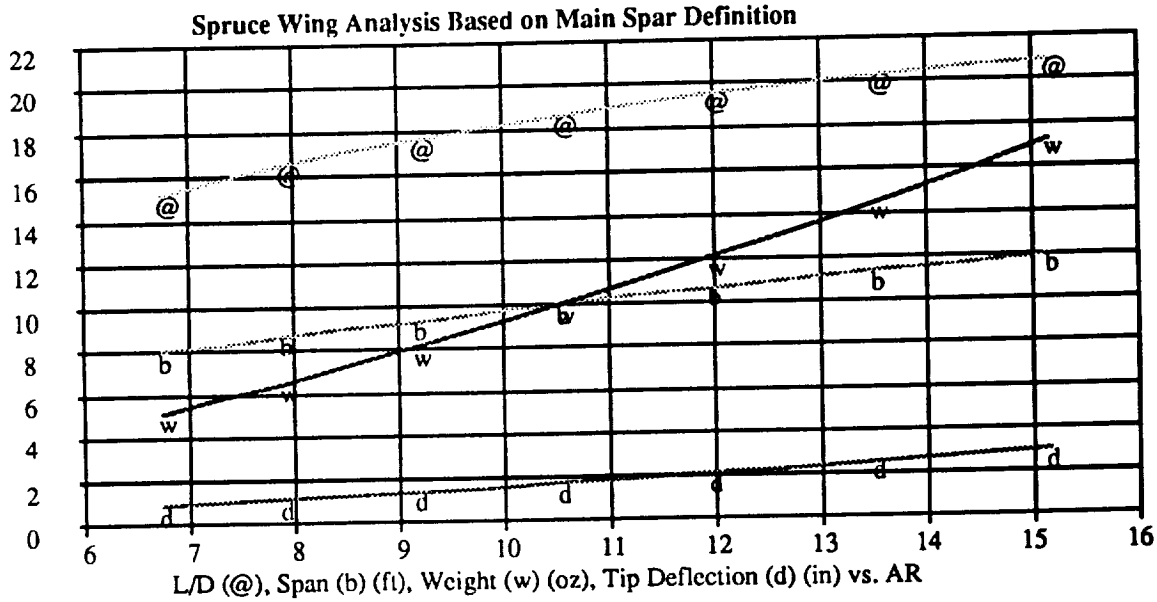

Appendix B
Calculation of the Efficiency Factor

The efficiency factor was estimated by taking the average of the efficiency factor values obtained from the Empirical Formula and Jensen's methods.

1. Empirical Formula $e=1.78*(1-0.045AR^{0.68})-0.64$

This equation, based on empirical data for straight-winged airplane, provides a good approximation although it was not determined for RPVs specifically (Ref 3). The efficiency factor is .765 for an aspect ratio of 9.62.

2. Jensen's Method $1/e = 1/e_{wing} + 1/e_{body} + 1/e_{other}$

In this equation, e_{wing} and e_{body} varying with aspect ratio and e_{other} is approximated as 20 (Ref 3). Referring to Figure B.1, the value of e_{wing} for a rectangular wing with an aspect ratio of 9.62 is approximately .76.

Figure B.1
Wing Efficiency Factor

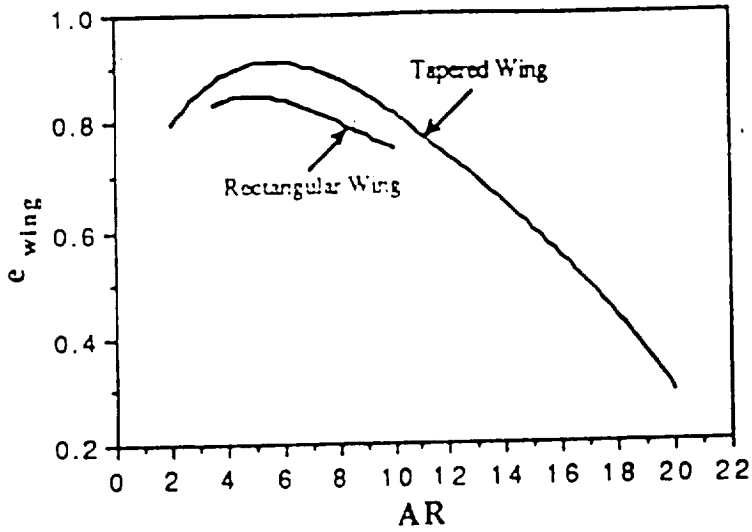

To determine a value for e_{body}, a body efficiency parameter is defined as $E_{body} = e_{body}S_{body}/S_{ref}$ where S_{body} is the cross-sectional

area of the body and Sref is the wing area. The value of 1.22 for E_{body} is obtained from Figure B.2 for a rectangular fuselage and an aspect ratio of 9.62. For S_{body}=20.23 in^2 and S_{ref}=1416 in^2, e_{body} is 85.39. Thus, the value of the efficiency factor obtained from Jensen's method is .726.

Figure B.2
Fuselage Efficiency Parameter

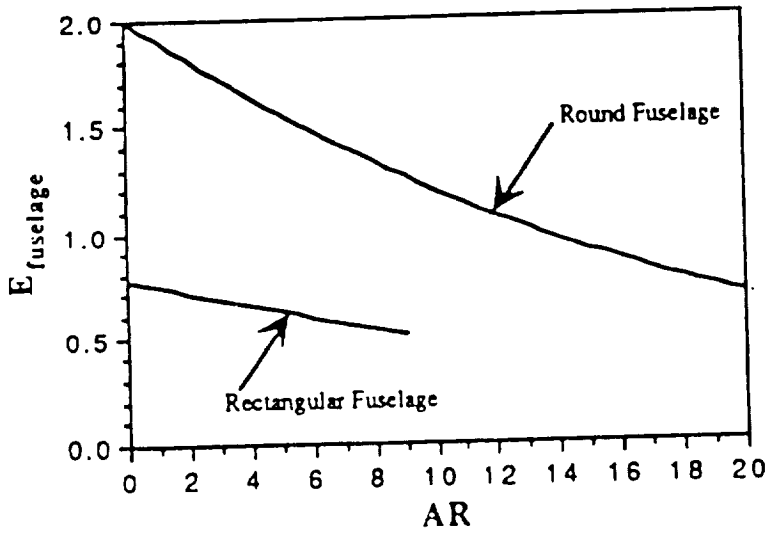

The two values differ by only 5.1%. The average of these efficiency factor values is .746. This averaged value is used in all calculations containing the efficiency factor.

Appendix C
Drag Breakdown

The drag of the Prime Mover was predicted using the drag breakdown method outlined in Jensen's thesis (Ref 3). This method estimates the total parasite drag by summing the contribution of each individual component of the airplane based on the wetted area and referencing it to the area of the wing according to the equation:

$$C_{Do} = \Sigma\, C_f\, S_{wet}/S_{ref}$$

where Cf=.0055 was selected based on skin friction coefficients of other model aircraft.

1. Fuselage
   S_{wet}=945 in^2
   C_{Do}=.003671

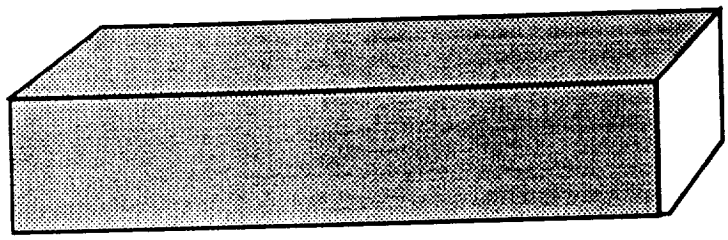

2. Battery Pack
   S_{wet}=35.6 in^2
   C_{Do}=.000138

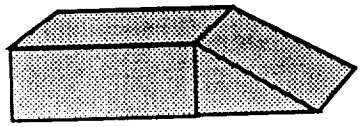

3. Frontal Section
   S_{wet}=55.9 in^2
   C_{Do}=.000217

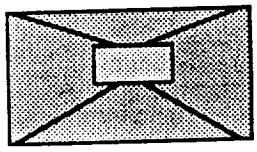

4. Rear Section
   S_{wet}= 33.4 in^2
   C_{Do}=.000130

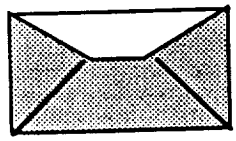

5. Wing
   S_{wet}= 2236 in^2
   C_{Do}=.008685

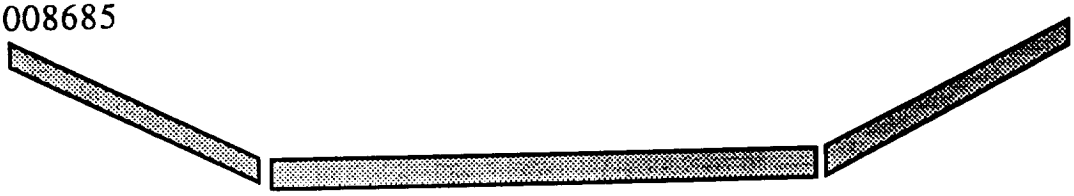

6. Horizontal Stabilizer
   S_{wet}= 416 in^2
   C_{Do}=.001616

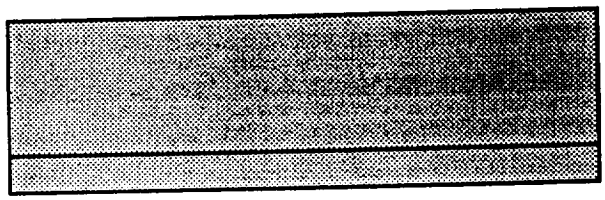

7. Vertical Stabilizer
   S_{wet}= 198 in^2
   C_{Do}=.000769

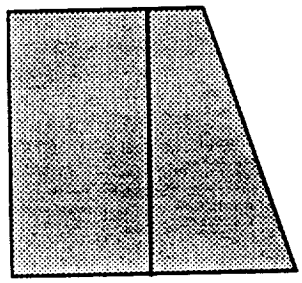

8. Landing Gear
   S_{wet}=79.9 in^2
   C_{Do}=.000310

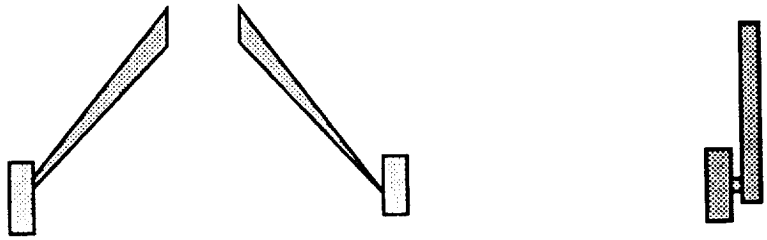

The total wetted area for the aircraft is 3999.8 in^2 and, given a reference area of 1416 in^2, the total parasite drag is .0155. Adding an additional 15% for interference, roughness, and proturberances provides a final estimated value for the parasite drag of .0179.

Appendix D
Sample Propeller Data

PROPELLER DATA SHEET

A) Propeller Designation: ZINGERJ 11-5

B) Number of Blades: 2 Diameter: 11 (Inches)

C) Select one of the following airfoil sections:
1) INVISCID FLAT PLATE
2) THIN FLAT PLATE
3) SYMMETRICAL
4) CLARK Y
5) RAF-6
--> 6) NACA44XXLOWRE

D) Blade thickness may be entered as either:
1) Fraction of chord
--> 2) Inches

E) Blade data may be entered at radial locations specified as:
1) Fractional Radius
--> 2) Inches

F) Radius* at which blade setting is measured: 3

G) Blade setting (i.e. ref angle for whole blade): 14.86

H) Enter the number of radial data positions: (3-9): 9

I)

Data Point	Radius*	Chord	Thickness*	Angle
1:1		.707	.234	38.51
2:1.5		.78	.198	27.95
3:2		.873	.191	21.7
4:2.5		.924	.181	17.66
5:3		.932	.171	14.86
6:3.5		.911	.157	12.81
7:4		.843	.138	11.25
8:4.5		.756	.116	10.02
9:5		.632	.095	9.04

J) Select desired refinment of analysis:
1) Analysis by simple blade element theory.
2) Analysis including induced velocity.
--> 3) Analysis including induced velocity and tip losses.

K) These Cl/Cd coefficient adjustments may be selected
1) No Cl/Cd adjustments
2) Mach number adjustment
3) Reynolds number adjustment
--> 4) Mach and reynolds number adjustments

L) Select altitude in thousands of feet: .025

M) Specify one of the following:
--> 1) Airspeed FIXED at: 19 MPH
2) Propeller RPM FIXED at:

N) Range of Advance Ratio to be used in calculations:
J min: .2 J max: .7

NOTES: First data point must be less than 30% radius; others must progress outward.
Designation must start with a letter and may not contain a comma.
For square tip blades (only) use tip as last data point.
Angles must be specified in degrees, lengths in inches.
* Units must be as specified in lines D and E.

ZINGERJ 11-5 PROPELLER

Performance Estimate

Analysis including induced velocity and tip losses.

DESCRIPTION: 2 Blades; 11 In. Dia.; NACA44XXLOWRE Airfoil; Blade set at 14.86 Degrees at 3 Inch Station
FLIGHT CONDITIONS: Calculations adjusted for both Mach and Reynolds numbers at 19 MPH and .025 thousand feet.

Blade Measurements

Fractional Radius,	X:	.3	.45	.6	.7	.75	.8	.85	.9	.95
Radial Position,	r:	1.7	2.5	3.3	3.8	4.1	4.4	4.7	4.9	5.2
Blade Chord,	C:	.8	.9	.9	.9	.8	.8	.7	.7	.4
Thickness,	In.	.1	.1	.1	.1	.1	.1	.1	.1	.1
Thickness Ratio,	T:	.15	.15	.15	.15	.15	.15	.14	.14	.15
Blade Angle,	Beta:	25.6	17.8	13.6	11.7	10.9	10.2	9.7	9.1	8.6
Geometric Pitch,	GP:	5	5	5	5	5	5	5	5	5
Solidity	S:	.094	.107	.107	.101	.095	.089	.086	.077	.046

Thrust, Power, Efficiency, and Velocities

J:	.2	.24	.29	.33	.37	.41	.46	.5	.54	.58	.63
Ct:	.073	.066	.06	.053	.046	.038	.029	.021	.012	3E-03	-6E-03
Cp:	.028	.028	.027	.026	.024	.021	.018	.015	.011	6E-03	1E-03
eta:	.519	.582	.64	.683	.712	.737	.727	.689	.613	.264	-3.999
Mt:	.244	.226	.208	.194	.18	.168	.158	.149	.141	.133	.127
RPM:	9120	7514	6389	5557	4917	4409	3996	3654	3366	3120	2907

Angles of Attack (Degrees)

X	J: .2	.24	.29	.33	.37	.41	.46	.5	.54	.58	.63
.3	12.9	6.6	5.1	3.6	2	.4	-1.1	-2.6	-4.1	-5.5	-7
.45	5.6	4.4	3.4	2.3	1.2	.1	-1.1	-2.2	-3.3	-4.3	-5.5
.6	4.3	3.2	2.4	1.6	.7	-.2	-1	-1.9	-2.8	-3.7	-4.5
.7	3.4	2.7	2	1.2	.5	-.3	-1	-1.8	-2.6	-3.3	-4.1
.75	3.1	2.4	1.8	1.1	.4	-.3	-1	-1.7	-2.5	-3.2	-3.8
.8	2.9	2.2	1.7	1	.4	-.3	-1	-1.7	-2.4	-3.1	-3.8
.85	2.6	2.1	1.5	.8	.3	-.4	-1	-1.7	-2.3	-3	-3.6
.9	2.4	1.9	1.3	.7	.2	-.5	-1.1	-1.7	-2.2	-2.9	-3.5
.95	2.4	1.9	1.4	.8	.2	-.4	-1	-1.6	-2.2	-2.8	-3.4

Reynolds Number (Millions)

X	J: .2	.24	.29	.33	.37	.41	.46	.5	.54	.58	.63
.3	.05	.04	.03	.03	.03	.03	.03	.03	.02	.02	.02
.45	.06	.06	.05	.05	.05	.04	.04	.04	.04	.04	.03
.6	.09	.08	.07	.07	.06	.06	.05	.05	.05	.05	.04
.7	.09	.08	.08	.07	.07	.06	.06	.06	.05	.05	.05
.75	.09	.08	.08	.07	.07	.06	.06	.06	.05	.05	.05
.8	.09	.08	.08	.07	.07	.06	.06	.06	.05	.05	.05
.85	.09	.08	.08	.07	.07	.06	.06	.06	.05	.05	.05
.9	.08	.08	.07	.07	.06	.06	.06	.05	.05	.05	.05
.95	.05	.05	.05	.04	.04	.04	.04	.03	.03	.03	.03

* Thickness values limited by available Cl and Cd data for selected airfoil section.
Advance ratio values limited by available Cl and Cd data for selected airfoil section.

Appendix E

Sample Cruise Conditions for Electric Motor Performance

Input	Name	Output	Unit	Comment
	Q	1.0701	psf	dynamic pressur
.002378	rho		slug/ft3	air density
30	vel		ft/sec	air speed
	Cd	.03641082		a/c drag coefficient
.0179	Cdo			zero lift drag coefficient
	Cl	.63938933		a/c lift coefficient
.74	eff			efficiency factor
9.5	AR			aspect ratio
1	n			load factor
6.5	W		lb	a/c weight
9.5	S		ft-ft	wing area
	Preq	15.05493	W	a/c power required - level flight
	ROC	-.0004831	ft/s	rate of climb
	Pavail	15.050672	W	power available from propeller
	v	9.2099145	volt	armature voltage
9.563	vset		volt	battery voltage
.08	Kb			battery constant
	i	4.4135691	amp	motor current draw
	motrpm	11128.572	rpm	motor speed (rpm)
.12	Ra		ohm	armature resistance
.00078	Kv		volt/rpm	motor speed constant
	proprps	4675.8706	rpm	propeller speed (rps)
2.38	gr			gear ratio
	J	.41979831		propeller advance ratio
.917	propd		ft	propeller diameter
	eta	.74524122		propeller efficiency
1.08	Kt		in-oz/amp	motor torque constant
.95	greff			gear efficiency
	fltime	815.66639	sec	flight time
1	batcap		amp-hr	battery capacity
	range	24469.992	ft	range
	CT	.0362363		
	CP	.0204121		
	moteff	.54803682		motor efficiency
	oeff	.40841963		overall efficiency

Rule

```
Q= .5*rho*vel^2
Cd=Cdo+Cl^2/(PI()*eff*AR)
Cl=(n*W)/(Q*S)
Preq=Q*S*Cd*vel
ROC=(Pavail-Preq)/W
v=vset-Kb*i
motrpm=(v-i*Ra)/Kv
proprps=motrpm/(60*gr)
J=vel/(proprps*propd)
CT=Ct(J)
CP=Cp(J)
eta=Ct(J)*J/Cp(J)
Pavail=eta*Cp(J)*rho*proprps^3*propd^5
Cp(J)*rho*proprps^3*propd^5=((Kt/Kv)*(v*i-i*i*Ra)*.0005454-floss(motrpm))*gre
fltime=batcap/i
range=vel*fltime*3600
k=-9.4225+6.0529E-3*60*proprps-1.3867E-6*(60*proprps)^2
f=(60*proprps)^3*1.4337E-10-(60*proprps)^4*5.5867E-15
moteff=k+f
```

Appendix F
Equations and Assumptions

F.1 Wing contribution to Cm

$Cm_{ow} = Cm_{acw} + Cl_{ow}$ (Xcg/c - Xac/c)

$Cm_{\alpha w} = Cl_{\alpha w}$ (Xcg- Xac)

assumptions: small angles - 15° max

cos 15° = 1 (actually = .966)

sin 15° = .262 (actually = .259)

L/D >> 1 (actually = 14)

Zcg is negligable since multiplied by sine

F.2 Horizontal stabilizer contribution to Cm

$Cm_{oh} = \eta_h * V_h * Cl_{\alpha h} * (\varepsilon_o + i_w - i_t)$

$Cm_{\alpha h} = -\eta_h * V_h * Cl_{\alpha h} * (1 - d\varepsilon/d\alpha)$

assumptions: $\eta_h = .97$ this is an estimate using ref.6 pg 47

$\varepsilon = \varepsilon_o + (d\varepsilon/d\alpha)\,\alpha_w$ }

$\varepsilon_o = 2*Cl_{ow}/(\pi AR_w)$ } ref.6 pg 47-48

$d\varepsilon/d\alpha = 2*Cl_{\alpha w}/(\pi AR_w)$ }

lt/Zcgt >> 1 (actually = 24)

F.3 Fuselage contribution to Cm

$$Cm_{of} = \frac{k2 - k1}{36.5 * S_w * c_w} \Sigma\, w_f^2\, (\alpha_{ow} + i_f)\, \Delta x$$ }

$$Cm_{\alpha f} = \frac{1}{36.5 * S_w * c_w} \Sigma\, w_f^2\, (d\varepsilon/d\alpha)\, \Delta x$$ } ref.6 pg 49-51

assumptions: k2-k1 = 0.95

station	Δx	wf	αow+if	$wf^2(\alpha ow+if)\Delta x$
1	0.33	0.283	-16	-.427
2	1.83	0.396	-2	-.575
3	1.48	0.396	-2	-.464
4	0.27	0.313	+32	+.849
				total = -.616

station	Δx	wf	x	$d\varepsilon/d\alpha$	$wf^2(d\varepsilon/d\alpha)\Delta x$
1	0.33	0.283	1.99	1.10	0.03
2	1.83	0.396	0.92	1.20	0.344
3	1.48	0.396	0.74	0.093	0.022
4	0.27	0.313	1.62	0.08	0.002
					total = 0.398

F.4 Setting the wing position

$Mcg = Mac + Lw\ (Xcg - Xac)$

$Cmcg = Cmac_w + Cl_w\ (Xcg/c - Xac/c)$

$Xac/c = Xcg/c + (Cmac_w/Cl_w)$

F.5 Wing and Fuselage contribution to Cn

$$Cn_{Bwf} = -K_n K_{rl} \frac{S_{fs} l_f}{S_w\ b}$$

assumptions: $K_n = .00075$

$K_{Rl} = 1.4$

F.6 Vertical stabilizer contirbution to Cn

$Cn_{Bv} = V_v\ Cl_{\alpha v}\ \eta_v(1+ d\sigma/ d\beta)$

assumptions: $\eta_v(1+ d\sigma/ d\beta) = 0.992 + 1.53\ (S_v/S_w) + 0.009\ AR_w$

ref.6 pg 71

F.7 Cl_B calculations (ref.4)

$(Cl_B)_{total} = (Cl_B)_w + (Cl_B)_v + (\Delta Cl_B)_1 + (\Delta Cl_B)_2 + (Cl_B)_{w,\Gamma=0}$

assumptions:

$(Cl_B)_w = -.20799$

$(Cl_B)_v = -.01129$

$(\Delta Cl_B)_1 = -.0006$

$(\Delta Cl_B)_2 = +.00016$

$(Cl_B)_{w,\Gamma=0} = -.00364$

F.8 Required EDA and actual panel angle(ref.4)

30 ft/s => 22°/s roll rate
desire 25°/s roll rate

$$\frac{\Gamma}{10°} = \frac{25}{22} * \frac{116.16}{100}$$

$\Gamma = 13.2°$

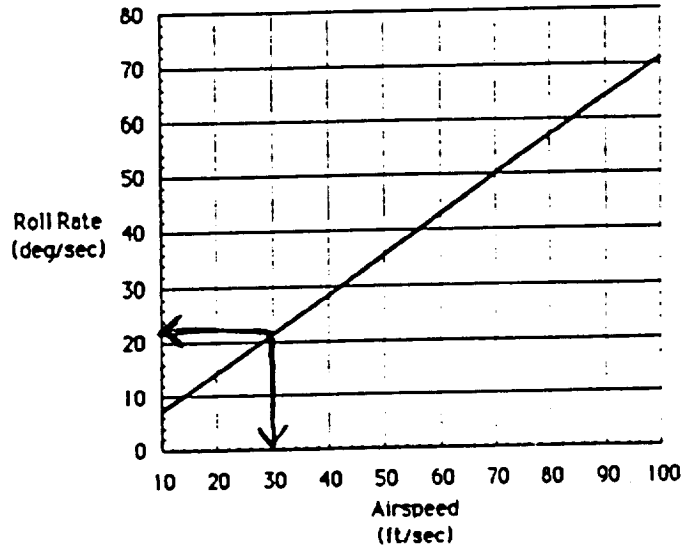

Break Point = 40% span
Moment Fraction = 0.775
13.2° EDA = 0.775 * panel angle
Panel angle = 17°

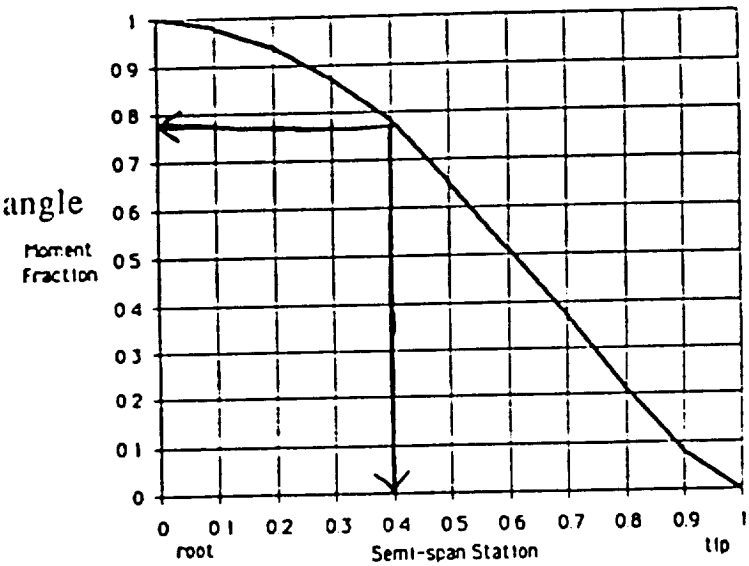

F.9 Required Yaw Angle (ref.4)

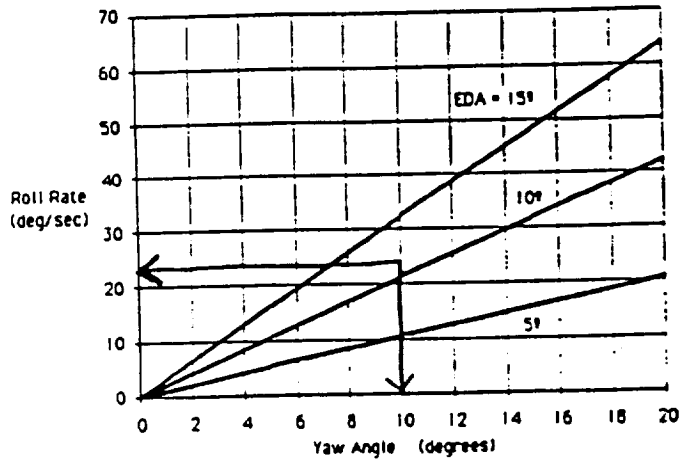

$$\frac{25°/s}{X} = \frac{100}{116.16} * \frac{13.2}{10}$$

X = 22°/s

Appendix G
Performance Calculations

The three computer codes listed use the same procedure to find a motor speed for a particular flight velocity. In "takeoff.f", lines 3 through 22 input the necessary variables. Note that the user must manually input the propeller coefficients as indicated in lines 67 through 78. In addition, a motor loss has been included in line 65 using a motor efficiency as a function of propeller RPM. Finally, the gearing efficiency is found in line 81 as the value 0.95.

Lines 56 through 89 of "takeoff.f" is the iterative process that finds the converging motor speed for a particular flight velocity. Once the motor speed has converged within a difference of 20 (line 89) the program utilizes the values found for motor RPM, coefficient of thrust and power, and current.

After the motor convergence is complete, various other calculations can begin. For each particular flight velocity and voltage setting, values for power, thrust, lift, and drag can be computed, thereby allowing an analysis of the kinematics of the aircraft. "Takeoff.f" uses a time-step process in lines 106 through 121 calculating distance travelled and velocity for each increment in time. When the velocity of the aircraft exceeds the takeoff velocity the program terminates. "Perf.f" and "pavail.f" both calculate the power available, power required, and rate of climb at each desired flight velocity and voltage setting. "Perf.f" finds the voltage setting and current require for cruise conditions (rate of climb approximately zero) and then calculates the range and endurance for each flight velocity.

Landing Calculations

$$X_{GR}=\frac{W}{g}\frac{1}{2B}\ln\left[1+\frac{B}{A}V_{TD}^2\right]$$

$$A=\mu W$$

$$B=C_D\frac{1}{2}\rho S$$

$$V_{TD}\cong V_{stall}=22.6 \text{ ft/ s}$$

$$W=6.7 \text{ lb}$$

$$\mu=0.15$$

$$S=9.68$$

$$C_D=0.019+\frac{1.14^2}{\pi(.74)(9.68)}=0.077$$

$$X_{GR}=43.8 \text{ ft}$$

Gliding Calculations

$$\gamma_{min} = \tan^{-1}\left[\frac{1}{L/D)_{max}}\right]$$

$$\left(\frac{C_L}{C_D}\right)_{max} = \frac{\sqrt{C_{Do}\pi e AR}}{2\,C_{Do}}$$

$C_{Do} = 0.019$

$e = 0.74$

$AR = 9.68$

$L/D)_{max} = 17.2$

$\gamma_{min} = 3.33^{o}$

Glide Dist)$_{max}$ = L/D)$_{max}$ x altitude = 17.2 x 25 ft = 430 ft

takeoff.f

```
      real j,kt,kv,mass,mrpm,mrpmn,mrps,mu,lift

      open(10,file ='take')
      read(10,*) wem
      read(10,*) cargo
      read(10,*) rho
      read(10,*) clmax
      read(10,*) clto
      read(10,*) cdo
      read(10,*) sref
      read(10,*) e
      read(10,*) ar
      read(10,*) dia
      read(10,*) kt
      read(10,*) kv
      read(10,*) rarm
      read(10,*) rbat
      read(10,*) batcap
      read(10,*) fusamp
      read(10,*) gearat
      read(10,*) mu
      close(10)

      dt=.01
      bvolts=14.4
c     dia=dia/12.

      pi=-4.*atan(-1.)
      dia4=dia**4
      dia5=dia**5

      rtot=rarm+rbat

      open(100,file='takeout')

      do 40 c=0.,32.,4.
      w=wem+c/16.
      mass=w/32.174
      clto=clmax/1.44
      cdto=cdo+clto**2/(pi*e*ar)
      ampmax=bvolts/(2.*rtot)
      pomax=((kt*bvolts**2)/(4.*rtot*kv))*2.*pi
      pomxhp=pomax*1.578e-7
      pomxwt=pomxhp/1.341e-3
      fac1=bvolts/(2.*rtot)
      fac2=(bvolts/rtot)**2
      batlos=0.
      time=0.
      icount=0
      v=0.
      s=0.
      vto=sqrt(2.*w/(rho*sref*clmax))*1.2

      amps=0.
      mrpm=(bvolts-ampmax*rtot)/kv
85    continue
      icount=icount+1

      iter=0
15    continue
      mrps=mrpm/60.
      iter=iter+1
      prps=mrps/gearat
      prpm=prps*60.
```

takeoff.f

```
    65          etam=-9.4225+6.0529e-3*prpm-1.3867e-6*prpm**2+1.4337e-10*prpm**3-5.5867e-1
5*prpm**4
    66          j=v/(prps*dia)
    67  c       10-6
    68  c       ct=.14079-8.2493e-2*j-8.7552e-2*j**2-7.4503e-2*j**3
    69  c       cp=6.4266e-4+.31747*j-.99812*j**2+1.5975*j**3-1.1167*j**4
    70  c       11-5
    71          ct=9.7987e-2-.11367*j-5.0432e-2*j**2-6.2163e-2*j**3
    72          cp=2.7985e-2-3.7795e-3*j+9.3626e-2*j**2-.38324*j**3+.20948*j**4
    73  c       12-4
    74  c       ct=7.6014e-2-.10035*j-8.643e-2*j**2-.10066*j**3
    75  c       cp=2.0033e-2+1.566e-3*j+1.7352e-2*j**2-.18709*j**3
    76  c       12-6
    77  c       ct=.12597-.16733*j-1.4419e-2*j**2-4.9687e-2*j**3
    78  c       cp=3.399e-2+2.6607e-2*j-6.2701e-2*j**2-7.5545e-2*j**3
    79          pmot=cp*rho*prps**3*dia5*1.152e4/etam
    80          if (pmot .ge. pomax) goto 1001
    81          amps=fac1-.5*sqrt(fac2-4.*pmot/.95*kv/(rtot*kt*2.*pi))
    82          mrpmn=(bvolts-amps*rtot)/kv
    83          d=abs(mrpm-mrpmn)
    84          mrpm=mrpm+(mrpmn-mrpm)*.5
    85          if (iter .gt. 1000) then
    86          print *, "motor speed calculation did not converge"
    87          goto 40
    88          endif
    89          if (d .gt. 20.) goto 15
    90          if (amps .gt. fusamp) then
    91          print *, "fuse current exceeded"
    92          stop
    93          endif
    94          prps=mrpm/(60.*gearat)
    95          thrust=ct*rho*prps**2*dia4
    96          drag=.5*rho*v**2*sref*cdto
    97          lift=.5*rho*v**2*sref*clto
    98          frict=mu*(w-lift)
    99          if (thrust .lt. frict) then
   100          print *, "friction exceeds static thrust"
   101          stop
   102          endif
   103          accel=(thrust-drag-frict)/mass
   104
   105
   106          delv=accel*dt
   107          ds=v*dt
   108          dbat=dt*amps/3600.
   109          v=v+delv
   110          s=s+ds
   111          batlos=batlos+dbat
   112          time=time+dt
   113          if(s .gt. 200.) then
   114          print *,"distance greater than 200 ft"
   115          goto 40
   116          endif
   117          if (time .gt. 60.) then
   118          print *, "time greater than 60 sec"
   119          stop
   120          endif
   121          if (v .lt. vto) goto 85
   122          wl=w/sref
   123          write(100,*) s
   124          roc=(thrust-drag)/w*v
   125          gamma=asin((thrust-drag)/w)
   126          print *, c, s
   127  c       print *, roc
```

takeoff.f

```
128   c       print *, "V takeoff=",vto
129   c       print *, "Time for run (sec)=",time
130   c       print *, "V at TO (ft/sec)=",v
131   c       print *, "Distance (ft)=",s
132   c       print *, "Battery Drain (amp-hrs)=",batlos
133   c       print *, "Advance Ratio at TO=", j
134   c       print *, "Thrust (lb) at TO=", thrust
135   c       print *, "Lift (lb) at TO=", lift
136   c       print *, "Drag (lb) at TO=", drag
137   c       print *, "Friction (lb) at TO=", frict
138   c       print *, "Current Draw at TO (amps)=", amps
139   40      continue
140
141           close(100)
142           stop
143
144   1001    print *, "Pmot exceeded Pmax"
145           print *, "Pmot=",pmot,"   Pmax=",pomax
146           stop
147           end
```

perf.f

```
      1           real j,kt,kv,mass,mrpm,mrpmn,mrps
      2
      3           open(10,file ='stuff')
      4           read(10,*) w
      5           read(10,*) cargo
      6           read(10,*) rho
      7           read(10,*) clmax
      8           read(10,*) cdo
      9           read(10,*) sref
     10           read(10,*) e
     11           read(10,*) ar
     12           read(10,*) dia
     13           read(10,*) kt
     14           read(10,*) kv
     15           read(10,*) rarm
     16           read(10,*) rbat
     17           read(10,*) batcap
     18           read(10,*) fusamp
     19           read(10,*) gearat
     20           close(10)
     21
     22           pi=-4.*atan(-1.)
     23           dia4=dia**4
     24           dia5=dia**5
     25           mass=w/32.174
     26           rtot=rarm+rbat
     27           w=w+cargo/16.
     28           vel=30.
     29           open (100,file='perfout')
     30   c       do 35 vel=0.,60.,1.
     31           cl=w/(.5*rho*vel**2*sref)
     32           cd=cdo+cl**2/(pi*e*ar)
     33           drg=.5*rho*vel**2*sref*cd
     34           preq=drg*vel*1.356
     35           roco=10.
     36           do 60 bvolts=6.,16.,.005
     37           ampmax=bvolts/(2.*rtot)
     38           pomax=((kt*bvolts**2)/(4.*rtot*kv))*2.*pi
     39           pomxhp=pomax*1.578e-7
     40           pomxwt=pomxhp/1.341e-3
     41           fac1=bvolts/(2.*rtot)
     42           fac2=(bvolts/rtot)**2
     43           mrpm=(bvolts-ampmax*rtot)/kv
     44           iter=0
     45   85      continue
     46           mrps=mrpm/60.
     47           iter=iter+1
     48           prps=mrps/gearat
     49           prpm=prps*60.
     50           etam=-9.4225+6.0529e-3*prpm-1.3867e-6*prpm**2+1.4337e-10*prpm**3-5.5867e-1
5*prpm**4
     51           j=vel/(prps*dia)
     52           ct=9.7987e-2-.11367*j-5.0432e-2*j**2-6.2163e-2*j**3
     53           cp=2.7985e-2-3.7795e-3*j+9.3626e-2*j**2-.38324*j**3+.20948*j**4
     54           pmot=cp*rho*prps**3*dia5*1.152e4/etam
     55           amps=fac1-.5*sqrt(fac2-4.*(pmot/.95)*kv/(rtot*kt*2.*pi))
     56           mrpmn=(bvolts-amps*rtot)/kv
     57           d=abs(mrpm-mrpmn)
     58           mrpm=mrpm+(mrpmn-mrpm)*.5
     59           if (iter .gt. 1000) then
     60   c       print *, "motor speed calculation did not converge"
     61           goto 60
     62           endif
     63           if (d .gt. 20.) goto 85
```

perf.f

```
      if (amps .gt. fusamp) then
      print *, "fuse current exceeded"
      goto 60
      endif
      prps=mrpm/(60.*gearat)
      thrust=ct*rho*prps**2*dia4
      pavail=thrust*vel
      pavlhp=pavail/550.
      pavlwt=pavlhp/1.341e-3
      roc=(pavlwt-preq)/w
      if (abs(roc) .gt. .1) then
              goto 60
      else
              if (abs(roc) .lt. roco) then
              endur=batcap/amps
              range=vel*endur*3600.
              battloss=amps/vel/3600.
              roco=abs(roc)
              endif
      endif
 60   continue
      write(100,*) vel, range, endur, battloss
 35   continue

      close(100)
      stop

1001  print *, "Pmot exceeded Pmax"
      print *, "Pmot=",pmot,"   Pmax=",pomax
      stop
      end
```

pavail.f

```
      real j,kt,kv,mass,mrpm,mrpmn,mrps

      open(10,file ='stuff')
      read(10,*) w
      read(10,*) rho
      read(10,*) clmax
      read(10,*) cdo
      read(10,*) sref
      read(10,*) e
      read(10,*) ar
      read(10,*) dia
      read(10,*) kt
      read(10,*) kv
      read(10,*) rarm
      read(10,*) rbat
      read(10,*) batcap
      read(10,*) fusamp
      read(10,*) gearat
      close(10)
      bvolts=14.4
      pi=-4.*atan(-1.)
      dia4=dia**4
      dia5=dia**5
      mass=w/32.174
      rtot=rarm+rbat

      open (100,file='pavout')
      open (101,file='rocout')
      open (102,file='prout')
      do 35 vel=0.,70.,5.
      cl=w/(.5*rho*vel**2*sref)
      cd=cdo+cl**2/(pi*e*ar)
      drg=.5*rho*vel**2*sref*cd
      preq=drg*vel*1.356
60    continue
c     do 60 bvolts=7.,14.4,.1
      ampmax=bvolts/(2.*rtot)
      pomax=((kt*bvolts**2)/(4.*rtot*kv))*2.*pi
      pomxhp=pomax*1.578e-7
      pomxwt=pomxhp/1.341e-3
      fac1=bvolts/(2.*rtot)
      fac2=(bvolts/rtot)**2
      mrpm=(bvolts-ampmax*rtot)/kv
      iter=0
85    continue
      mrps=mrpm/60.
      iter=iter+1
      prps=mrps/gearat
      prpm=prps*60.
      etam=-9.4225+6.0529e-3*prpm-1.3867e-6*prpm**2+1.4337e-10*prpm**3-5.5867e-1
5*prpm**4
      j=vel/(prps*dia)
      ct=9.7987e-2-.11367*j-5.0432e-2*j**2-6.2163e-2*j**3
      cp=2.7985e-2-3.7795e-3*j+9.3626e-2*j**2-.38324*j**3+.20948*j**4
      pmot=cp*rho*prps**3*dia5*1.152e4/etam
      if (pmot .ge. pomax) goto 1001
      amps=fac1-.5*sqrt(fac2-4.*(pmot/.95)*kv/(rtot*kt*2.*pi))
      mrpmn=(bvolts-amps*rtot)/kv
      d=abs(mrpm-mrpmn)
      mrpm=mrpm+(mrpmn-mrpm)*.5
      if (iter .gt. 1000) then
      print *, "motor speed calculation did not converge"
      goto 60
      endif
```

pavail.f

```
64          if (d .gt. 20.) goto 85
65          if (amps .gt. fusamp) then
66          print *, "fuse current exceeded"
67          goto 60
68          endif
69          thrust=ct*rho*prps**2*dia4
70          pavail=thrust*vel
71          pavlhp=pavail/550.
72          pavlwt=pavlhp/1.341e-3
73          roc=(pavlwt-preq)/w
74          write(100,*) vel,bvolts,pavlwt
75          write(101,*) vel,bvolts,roc
76  c60     continue
77          write(102,*) vel,preq
78  35      continue
79
80          close(100)
81          close(101)
82          close(102)
83          stop
84
85  1001    print *, "Pmot exceeded Pmax"
86          print *, "Pmot=",pmot,"   Pmax=",pomax
87          stop
88          end
```

Appendix H
Two-dimensional Truss Analysis

The Prime Mover will be subjected to a variety of loads during it's life. These vary from lifting forces, to weight forces, to catapult forces. Each of these forces offers their individual challenges in fuselage design.

It was Exodus's goal to produce an aircraft fuselage capable of withstand a load factor of 4.0 in landing situations, 2.5 in cruise conditions, and 2.0 during catapult launching. Due to the complexity of structural testing, three design options were studied. Each of these were analyzed separately.

By the assumption that the forces on the aircraft are nearly symmetric, one side of the fuselage is analyzed in a two dimensional truss method. Fixing certain junctures of the truss design allowed for a static analysis.

The forces were simulated by point loads at fuselage nodal locations in a two dimensional truss analysis, where each node is defined by a junction of two or members. Therefore, if a force was to be distributed between nodes 5 and 6, half the load would be placed at each location. Forces included the following depending on the load environment: landing gear weight, equipment weight, cargo weight, wing weight, battery weight, engine weight, empennage weight, fuselage weight, wing lift force, landing forces, engine forces, and catapult forces.

These forces were multiplied by the desired load factors. The optimal designs of each initial design were compared for given nodal locations. The saw tooth truss design was chosen as the strongest because of it's ability to handle compressive and tensional loads.

The program was then altered to allow for further optimization. The next two pages include the input data file used to analyze the final concept in a 4.0 g landing environment. The program that follows determines the minimal cross sectional area of any member dependent on material properties and the internal forces produced from the given loads.

```
FUSELAGE-2-D
29      55      0       0
1       0       0       1       60.     0.      4.5     0.      0.      -.44
2       1       0       1       56.     0.      4.5     0.      0.      -.44
3       1       0       1       52.     0.      4.5     0.      0.      -.064
4       1       0       1       47.     0.      4.5     0.      0.      -.064
5       1       0       1       43.     0.      4.5     0.      0.      -1.34
6       1       0       1       39.     0.      4.5     0.      0.      -1.34
7       1       0       1       35.     0.      4.5     0.      0.      -1.
8       1       0       1       31.     0.      4.5     0.      0.      -1.
9       1       0       1       27.     0.      4.5     0.      0.      -.064
10      1       0       1       22.     0.      4.5     0.      0.      -.064
11      1       0       1       18.     0.      4.5     0.      0.      -.064
12      1       0       1       14.     0.      4.5     0.      0.      -.064
13      1       0       1       10.     0.      4.5     0.      0.      -.064
14      1       0       1       6.      0.      4.5     0.      0.      -.064
15      0       0       0       4.25    0.      4.5     0.      0.      4.405
16      0       0       0       4.25    0.      0.      0.      0.      -.372
17      1       0       1       6.      0.      0.      0.      0.      -.372
18      1       0       1       10.     0.      0.      0.      0.      -.372
19      1       0       1       14.     0.      0.      0.      0.      -.372
20      1       0       1       18.     0.      0.      0.      0.      -.372
21      1       0       1       22.     0.      0.      0.      0.      -.372
22      1       0       1       27.     0.      0.      0.      0.      -.372
23      1       0       1       31.     0.      0.      0.      0.      -.372
24      1       0       1       35.     0.      0.      0.      0.      -.372
25      1       0       1       39.     0.      0.      0.      0.      -.372
26      1       0       1       43.     0.      0.      0.      0.      -.372
27      1       0       1       47.     0.      0.      0.      0.      -.372
28      1       0       1       52.     0.      0.      0.      0.      6.27
29      1       0       0       56.     0.      0.      0.      0.
1       1       2       .0625   65000.
2       2       3       .0625   65000.
3       3       4       .0625   65000.
4       4       5       .0625   65000.
5       5       6       .0625   65000.
6       6       7       .0625   65000.
7       7       8       .0625   65000.
8       8       9       .0625   65000.
9       9       10      .0625   65000.
10      10      11      .0625   65000.
11      11      12      .0625   65000.
12      12      13      .0625   65000.
13      13      14      .0625   65000.
14      14      15      .0625   65000.
15      15      16      .3      65000.
16      16      17      .0625   65000.
17      17      18      .0625   65000.
18      18      19      .0625   65000.
19      19      20      .0625   65000.
20      20      21      .0625   65000.
21      21      22      .0625   65000.
22      22      23      .0625   65000.
23      23      24      .0625   65000.
24      24      25      .0625   65000.
25      25      26      .0625   65000.
26      26      27      .0625   65000.
27      27      28      .0625   65000.
28      28      29      .0625   65000.
29      29      1       .03125  65000.
30      29      2       .03125  65000.
31      28      3       .03125  65000.
32      27      4       .03125  65000.
33      26      5       .03125  65000.
34      25      6       .03125  65000.
35      24      7       .03125  65000.
```

36	23	8	.03125	65000.
37	22	9	.03125	65000.
38	21	10	.03125	65000.
39	20	11	.03125	65000.
40	19	12	.03125	65000.
41	18	13	.03125	65000.
42	17	14	.03125	65000.
43	29	3	.0156	1300000.
44	3	27	.0156	1300000.
45	27	5	.0156	1300000.
46	5	25	.0156	1300000.
47	25	7	.0156	1300000.
48	7	23	.0156	1300000.
49	23	9	.0156	1300000.
50	9	21	.0156	1300000.
51	21	11	.0156	1300000.
52	11	19	.0156	1300000.
53	19	13	.0156	1300000.
54	13	17	.0156	1300000.
55	17	15	.0156	1300000.

```
C       Two Dimensional Truss Analysis and Optimization Program
C       Internal Stress and Nodal displacement were compared to
C              that of SPACETRUSS and found extremely accurate.
C       The initial areas of the members are read from the input file
C       entitled Alanding.  These areas are varied based on decreasing
C       the area of the member with the highest load factor without
C       exceeded structural limitation of a 4.0 g landing load.

        Dimension node(30),memb(60),xpos(30),ypos(30),zpos(30),xfor(30),yfor(30),zf
        REAL KSPRING,xpos(125),zpos(125),FII(125),PCR(125),C(125,125),X(125),CIV(12
        REAL U(125),V(125),FX(125),FY(125),DEF(125),KFORS(125,125),FORCE(125,125),S
        INTEGER CR,start(60),finish(60)

        OPEN(12, file='Alanding')
        WRITE(6,*) 'Fuselage design A at ground conditions n=4'
        PI=4.*atan(1.)
        Density=.0058

        READ(12,'(a)') junk
        WRITE(6,*)
        WRITE(6,*) ' This is a 2 dimensional analysis.'
        WRITE(6,*) ' All nodes are constrained in the y component.'
        WRITE(6,*) ' This is an analysis of the side of the fuselage only.'
        READ(12,*) nnodes,nmembs,junk1,junk2
        WRITE(6,*) 'There are',nnodes,'nodes and',nmembs,'members'
        N=2*nnodes

C       THIS DO LOOP ALLOWS FOR THE READING OF THE POSITIONS OF EACH
C       JOINT TO BE USED IN CALCULATING LENGTH, THETA, AND THE
C       SPRING CONSTANT VALUES

        For=0
        moment=0
        Kount=0

        DO 20 Ia=1,nnodes
        READ(12,*) node(Ia),junk1,junk2,junk3,xpos(Ia),ypos(Ia),zpos(Ia),xfor(Ia),y
        If (junk1 .eq. 0) WRITE(6,*) 'Constrained in x direction at node',Ia
        If (junk3 .eq. 0) WRITE(6,*) 'Constrained in z direction at node',Ia
        For=For+zfor(Ia)
        moment=moment+xpos(Ia)*zfor(Ia)
 20     Continue

        WRITE(6,*)
        WRITE(6,*) 'Sum of the Forces =', For
        WRITE(6,*) 'Sum of the Moments =', moment
        WRITE(6,*)

 789    Kount=Kount+1
        cop=0
        TOTWE=0
        DO 10 I=1,N
        DO 10 J=1,N
        CIV(I,J)=0
 10     C(I,J)=0
        D=0

        DO 30 Ib=1,nmembs
        If (Kount .eq. 1) READ(12,*) memb(Ib),start(Ib),finish(Ib),Area(Ib),E(Ib)
        If(Ib .ge. 44) DENSITY=.016
        JA=start(Ib)
        JB=finish(Ib)
        D=SQRT((zpos(JB)-zpos(JA))**2 + (xpos(JB)-xpos(JA))**2)
        THETA=ATAN2(zpos(JB)-zpos(JA),xpos(JB)-xpos(JA))
        KSPRING=E(Ib)*Area(Ib)/D
        WEIGHT(Ib)=D*Area(Ib)*DENSITY
```

```
      TMOIN=(Area(Ib)**2)/12
      TOTWE=TOTWE+WEIGHT(Ib)
      Pcr(Ib)= PI*PI*E(Ib)*TMOIN/(D**2)

C*******Going to the subroutine************!!!
      NJOINTS=nnodes
      CALL KMAT(C,THETA,KSPRING,JA,JB,NJOINTS)
C*******Made it back!!!!

      LENGTH(JA,JB)=D
      ANGLE(JA,JB)=THETA
      KFORS(JA,JB)=KSPRING
   30 Continue

C*****************    PARTITION MATRIX  ***************
C     THE CRITICAL ROW NUMBER WILL BE READ- MEANING THE ROW IN WHICH DISPLACEMENT

      CR=7
      NEWA=CR-1
      NEWN=N-CR+1

      Do 42 lit=1,N
      Do 43 lat=1,N
      CIV(lit,lat)=C(lit,lat)
c     WRITE(6,*) lit,lat,C(lit,lat)
   43 Continue
   42 Continue

      Do 761 lit=1,N
      CIV(2,lit)=C(29,lit)
      CIV(3,lit)=C(30,lit)
      CIV(4,lit)=C(31,lit)
      CIV(5,lit)=C(32,lit)
      CIV(6,lit)=C(58,lit)
      Do 762 lat=7,33
  762 CIV(lat,lit)=C(lat-5,lit)
      Do 763 lat=34,58
  763 CIV(lat,lit)=C(lat-1,lit)
  761 continue

      Do 764 lit=1,N
      C(lit,2)=CIV(lit,29)
      C(lit,3)=CIV(lit,30)
      C(lit,4)=CIV(lit,31)
      C(lit,5)=CIV(lit,32)
      C(lit,6)=CIV(lit,58)
      Do 765 lat=7,33
  765 C(lit,lat)=CIV(lit,lat-5)
      Do 766 lat=34,58
  766 C(lit,lat)=CIV(lit,lat-1)
  764 continue

C     Input forces
      Do 767 I=1,NEWN
  767 FII(I)=0

      do 768 I=2,28,2
  768 FII(I-1)=zfor(I/2)
      do 769 I=30,NEWN+1,2
  769 FII(I-1)=zfor(I/2+2)

      DO 60 Id=1,NEWN
      DO 60 Ie=1,NEWN
      CIV(Id,Ie)=C(Id+NEWA,Ie+NEWA)
c     Write(6,*) Id,Ie,'          ',C(Id,Ie)
   60 Continue
```

```
C*************** Gaussian Section ***********
        DO 310 ib=1,N
        X(ib)=0
  310   continue

        Do 330 K=1,NEWN
        CC= CIV(K,K)

        FII(K)= FII(K)/CC

        DO 320 I=K,NEWN
  320   CIV(K,I)= CIV(K,I)/CC

        DO 330 I=K+1,NEWN
        CC= CIV(I,K)
        FII(I)= FII(I) - CC*FII(K)

        DO 330 J=K,NEWN
        CIV(I,J)=CIV(I,J)-CIV(K,J)*CC
  330   continue

        DO 340 Ih=NEWN,1,-1
        SUM=0

        DO 350 Ij=NEWN,Ih,-1
        PROD=CIV(Ih,Ij)*X(Ij)
  350   SUM=SUM+PROD

  340   X(Ih)=FII(Ih)-SUM

C*********************DEFINE RESULTS*****************************


        DO 80 IA=57,33,-1
   80   X(IA)=X(IA-5)
        DO 90 IB=28,2,-1
   90   X(IB)=X(IB-1)
        X(1)=0.
        X(29)=0.
        X(30)=0.
        X(31)=0.
        X(32)=0.
        X(58)=0.

        DO 93 INA=1,nnodes
        IOP=2*INA-1
        IUP=2*INA
        U(INA)=X(IOP)
   93   V(INA)=X(IUP)

C       **********************Compare these displacements to SPACETRUSS*****
c       DO 95 IYP=1,nnodes
c       WRITE(6,*) 'U',IYP,U(IYP)
c   95  WRITE(6,*) 'V',IYP,V(IYP)


C*******That completes the part on displacements now we must find the reaction forc

        DO 222 I=1,nnodes
        FX(I)=xfor(I)
  222   FY(I)=zfor(I)


C**************USING THESE FORCES AND DISPLACEMENTS ......
```

```
C       --------------Deflection---------------
        DO 102 I=1,nnodes
        DEF(I)=SQRT(U(I)**2+V(I)**2)
C       WRITE(6,*) 'DEF(',I,')=',DEF(I)
  102   Continue

C       ---------------Forces and Stresses-------------
        tackle=0
        tbone=0

        DO 105 J=1,nmembs
        KA=start(J)
        KB=finish(J)
        tat=0

        FORCE(KA,KB)= (KFORS(KA,KB)*((U(KB)-U(KA))*COS(ANGLE(KA,KB))+(V(KB)-V(KA))*
        If(FORCE(KA,KB) .lt. 0) then
        Forrat=(FORCE(KA,KB)/-Pcr(J))
        else
        Forrat=1
        endif
        STRESS(KA,KB)=FORCE(KA,KB)/AREA(J)
        SHEAR(J)=STRESS(KA,KB)/2
        If(STRESS(KA,KB) .gt. 0) then
        If(J .lt. 44) Strrat=STRESS(KA,KB)/400
        If(J .ge. 44) Strrat=STRESS(KA,KB)/750
        else
        Strrat=1
        endif

        If(FORCE(KA,KB) .eq. 0) Forrat=1
        If(Forrat .gt. 1) Write(6,*)'***Force Ratio Exceeded in member',J,'     Are
        If(Strrat .gt. 1) Write(6,*)'***Stress Ratio Exceeded in member',J,'     Ar
        If (J .lt. 44)then
        If(SHEAR(J)/200 .gt. 1) Write(6,*)'***Shear Ratio Exceeded in member',J,'
        else
        If(SHEAR(J)/750 .gt. 1) Write(6,*)'***Shear Ratio Exceeded in member',J,'
        endif

C       -------------Testing Force and Stress Ratios----

        If(ABS(Forrat-1) .gt. data) then
        tackle=Forrat
        tbone=Area(J)
        data=Abs(Forrat-1)
        recall=J
        endif
        If(Abs(Strrat-1) .gt. data) then
        tackle=Strrat
        tbone=Area(J)
        data=Abs(Strrat-1)
        recall=J
        endif

C       -------------Safety Factor-----------------

  105   CONTINUE


        Write(6,*) '    Member=',recall
        Write(6,*) '    Ratio=',tackle
        Write(6,*) '    Current Area=',tbone
        Write(6,*) 'Would you like to change area?'
        Write(6,*) 'If yes, input member'
        Write(6,*) 'If no, input 999'
```

```
      Read(5,*) recall
      If(recall .gt. 990) goto 212
      Write(6,*) 'Input area'
      Read(5,*) exit

      If ((recall .ge. 1) .and. (recall .le. 14)) then
              do 912 i=1,14
912           Area(i)=exit
              write(6,*) 'Area     1-14',Area(1)
      else if((recall .ge. 16) .and. (recall .le. 28)) then
              do 913 i=16,28
913           Area(i)=exit
              write(6,*) 'Area     16-28',Area(16)
      else if((recall .ge. 30) .and. (recall .le. 42)) then
              do 914 i=30,42
914           Area(i)=exit
              write(6,*) 'Area     30-42',Area(30)
      else if((recall .ge. 43) .and. (recall .le. 54)) then
              do 915 i=43,54
915           Area(i)=exit
              write(6,*) 'Area     43-54',Area(44)
      else
              Area(recall)=exit
              write(6,*) 'Area      ',recall,'    ',exit

      data=0
      exit=0
      endif
      Goto 789

212   WRITE(6,*) 'The total weight of the structure in onces=',TOTWE*16
      Write(6,*)
737   FORMAT (2x,'Member',8x,'TENSION',9x,'STRESS',9x,'Area')
747   FORMAT (2x,I2,6x,F10.6,6X,F10.6,6X,F10.5)

      Write(6,737)
      strtot=0
      strcount=0
      fortot=0
      forcount=0

      Do 822 J=1,nmembs
      KA=start(J)
      KB=finish(J)
      if (STRESS(KA,KB) .ge. 0) then
              Strrat=STRESS(KA,KB)/400
              strtot=strtot+Strrat
              strcount=strcount+1
      else
              Strrat=1
      endif
      If(FORCE(KA,KB) .lt. 0) then
              Forrat=FORCE(KA,KB)/Pcr(J)
              fortot=fortot+Forrat
              forcount=forcount+1
      else
              Forrat=1
      endif
      WRITE(6,747) J,Forrat,Strrat,Area(J)
822   Continue
      Write(6,*)
      Write(6,*)'Average safety factor in compression is',-fortot/forcount
      Write(6,*)'Average safety factor in tension is',strtot/strcount

      Write(6,*)'Thats all folks.............'
      STOP
```

```
      END
C***************Subroutine*****************************
      SUBROUTINE KMAT(C,THETA,KSPRING,I,J,nnodes)
C
C             THIS TAKES K AS INPUT AND ADDS CONTRIBUTION TO
C             CURRENT MEMBER
C
      REAL C(125,125),R(2,125),KE(2,2),T(2,125),KSPRING

C
C     BEGIN BY FINDING R
C
      Na=2*nnodes

      DO 210 Ik=1,2
      DO 210 Il=1,Na
  210 R(Ik,Il)=0

      R(1,2*J-1)=COS(THETA)
      R(1,2*J)=SIN(THETA)
      R(2,2*I-1)=COS(THETA)
      R(2,2*I)=SIN(THETA)
C
C     DEFINE KE
C
      KE(1,1)=KSPRING
      KE(2,2)=KSPRING
      KE(1,2)=-KSPRING
      KE(2,1)=-KSPRING
C
C     MULTIPLY KE * R
C
      DO 220 II=1,2
      DO 220 JJ=1,Na
      T(II,JJ)=0.
      DO 220 KK=1,2
      T(II,JJ)=T(II,JJ)+KE(II,KK)*R(KK,JJ)
  220 Continue

      DO 230 II=1,Na
      DO 230 JJ=1,Na
      DO 230 KK=1,2
      C(II,JJ)=C(II,JJ)+R(KK,II)*T(KK,JJ)
  230 Continue

      RETURN
      END
```

Appendix I
Economic Analysis

	A	B	C	D	E	F
1	UPC=	376000		ECONOMIC RESULTS		
2	OCPF=	9				
3	MCPF=	25		UVCPF	0.00032169	
4	FCPF=	1604		UWCPF=	0.00804214	
5	NFLEET=	42		FLC ($) =	57069600	
6	NCYC=	600		FLV (CU. IN.) =	20160000	
7	DESVOL=	800		FLW (OZ.)	806400	
8	DESWGT=	32		FCPOF ($/OZ)	70.7708333	
9	DRANGE=	8800		FCPCI ($/CU. IN.) =	2.83083333	
10	FLVPD=	29400		FLIFE (DAYS)	300	
11	FFPD=	84		FCPVOL($/CU. IN.) =	6.47047619	
12						
13						
14						
15		.....	IN ORDER FOR PROPER PRICING SCHEMES,			.....
16			AVERAGE VALUES WERE USED NOT			
17			MAXIMUM VALUES			
18						
19						
20						
21		CARGO LOAD PER DAY PER CITY				
22			LOAD (IN)			
23		CITY	DEPARTING	ARRIVING		
24		A	2060	1960		
25		B	2760	2760		
26		F	2910	2910		
27		G	2620	2720		
28		H	1560	1560		
29		I	2450	2450		
30		J	3450	3450		
31		K	3950	4050		
32		L	2830	2730		
33		M	2310	2210		
34		N	2500	2600		
35		TOTAL	29400	29400		
36						
37						
38		NON-OVERSEAS LOAD (IN)			OVERSEAES LOAD (IN)	
39	CITY	DEPARTING	ARRIVING		DEPARTING	ARRIVING
40	A	500	300		1560	1660
41	B	300	500		2460	2260
42	F	1560	1460		1350	1450
43	G	1400	1500		1220	1220
44	H	1060	1160		500	400
45	I	1550	1550		900	900
46	J	1900	1800		1550	1650
47	K	1950	1950		2000	2100
48	L	750	750		2080	1980
49	M	700	700		1610	1510
50	N	750	750		1750	1850
51	TOTAL	12420	12420		16980	16980
52						
53						
54		NON-OVERSEAS PRICE ($/CU. IN.) =			8.7404762	
55		OVERSEAS PRICE ($FLIFE) =			11.010476	
56						